Received: 31 March 2025 | Revised: 14 July 2025 | Accepted: 30 August 2025

DOI: 10.1111/andr.70118

ANDROLOGY

WILEY

ORIGINAL ARTICLE

The sensory penis: A comprehensive immunohistological and ontogenetic exploration of human penile innervation

Alfonso Cepeda-Emiliani[1] | María Otero-Alén[2] | Juan Suárez-Quintanilla[1] | Marina Gándara-Cortés[1,3] | Tomás García-Caballero[1,3] | Rosalía Gallego[1] | Lucía García-Caballero[1]

[1]Department of Morphological Sciences, School of Medicine and Dentistry, University of Santiago de Compostela, Santiago de Compostela, Spain

[2]Health Research Institute of Santiago (IDIS), Santiago de Compostela, Spain

[3]Department of Pathology, University Clinical Hospital, Santiago de Compostela, Spain

Correspondence
Alfonso Cepeda-Emiliani, Department of Morphological Sciences, School of Medicine and Dentistry, University of Santiago de Compostela, Santiago de Compostela, Spain.
Email: alfonsomario.cepeda@rai.usc.es

Abstract

Background: Penile sexual sensation relies on intricate neural structures that remain incompletely characterized. Immunohistological insights into their development and organization can enhance understanding of penile neuroanatomy and function, while optimizing surgical outcomes.

Objectives: To elucidate the ontogeny, organization, and immunohistological features of human penile innervation in fetal and adult specimens, primarily focusing on the frenular delta, sensory corpuscles, and related structures to address gaps in anatomical knowledge and inform surgical practices.

Materials and methods: Formalin-fixed, paraffin-embedded tissues from 30 fetal (8–24 weeks) and 14 adult cadaveric penile specimens were analyzed. Routine histological stains and immunohistochemical markers targeting neural structures were applied. Serial sections were examined for histology, neuroanatomical mapping, sensory corpuscle characterization, and neural density assessments.

Results: Fetal penile neurodevelopment exhibited two phases: the pre-corpuscular stage (8–16 weeks), marked by axonal hyperinnervation and exuberant ventral intraepithelial nerve fibers, and the corpuscular stage (17–24 weeks), characterized by Pacinian corpuscle emergence and targeted neural pruning. Adult specimens showed region-specific neural distributions, with heightened densities in the frenular delta. Intracorporeally, sensory corpuscles exhibited a bimodal intraspongiosal distribution, with Pacinians in the bulb and glans. Molecular profiles of sensory corpuscles, including novel immunoreactivities, were comprehensively documented. The preputial dartos and vasculature displayed dense autonomic innervation. A superficial glans tunica albuginea was identified, with implications for neural organization.

Discussion: These findings reveal previously unrecognized transitions during fetal penile neural development and into adulthood, providing a foundation for the neurodevelopmental biology of the human penis and documenting the frenular delta's unique innervation. The characterization of penile neural components and the glans tunica

albuginea addresses longstanding anatomical and sexological questions. Our results inform current debates on penile circumcision and neurotomy.

Conclusion: This study provides a comprehensive ontogenetic framework of penile innervation, emphasizing the frenular delta as a specialized center of sexual sensation.

KEYWORDS
foreskin, immunohistochemistry, mechanoreceptors, nerve endings, penis, peripheral nervous system

1 | INTRODUCTION

The human penis functions as a sophisticated sensory organ for sexual stimuli, transmitting signals to spinal centers that mediate sexual reflexes and to supraspinal sites responsible for the subjective experience of sexual sensation and orgasm.[1,2] Although erogenous zones exist throughout the entire body, the penis is the primary peripheral organ for sexual sensation in individuals with this anatomy, because of its specialized structure, including unique nerve fiber types, corpuscular receptors, and central connections that integrate sensory input with arousal and reflex pathways.[3] The frenular delta, which is part of the ventral prepuce, along with the rest of the prepuce and the glans, are the primary erogenous zones of the penis, containing dense neural structures essential for the perception of sexual pleasure.[4–13] Among these regions, the frenular area has long been recognized as a crucial epicenter of penile sexual sensation, generating intensely pleasurable and highly specialized sensations upon stimulation (Table S1).[14–21] More recently, immunohistological studies have revealed the intricate innervation of the developing frenular region during fetal development,[6,22,23] brain imaging has demonstrated unique neural responses to frenular stimulation,[5] and self-reports[4,5,8,9,24] consistently identify it as the primary site of penile sexual sensitivity, collectively reinforcing its fundamental role in the perception of sexual pleasure.

The frenular delta is richly innervated by partially overlapping perineal and dorsal nerve branches (Figure 1A) and by heightened concentrations of nerve bundles and corpuscular receptors.[6,25–27] However, the precise embryological origins of this innervation remain elusive. Insights from the ontogeny of fetal penile innervation are necessary for understanding how these peripheral neural networks develop and specialize for sexual sensation and reflexes (Figure 1B). Additionally, comprehensive visual documentation of the adult frenular delta's neural supply remains lacking, leaving gaps in our understanding of the precise distribution, density, and organization of its innervation.[28] The so-called genital corpuscles, enigmatic mechanosensory end organs associated with sexual sensation and long documented in the prepuce,[29–36] are especially dense in the frenular region.[6,13] However, their immunohistology remains largely unexplored, particularly regarding the structure and role of their capsular cells and the molecular composition of their axons.

The most comprehensive study on glans sensory innervation to date was conducted by Halata and Munger in 1986 using silver impregnations and electron microscopy.[13] They reported a 10:1 ratio of free nerve endings (FNEs) to sensory corpuscles, with genital corpuscles concentrated along the corona and frenular region, FNEs in almost every dermal papilla, no innervated Merkel cells, and low densities of Pacinian corpuscles in the glans corpus spongiosum. Although detailed, their results were primarily focused on corpuscular receptors, and the lack of low-power microphotographs in their study limits the ability to evaluate overall neural distribution and tissue organization. More advanced research is needed to better elucidate the innervation and structure of the glans and their role in sexual function, particularly using modern immunohistological techniques. A precise understanding of how the dorsal nerves reach the glans lamina propria remains unclear, particularly regarding whether they perforate a superficial tunica albuginea rich in elastic fibers[39–41] (Figure 1C) or if this structure is absent, as suggested by standard histology and uropathology textbooks.[13,42,43] Although the glans is commonly regarded as the distal extension of the corpus spongiosum (a view that has been questioned),[44] relatively little is known about the sensory properties of the corpus spongiosum proximal to the glans and of other erectile tissues, such as the corpora cavernosa.

Recent immunohistochemical studies on preputial innervation[6,45,46] have built on previous foundational work,[11,12] offering greater detail on the sensory corpuscles, FNEs, nerve bundles, and their molecular profiles within the prepuce. Beyond its rich sensory innervation, the prepuce contains a dense layer of smooth muscle forming its central axis (dartos),[6,11,42] with its innervation described by Bourlond and Winkelmann,[47] Perez Casas et al.,[48] and Cepeda-Emiliani et al.[6] The preputial dartos is continuous with the proximal penile dartos (peripenic muscle of Sappey) and the scrotal dartos. Although some bundles of the penile dartos muscle are located at the coronal sulcus, the vast majority are confined to the prepuce.[11] The preputial dartoic innervation suggests that the dartos smooth muscle is neurally equipped to carry out complex physiological functions, enabling controlled contractions that contribute to penile skin tension, elasticity, and responsiveness during sexual activity. However, no studies to date have investigated the physiological properties of the preputial dartos, despite its likely role in preputial and penile physiology and regulating penile skin tone.

The detailed investigation presented in the current study provides a comprehensive histological and immunohistological examination of key topics in contemporary penile research, addressing each of the aforementioned areas in depth. The following

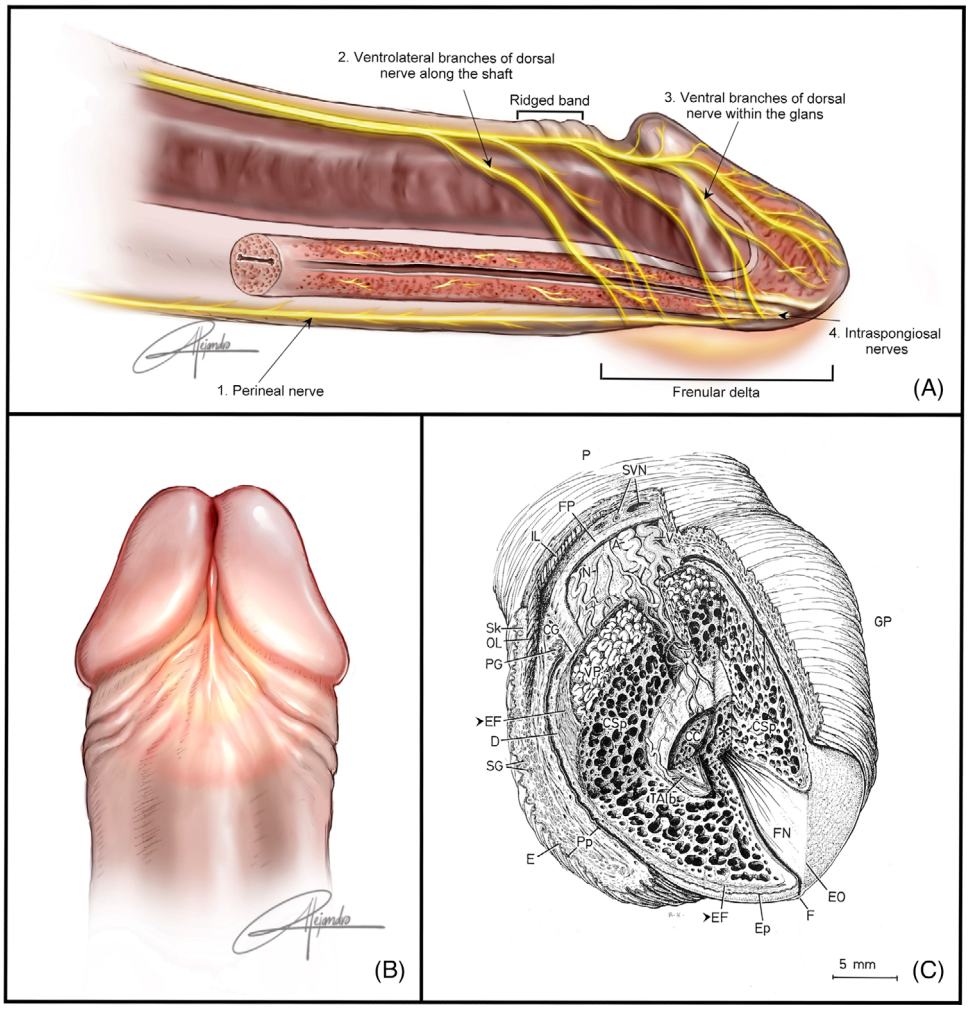

FIGURE 1 Innervation of the frenular delta and microanatomical organization of the glans and prepuce. (A) The frenular delta is innervated by the overlap of the perineal nerve, ventrolateral branches of the dorsal nerve along the shaft, and ventral branches of the dorsal nerve within the glans corpus spongiosum. This unique pattern of nerve convergence likely results in heightened densities of nerve bundles, corpuscular receptors, and free nerve endings (FNEs) in this region, contributing to the specialized sexual sensations and responses associated with the frenular delta. The illustration is not intended to be anatomically exact but rather to convey a concept of penile innervation in a simplified manner to enhance understanding of the frenular delta's sensory significance. Thus, anatomical dissections reveal a complex three-dimensional branching of the dorsal nerve within the glans, with ventral branches supplying the frenular area.[86] This contrasts with the two-dimensional branching of the ventrolateral dorsal nerve along the tunical shaft surface.[86] In anatomical dissections,[110] these branches display a horsetail-like arrangement as they spread ventrodistally, emitting intraspongiosal perforators (not illustrated) that supply the anterior and distal urethra at the frenular level,[86–89] further contributing to the complexity of penile innervation in this region. Kinsey[17] (Table S1) suggested that distal deep urethral innervation contributes to the sensations of sexual reward associated with this penile region. (B) Anatomy of the frenular delta in a frontal view depicting the V-shaped or inverted Y-shaped delta into which the ventral prepuce and frenulum typically retract.[10] This region is widely reported by men as the primary source of penile erogenous sensation, reflecting its significant role in sexual arousal and response.[4, 5, 8, 9, 24] However, the illustration is not intended to precisely map the anatomy to somatosensory perceptual experience, and this penile pleasure center may cover a more diffuse region within the distal third of the ventral penile aspect and deeper spongiosal and distal urethral regions, as suggested by Kinsey.[17] The experimental practice of penile selective neurotomy, discouraged by urological guidelines,[123] targets the perineal nerve and ventrolateral branches of the dorsal nerve at the frenular level, posing a high risk of permanently impairing this erotogenic center. It also risks damaging the urethral perforating branches that originate from the ventrolateral dorsal nerve. Deep ventral circumcision incisions can cause similar sensory damage.[28] Additionally, circumcision can cause proximal displacement of this penile center of sensation toward the middle third of the ventral penile aspect, as supported by a recent survey study.[37] This concept aligns with classical theorizations by Bryk[38] of post-circumcision proximal relocation of penile erogenous zones, with speculations by Schober et al.[8] on post-circumcision penile dermatomal migration, and partially with Zaliznyak et al.'s[37] speculation that circumcision induces neural rewiring of the penis. (C) India ink drawing by Krstić[40] of the microanatomical organization of the human penile glans and prepuce. The scale bar is part of the original drawing. Note the elastic fiber (EF) layer (arrowheads) parallel to the glans epithelium, situated between the dermis (D) and corpus spongiosum (CSp) of the glans. Elastic fibers delaminate radially into the underlying spongiosal connective tissue. Krstić stated (p. 384): "The dermis (D) of the glans is very rich in nerve endings, genital corpuscles, and EF; these fibers are disposed as an entire elastic layer immediately enveloping the CSp of the glans. The elastic layer has been partly removed to show the extensively developed venous plexus (VP) of the CSp from the exterior." Despite detailed characterization and illustration of this superficial EF layer in the

subsections of this introduction synthesize the key elements from all these lines of research, providing a theoretical and conceptual framework that sets the stage for the detailed findings presented in Section 3.

1.1 | Ontogeny of human penile innervation and its role in sexual sensation: mapping axonal guidance, pruning, and gradient-driven pathways

Neurodevelopmental studies on fetal penile innervation are limited, with only a few employing light microscopic immunohistology[23,49–55] and laser scanning confocal microscopy.[22] Although the data remain sparse and fragmentary, orderly pattern and underlying coherence can be extracted from the available findings. From approximately 8–9 weeks of fetal age to the fully developed fetal penis, innervation appears to show a bias toward the distal ventral aspect, where greater neural densities are observed, initially because of numerous branches of the dorsal nerve extending into this region. Aksel et al.,[22] using protein gene product 9.5 (PGP9.5), provided detailed visualizations of these dense ventral branches of the dorsal nerve throughout 9–12 weeks of fetal age in both the fetal penis and clitoris (see their Figures 8A and 9A).

As the penile urethra forms in the ventral aspect, the ventral mesenchyme of the urethral folds embracing the open urethral groove also carries a dense supply of axons.[22,56] As urethral formation extends into the glans region, this dense ventral axonal supply overlaps with the innervation derived from the ventral branches of the dorsal nerve, further increasing the innervation density in the distal ventral region. This fetal penile region corresponds to the prospective frenular region and, in the adult intact penis in the classical anatomical position (penis erect and prepuce retracted),[57,58] to the distal third of the ventral penile aspect. Thus, in our previous immunohistochemical study[6] based on fetal and adult data, we hypothesized that this region represents a convergence zone for branches of all penile extracorporeal nerves, with significant implications for penile sexual sensation. This dense ventral somatosensory nerve supply (Figure 1A) likely enhances the acute perception of sexual sensation in this area (Figure 1B). This neurodevelopmental process could serve as a hypothetical embryological basis for the innervation overlap between dorsal and perineal nerves documented in this penile region by electrophysiologists.[26,27]

In addition to the fetal ventral branches of the dorsal nerve, we previously demonstrated the presence of age-dependent exuberant PGP9.5$^+$ and pan-TRK$^+$ intraepithelial nerve fibers within disproportionately thickened epithelial sheets of the fetal ventral prepuce and future frenulum.[6] In that study, we observed a proportional relation between fetal penile epithelial thickness and underlying stromal neural densities, which was strikingly pronounced ventrally, suggesting that ventral epithelial thickness and epithelial-neural interactions in general play a central role in penile neurodevelopment.

A general theoretical framework to explain these phenomena, grounded in principles of neurodevelopmental biology,[59] suggests that throughout penile morphogenesis, intermediate and final target tissues of developing penile nerves produce neurotrophic and/or neurotropic molecules with short- and/or long-range chemoattractant effects on penile nerves. These molecules may include nerve growth factor (NGF), brain-derived neurotrophic factor (BDNF), neurotrophin-3 (NT-3), glial cell line-derived neurotrophic factor (GDNF), and morphogens such as bone morphogenetic proteins (BMP) and Sonic hedgehog (Shh), along with canonical axonal guidance molecules like netrins, semaphorins, ephrins, and Slit-Robo ligands, which establish gradients to direct axonal growth and targeting.[59–62] Although neuronal pathfinding mechanisms in the penis remain unknown, it appears that throughout urethral formation, the proliferating ventral thickened epithelia and underlying stroma may secrete higher concentrations of specific axonal guidance ligands, establishing gradients that interact with axonal receptors and contribute to the observed ventral innervation bias. The selective upregulation of specific axonal receptors could further refine this targeted innervation pattern.

Additionally, other established principles of neural development, such as initial axonal hyperinnervation, subsequent axon pruning, and refined postnatal innervation (documented processes in other parts of the nervous system, including brain and spinal cord), provide a working hypothesis for understanding the maturation of neural networks in penile tissue.[56,59–62] An initial excessive overgrowth of nerve fibers (hyperinnervation) ensures a robust network of connections between neurons and target cells, serving as a preparatory phase that provides a rich substrate from which exuberant fibers are selectively eliminated (neural pruning). This process, often driven by competition for

glans, its existence remains controversial in contemporary literature. Major studies[13] and standard histology textbooks[42] fail to document this layer, whereas a recent study[39] supports its existence. Scattered sebaceous glands (SG) are predominantly restricted to the dermis of the outer prepuce, whereas the existence of preputial glands (PG) near the coronal sulcus and frenulum, often described as Tyson's glands, has not been demonstrated. Also note the outer (OL) and inner (IL) layers of penile skin smooth muscle bundles (dartos) extending into the prepuce (Pp). Krstić noted that the OL and IL contain circularly and longitudinally oriented smooth muscle, respectively. The smooth muscle of the preputial dartos layer has also been described as having a mosaic-like, whorled, or plexiform pattern, with a circular or transverse sphincteric configuration distally. The EFs in the spongiosal connective tissue (CSp) are typically more pronounced under light microscopic observation than illustrated. Complexities of the glans fibrous skeleton, including the distal or corporoglans ligament (a direct extension of the distal cavernosal tunica albuginea), are not depicted in Krstić's drawing, although they are easily observed during gross inspection. "*" end portion of the pars spongiosa urethrae. A, arteriae; CC, corpora cavernosa; CG, corona glandis; CSp, corpus spongiosum; D, dermis; E, epidermis; EF, elastic fibers; EO, external orifice; EP, epidermis; F, frenulum praeputii; FN, fossa navicularis; FP, fascia penis; GP, glans penis; IL, inner layer smooth muscle cells; N, nervi dorsalis penis; OL, outer layer smooth muscle cells; P, penis; PG, preputial glands; Pp, prepuce; SG, sebaceous glands; SK, skin; SVN, superficial dorsal blood vessels and nerves; TAlb, tunica albuginea; V, venae; VP, venous plexus. *Source*: Reproduced with permission from Springer Nature.

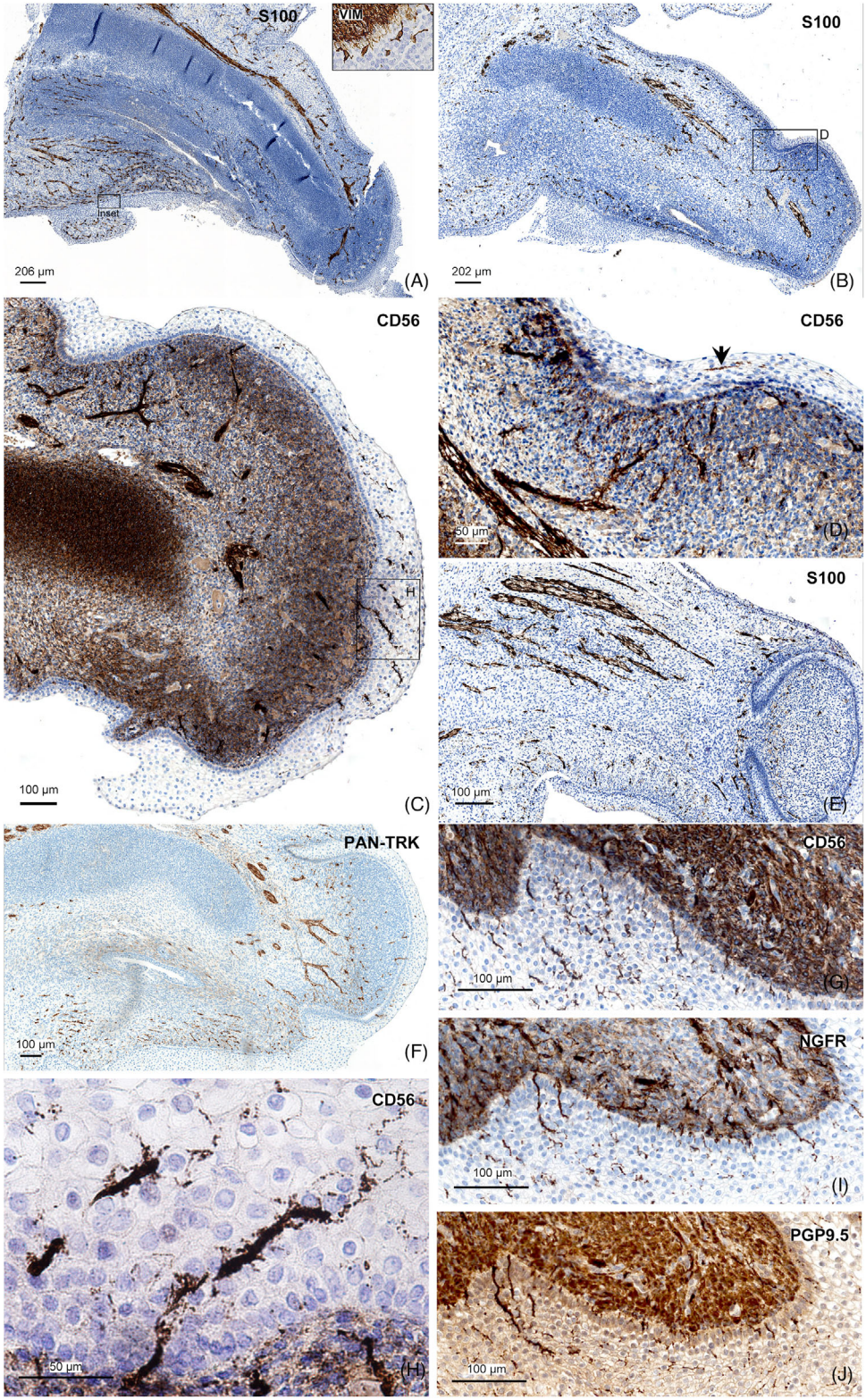

FIGURE 2 Early human fetal penile neurodevelopment in six sagittally sectioned specimens. Pre-corpuscular stage of penile neurodevelopment. Approximate fetal ages: 8 (A), 10 (B and D), 10 (C and H), 12 (E), 12 (F), and 12 (G, I, and J) weeks. (A) An 8-week specimen displays a prominent S100^{+} dorsal nerve branch coursing dorsal to the mesenchymal hypercellular condensation of the developing corpora cavernosa. This branch gives rise to numerous perpendicular projections dorsally and penetrates the glans mesenchyme, where it descends and radiates multiple fan-like branches, terminating ventrally near the prospective frenulum. No epithelial or mesenchymal remodeling indicative of early prepuce formation is evident at this stage. Notably, the blood vessel-rich ventral stroma surrounding the developing urethra exhibits a very dense network of thinner S100^{+} nerve fibers. Neural fibers contact the basal epithelial surfaces, although intraepithelial nerve fibers are scarce at this age. The inset in the upper right corner, located approximately 20 µm lateral to the corresponding small rectangle, shows intraepithelial VIM^{+}

neurotrophic factors, ensures the retention and refinement of the most functional connections. Whether this sequence of hyperinnervation, pruning, and refinement occurs in the fetal penis remains an open question, a hypothesis further explored and supported in our study.

Further investigation of these fetal developmental phenomena is crucial for deepening our understanding of penile neurodevelopment and its implications for sexual sensation and function. Exploring the specific axonal guidance cues and receptor–ligand interactions that govern the spatial distribution of adult penile nerves may provide valuable insights into the mechanisms underlying sexual sensation, particularly in the frenular area. These findings may also inform approaches to penile surgeries that enhance sexual health outcomes and uncover mechanisms underlying congenital penile abnormalities, such as hypospadias. The identification of molecules involved in penile axonal pathfinding could reveal their possible dual role in establishing functional neural circuits and contributing to such conditions. This aligns with the hypothesis by Aksel et al.,[22] who suggested that disruptions in neurovascular ontogeny may underlie the development of human hypospadias.

1.2 | Penile sensory corpuscles and their molecular profiles: genital-specific corpuscles of sexual sensation and CD10 in Pacinian corpuscles

As fetal penile development progresses into postfetal stages, preputial and glans axons, guided by intrinsic and extrinsic molecular cues, reorganize with Schwann cells to form complex multicellular structures known as sensory corpuscles or low-threshold mechanoreceptors (with limited data on these molecular cues in human development). These structures, also referred to as corpuscular receptors or neuroreceptors, sensory end organs, or sensory nerve formations, begin to develop at an unknown fetal age in the penis. Classical sensory corpuscles include Meissner, Pacinian, Ruffini, and Golgi-Mazzoni corpuscles. The so-called mucocutaneous end organs,[63–66] Krause corpuscles, and genital corpuscles belong to a family of sensory corpuscles traditionally associated to sexual sensation, making them of particular interest.[67,68]

Notably, as early work by Ramón y Cajal,[30] Dogiel,[29] Ohmori,[31] and others[32,34,36] demonstrated, genital corpuscles are a normal and well-documented component of preputial sensory innervation.[6,42,68] Pacinian corpuscles, which detect vibration (a stimulus known to correlate positively with sexual function[69]), are also a consistent feature of preputial innervation, as repeatedly reported in the vast majority of studies on preputial sensory corpuscles. Even in studies with minimal sample sizes, such as De Girolamo and Cecio[36] ($n = 1$) and Bläuer et al.[70] ($n = 3$), preputial Pacinians are readily documented, underscoring how easily these structures are recognized in preputial tissue.

Sensory corpuscles generally share a common structural pattern or theme, consisting of sensory axons enriched with axolemma Piezo2 expression and protruding spine-like cytoplasmic processes.[71] These axons and their spines are closely associated with variably arranged Schwann or lamellar cells, which are also responsive to mechanical stimuli.[72] Together, the axons and Schwann cells are encased in a connective tissue capsule that may be complete, partial, or absent. This functional organization suggests a bi-cellular mechanism for touch detection, involving coordinated interactions between the axon and lamellar cells.[72] Penile sensory corpuscles and FNEs represent points of afferent origin for reflex arcs related to erection and ejaculation.[2] The literature suggests that penile sensory corpuscles are most concentrated in the frenular delta and region,[6,13,25] with additional high densities in the preputial ridged band[11,12] and glans corona,[13] and a gradual decrease in density toward proximal penile regions. Similarly, the nerve bundles supplying these corpuscles may follow a ventral-to-dorsal and distal-to-proximal density gradient, with higher densities observed ventrally and distally.[6,25]

Although these mechanosensory structures have been observed in the human penis since the late 19th century with silver impregnation techniques,[29,31] few studies provide detailed immunohistochemical data on human penile sensory corpuscles.[6,11,12,42,45,46,70,73–78] In the penis, the axons of sensory corpuscles express markers such as neurofilaments (NFs), neuron-specific enolase (NSE), PGP9.5, and pan-TRK, whereas Schwann or lamellar cells express Wilms' tumor protein (WT1), S100, CD56, nestin, vimentin, Bcl-2, and SOX10, with their

spindle- or dendritic-shaped cells originating from the underlying mesenchyme. (B) A 10-week specimen shows the emergence of the glans-shaft junction and early prepuce formation dorsally, marked by increased concentrations of subepithelial nerve fibers (as further detailed in nearby section D). (C) 10-week specimen with intensely stained $CD56^+$ intraepithelial nerve fibers of varying diameters within the distal glans. Diffuse background staining is observed throughout the glans mesenchyme, with intraepithelial nerve fibers detected in the most superficial epithelial layers. $CD56^+$ subepithelial neural densities are noted dorsally at the developing glans-shaft junction, similar to (D). (D) Located approximately 182 μm lateral to the corresponding rectangle in B, this section shows $CD56^+$ nerve fibers ascending perpendicularly toward the glans-shaft junction from a thicker dorsal nerve branch in the lower left corner. Low levels of intraepithelial nerve fibers are noted (arrow). (E) 12-week specimen sectioned lateral to the midline, where the corpora cavernosa and urethra are out of the plane of section. Numerous thick $S100^+$ dorsal nerve lateral branches extend toward the glans and prepuce. Postnatally, these lateral branches exhibit the characteristic horsetail-like pattern as they spread ventrodistally, as described in Figure 1A. (F) A 12-week specimen reveals pan-TRK^+ dorsal nerve branches terminating in the ventral glans near the future frenulum, with independent pan-TRK^+ dense axonal contingents traveling ventrally beneath the urethra. The ventral penile epithelium begins to show disproportionate thickening associated with underlying dense ventral neural densities. As part of natural interspecimen variability, elevated levels of intraepithelial nerve fibers were observed in the ventral prepuce of other specimens of the same age, evidenced by $CD56^+$ (G), $NGFR^+$ (I), and protein gene product 9.5 ($PGP9.5^+$) (J) intraepithelial nerve fibers in the same region. (H) Higher magnification of the rectangle in C, providing detailed visualization of the peripheral axon branching pattern of these intraepithelial fibers, characterized by laterally extending fibers emerging from parent axons.

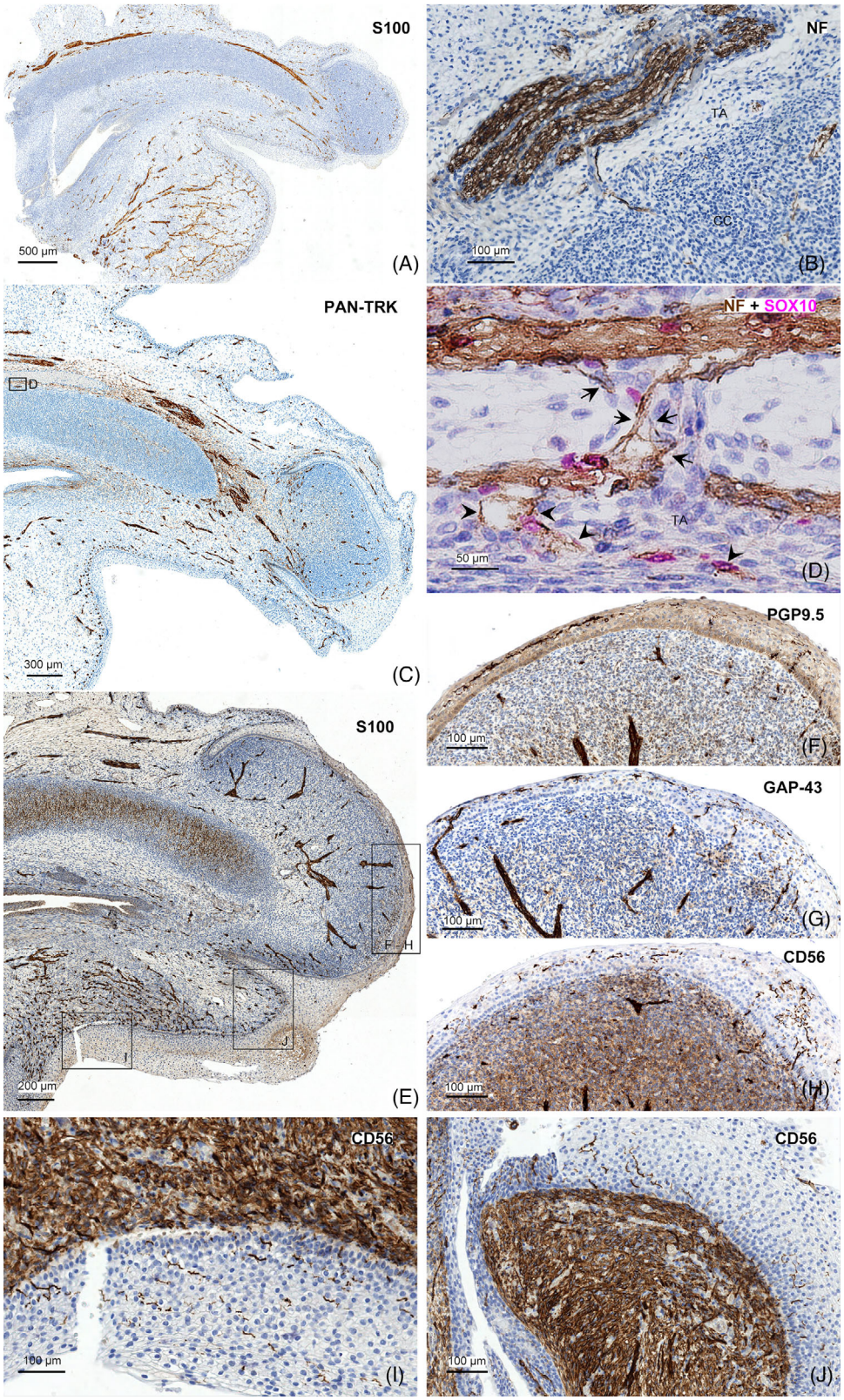

FIGURE 3 Neurodevelopmental processes in four sagittally sectioned human fetal penile specimens. Pre-corpuscular stage of penile neurodevelopment. Approximate fetal ages: 12 (A), 13 (B), 14 (C and D), and 12 (E–J) weeks. (A) A 12-week specimen displaying dense $S100^{+}$ perineal nerve arborizations in the scrotum, along with a prominent dorsal nerve branch that provides innervation to the dorsal prepuce before entering the glans. The dorsal nerve branch courses ventrally (partly out of the plane of section) and terminates near the future frenulum. The early ventral prepuce and proximal ventral penile region show a rich density of nerve fibers (partially out of the plane of section). Note the contrast between the thicker ventral penile and scrotal epithelia and the thinner dorsal preputial and dorsal proximal penile epithelia. (B) A thin neurofilament (NF^{+}) nerve fiber from a 13-week specimen defasciculates from a thick dorsal nerve branch, perforates the developing tunica

basal lamina composed of collagen type IV (COL-IV). The outer core of preputial Pacinian corpuscles expresses the perineurial markers glucose transporter 1 (Glut-1), epithelial membrane antigen (EMA), vimentin, and COL-IV, whereas the intermediate layer between the inner and outer cores expresses CD34. Thus, the Pacinian Glut-1$^+$ and EMA$^+$ outer core is considered an extension of the Glut-1$^+$ and EMA$^+$ peripheral nerve perineurium, whereas the CD34$^+$ intermediate layer is considered an extension of the CD34$^+$ endoneurium. In dermal papillae, the capsules of penile sensory corpuscles variably express the endoneurial marker CD34 but typically lack perineurial markers. However, it remains unclear whether the capsules of deep-dermal preputial genital corpuscles also express perineurial markers like Glut-1 or EMA.

Current data likely capture only a very small fraction of the potential immunoreactivities within sensory corpuscles. With their high densities in the penis and limited immunohistochemical data available, penile tissues offer a valuable opportunity to expand our knowledge of the molecular profiles of sensory corpuscles. Penile sensory corpuscles may reveal unique regional and organ-specific specializations, shedding light on the diversity of these structures and the functional specialization required for precise sensory processing related to sexual sensation.

1.3 | CD10 expression in Pacinian corpuscles

CD10 is a 100 kDa single-pass transmembrane cell surface glycoprotein and a key endopeptidase involved in the inactivation of peptides that regulate cell differentiation.[79] CD10 functions as an ectoenzyme, acting on a large diversity of extracellular substrates to facilitate their breakdown or degradation.[80] These substrates include neuropeptides such as substance P and calcitonin gene-related peptide, as well as various secreted, circulating, or membrane-associated peptides. Through these functions, CD10 has been implicated in a variety of physiological and pathological processes, including fetal development, tissue morphogenesis, stem cell regulation, oncogenesis, and Alzheimer's disease.[81] To the best of our knowledge, CD10 expression in sensory corpuscles has not been previously evaluated, although it has been reported in peripheral myelin and perineurium using immunohistochemistry.[82–84] Recent in-house, previously unpublished analyses by our group, using two Dako-Agilent CD10 antibody clones (DAK-CD10 and 56C6) on human adult glans and preputial tissues, revealed that Pacinian corpuscles in these regions typically express CD10 in the outer core lamellar cells. This novel immunoreactivity, along with its distinct staining pattern and potential physiological significance for Pacinian structure, is described for the first time in this study using single and double immunohistology.

1.4 | Intracorporeal sensory corpuscles: exploring the sensory role of erectile tissue

Excluding the glans corpus spongiosum, mechanosensory end organs located deep within the human penile erectile tissues have not been previously described systematically. Traditionally, the corporeal bodies have not been regarded as sensory tissues, with greater emphasis placed on the autonomic and local molecular regulation of intracavernosal smooth muscle in the motor process of erection. Consequently, the potential functional role of intracorporeal deep sensory inflow from FNEs or sensory corpuscles has been largely overlooked. Cortical responses to forceful penile cavernosal stimulation have been mapped to the deepest portion of the paracentral lobule, suggesting dual sensory innervation of the penis via the pudendal and cavernous nerves.[85] Although the corpus spongiosum is autonomically innervated by pelvic plexus-derived nerve fibers, the ventral branches of the dorsal nerve (Figure 1A) emit perforating sub-branches to the anterior urethra.[86–89] A more detailed histological examination of the corporeal bodies could reveal previously unrecognized somatosensory structures potentially involved in reflex innervation pathways. These neural structures may detect stimuli such as vascular engorgement and pressure changes during erection. In the corpus spongiosum, they might also perceive the passage of semen during ejaculation and urine during micturition, as well as other physiological stimuli.

albuginea (TA), and enters the fetal corpora cavernosa (CC). (C) 14-week specimen with pan-TRK$^+$ dorsal nerve branches distal to the CC that take a ventral course to reach the ventral glans. Dorsal nerve branches entering the dorsal prepuce are clearly visible. The perineal nerve, partially out of the plane of section, is seen ventrally innervating the ventral prepuce and future frenular area. Distal pan-TRK$^+$ intraepithelial nerve fibers are observed within the glandopreputial common epithelium. (D) A section approximately 34 μm medial to the supracorporeal region indicated by the rectangle in C, showing multiple NF$^+$ (brown) neural anastomoses (arrows) between the dorsal nerve (superiorly) and a thinner nerve (inferiorly) adjacent to the tunica albuginea (TA). These neural anastomoses are invested with SOX10$^+$ Schwann cell nuclei (magenta). A tunical perforating nerve branch (arrowheads) is observed emerging from the inferior thinner nerve. The three-dimensional character of the neural anastomoses (arrows) was clearly visualized in our 4 μm sections. (E) A 12-week specimen displaying high ventral S100$^+$ preputial neural density, associated with disproportionate ventral epithelial thickness compared to the dorsal aspect. Dorsal nerve branches are seen entering the dorsal prepuce. Similar to specimens in A and C, as well as Figure 2A,F, a main descending dorsal nerve branch terminates in the ventral glans near the future frenulum, giving off multiple radial branches targeting the glans epithelium. (F–H) Serial sections approximately 22 μm apart from each other in the distal glans tip region indicated in E, showing protein gene product 9.5 (PGP9.5$^+$) (F), GAP43$^+$ (G), and CD56$^+$ (H) intraepithelial nerve fibers. As these intraepithelial fibers approach the epithelial surface, their orientation shifts to run parallel to the surface (F and G), likely because of the presence of the transient overlying periderm layer, which restricts their longitudinal growth. (I) Higher magnification of the ventral region indicated in E, depicting dense CD56$^+$ intraepithelial nerve fibers in an adjacent serial section. (J) Higher magnification of the distal ventral preputial region indicated in E, again showing dense CD56$^+$ intraepithelial nerve fibers, from the same tissue section as I. CC, corpora cavernosa; TA, tunica albuginea.

1.5 | The preputial dartos: ontogeny and innervation of a sexually dimorphic histological layer

The human penile prepuce contains a dense layer of innervated smooth muscle, known as the dartos layer, which forms the central axis of the prepuce between the dermis and lamina propria.[11,42] This muscular formation is embedded within a fibroelastic, highly vascular connective tissue, interspersed with aggregations of nerve bundles. The preputial dartos is sexually dimorphic, as the clitoral prepuce lacks a layer of smooth musculature,[11,90] suggesting that the dartos plays specialized functional roles in the penis. Histologically, the dartoic muscle bundles exhibit varied orientations, forming mosaic-like,[91,92] whorled,[91] or plexiform[6] patterns, which transition to a circular or transverse sphincteric configuration distally.[11,42]

The dartos is richly innervated by FNEs and dense varicose neural plexuses intimately associated with the smooth myocytes and adjacent blood vessels, suggesting en passant synapses that enable neurotransmitter release along the nerve fibers.[6,47,48] This neuromuscular network or "autonomic ground plexus"[93] can be visualized using markers such as CD56, NSE, tyrosine hydroxylase (TH), and neuronal nitric oxide synthase (nNOS), with nNOS marking the least dense population of dartoic nerves, whereas the other markers reveal more abundant innervation.[6] The presence of TH and nNOS suggests a degree of possible dual autonomic regulation of preputial smooth muscle.[6] However, the complete neurochemical profile of this neuromuscular supply has yet to be fully elucidated. Other molecules associated with autonomic function, such as vasoactive intestinal peptide (VIP) and neuropeptide Y (NPY), may contribute to the regulation of dartoic smooth muscle as modulatory cotransmitters, but their expression has not yet been examined.

Although the preputial dartos can be readily visualized early in fetal development using immunohistochemistry and smooth muscle actin (α-SMA) antibodies,[6,90] its detailed ontogeny remains largely uncharted. This lack of comprehensive research leaves significant gaps in our understanding of this anatomical structure. More research is needed to clarify the development and functional roles of the preputial dartos in penile physiology, particularly its contributions to sexual sensation, penile skin mechanics, and its involvement in preputial and penile pathologies, as well as complications arising from circumcision.[94]

1.6 | Tunica albuginea of the glans: revisiting an unresolved anatomical question

Regarding the basic anatomy and histology of the glans, an unresolved issue is whether the glans corpus spongiosum is surrounded superficially by a tunica albuginea encapsulating the glans erectile tissue. Two schools of thought have addressed this question. In his seminal illustrations (Figure 1C), Krstić[40] implicitly supported a model that organizes the histological layers of the glans into four distinct levels from superficial to deep: (i) epithelium, (ii) lamina propria, (iii) an elastic fiber-rich layer, and (iv) the corpus spongiosum of the glans. According to Krstić,[40] the elastic fiber layer completely envelops the glans corpus spongiosum. Szymonowicz and Krause,[41] in their classical treatise on human histology, also described a distinct layer of elastic fibers traversing the surface of the glans and its connections to fascicles of elastic fibers within the underlying glans corpus spongiosum. Lee et al.[39] recently provided macroscopic and histological evidence supporting this four-layer model, identifying an irregular tissue level rich in elastic fibers between the glans lamina propria and spongiosal tissue (see their figures 4 and 5). This layer was perforated by dorsal nerve branches that formed fine reticular neural networks in the lamina propria. In the model proposed by Lee et al.,[39] the elastic fiber-rich layer is designated as the glans tunica albuginea and corresponds to the superficial elastic fiber layer described by Krstić[40] (Figure 1C) and Szymonowicz and Krause.[41] The unstated rationale for designating this layer as the "tunica albuginea" appears to be its anatomical continuity with the corporeal tunica albuginea via the distal or corporoglans ligament, as well as the observation that the cavernosal and spongiosal erectile tissues are typically enveloped by a tunica albuginea.

The other school of thought is that the glans lacks a tunica albuginea. Halata and Munger[13] and Velazquez et al.[42] describe a model of the glans histological layers with three levels from superficial to deep: (i) epithelium, (ii) lamina propria, and (iii) corpus spongiosum, with a smooth transition or blending between the lamina propria and corpus spongiosum. This model contrasts with the four-layer model that includes an elastic fiber-rich layer, or tunica albuginea, between the lamina propria and corpus spongiosum. Clarifying whether the glans possesses a tunica albuginea could enhance our understanding of the structural and functional properties of the glans and its sensory innervation. Such insights may help elucidate physiological phenomena related to the erectile tissue of the glans, improve our understanding of anatomical factors influencing the distribution of nerve endings and the spread of penile cancer, and contribute to resolving long-standing anatomical issues.

1.7 | Aims

The primary aims of this extensive study were to provide comprehensive histological and immunohistological evidence across all of the aforementioned areas using formalin-fixed and paraffin-embedded (FFPE) tissues, integrating previously fragmented lines of research to create a unified understanding of this complex anatomy.

2 | MATERIALS AND METHODS

This research adhered to Spanish legislation and the 1964 Helsinki Declaration and its subsequent amendments and was conducted with prior approval by the Santiago-Lugo Research Ethics Committee (code 2021/179).

2.1 | Fetal specimens

Thirty normal fetal penile specimens, aged approximately 8–24 weeks (mean: 16 weeks, SD: 5), were obtained with informed consent from the Pathology Department of the University Clinical Hospital of Santiago de Compostela, following either elective pregnancy terminations or spontaneous abortions, as well as fetal autopsies. All fetuses were fixed in 10% neutral buffered formalin, most for several days before examination. None were macerated, and none exhibited gross caudal malformations or features suggestive of syndromic conditions affecting genital development. Congenital anomalies unrelated to the urogenital system[95,96] were present in approximately half of the cases (n = 17): four with central nervous system defects (hydrocephalus, anencephaly, and trisomy 21 in two), three with complex cardiac defects (tetralogy of Fallot in two and hypoplastic left heart), and the remaining 10 with isolated minor anomalies, including cleft lip and/or palate, polydactyly, syndactyly, and limb malformations. Fetal ages were estimated based on foot length measurements, following Cunha et al.,[23,97] using the estimated time of fertilization as the reference. Genetic sex was determined in 24 specimens, including the youngest, by polymerase chain reaction of cell-free fetal DNA from maternal blood samples. Access to de-identified patient clinical histories enabled these determinations. Gonadal sex was confirmed by identifying testes in sufficiently mature specimens. Histological evaluation defined the penile anatomy as normal if the glans, corpora cavernosa, corpus spongiosum, urethra, and scrotum were present in normal positions and exhibited age-appropriate morphology,[90] irrespective of congenital malformations elsewhere. All specimens met these anatomical criteria. Most penile specimens were part of larger fetal pelvic specimens embedded in paraffin en bloc, containing variable extra-penile structures such as the scrotum, pubic bone, prostate, urinary bladder, seminal vesicles, testes, pelvic plexus, distal colon, caudal spinal cord, dorsal root ganglia, sympathetic chain, and vertebral column. These additional tissues are being analyzed in parallel investigations by our group. For this study, the focus was on penile specimens sectioned in sagittal (n = 10), coronal (i.e., frontal) (n = 10), and transverse (n = 10) planes.

2.2 | Adult cadaveric specimens

Fourteen adult cadaveric penile specimens were included in this study, all donated to the Body Donation and Dissecting Room Center of the Complutense University of Madrid for educational and research purposes. The mean age of the donors at death was 68 years (range: 45–96 years, SD: 18). Among these, 11 complete, normal, intact (non-circumcised) penile specimens were obtained from fresh cadavers and immersion-fixed in 10% neutral buffered formalin for several days after grossing to ensure optimal fixative penetration. Additionally, three normal, intact penile specimens were retrieved from embalmed cadavers aged 51, 63, and 96 years. These cadavers had been fixed approximately 2 months prior to specimen collection via femoral arterial perfusion with an ethanol-based embalming mixture (PanReac Applichem, product code 214632.0716). The tissue morphology of these specimens was optimal for evaluation. Preliminary analyses conducted by us demonstrated that this fixative provided optimal preservation of the critical tissue antigens essential for this study, ensuring suitability for immunohistochemistry. A polymer-based (EnVision) method with heat-induced epitope retrieval (HIER) at high pH, as routinely performed in our pathology laboratory, was effective for these specimens. Although HIER is traditionally used with FFPE tissue, its application to alcohol-fixed tissue enhanced staining specificity, reduced background, and maintained excellent morphology and signal intensity. These observations align with findings by Cizkova et al.,[98] who documented similar benefits of HIER for alcohol-fixed cytological samples.

The time between death and fixation did not exceed 24 h in any case. Except for two donors with unknown causes of death and one with metastatic prostate cancer, the causes of death were unrelated to the genitourinary system. No external genital abnormalities or history of penile surgery were identified, confirmed by gross inspection. The penile specimens included the prepuce, glans, midshaft, proximal penis, penile root (including crura and bulb), portions of the suspensory apparatus, and fragments of the bulbospongiosus muscle. Seven specimens were fixed with the prepuce covering the glans, whereas the remaining seven were fixed with the prepuce retracted or partially retracted. Transverse sections of the midshaft and bulbar urethras were obtained from all specimens. In eight specimens, the glans region was sectioned transversely, whereas sagittal sections from the glans region were obtained in the remaining six. Additionally, separate fragments of preputial tissue were collected from all specimens.

2.3 | Routine and special stains

All fetal and adult tissues were dissected, placed into standard or Supa Mega (Cell Path, EAO-0102-02A) cassettes, and processed overnight using an automated system before paraffin embedding. Four-µm-thick serial and semi-serial sections from each block were prepared for basic histological analysis. These sections were stained with hematoxylin and eosin (H&E) using a Dako-Agilent CoverStainer, as well as with Masson's trichrome (MT), elastic fiber stain, and reticulin fiber stain kits using the Dako-Agilent Artisan Link Pro Special Staining System. The elastic fiber stain, a modification of Verhoeff's stain, utilizes Van Gieson solution as a counterstain to differentiate collagen (red) from elastin (black). The reticulin stain highlights reticulin fibers, a form of immature connective tissue primarily composed of type III collagen. Reticulin fibers are abundant in fetal and embryonic tissues, with their density significantly decreasing in adult tissues. In adults, they are predominantly localized to structures such as basement membranes, smooth and skeletal muscles, peripheral nerves, blood vessels, liver, spleen, bone marrow, and kidneys. Both elastic and reticulin fibers stain black with these specialized techniques.

2.4 | Single and double immunohistochemistry

Four-μm-thick serial and adjacent sections from each tissue block were also mounted on FLEX IHC microscope slides (Dako-Agilent). Immunostaining was performed using an Autostainer Link 48 (Dako-Agilent) and the EnVision FLEX detection system (Dako-Agilent), following the manufacturer's instructions. Pretreatment was performed in a PT Link module (Dako-Agilent) for 20 min prior to staining. The protocols involving overnight incubation of primary antibodies (nNOS, NPY, TH, and VIP) were performed manually up to the incubation step and then completed using the Autostainer Link 48. Tissue antigens were visualized with EnVision FLEX/HRP diaminobenzidine and EnVision FLEX/HRP magenta chromogen solutions (Dako-Agilent). The full list of antibodies is detailed in the subsequent section.

Approximately 100 to 300 sections per specimen were examined by light microscopy. The sections were obtained from a single paraffin block for fetal specimens or from multiple paraffin blocks for adult specimens. Every 10th–14th section was used for routine and special stains, with selected intervening sections reserved for single and double immunohistology. The fetal paraffin blocks at the penile level were fully sectioned and examined without discarding any tissue. Numerous unstained slides from each specimen were stored at −20°C for parallel and future investigations.

2.5 | Antibodies

A comprehensive antibody battery was employed in this study to target a wide range of peripheral neural and associated structures, including axonal and non-axonal components of sensory corpuscles, perineural and endoneurial regions of peripheral nerves, and vascular and smooth muscle elements. Briefly, axonal markers included NF, PGP9.5, Pan-TRK, growth-associated protein 43 (GAP-43), and NSE; Schwann cell markers included S100, SOX10, nestin, Bcl-2, NGFR, and CD56; perineurial and endoneurial markers included EMA, Glut-1, COL-IV, vimentin, and CD34. CD31 specifically labeled vascular endothelium, D2-40 targeted lymphatic endothelium, and TH, VIP, NPY, and nNOS labeled autonomic nerve fibers. Additional markers included α-SMA for smooth muscle and perineurial cells, CD10 for perineurium[82–84] and the outer core of Pacinian corpuscles, and synaptophysin (SYN) as a marker of presynaptic vesicles in axons of mechanosensory endings and unmyelinated fibers. Notably, CD56 and NGFR also label axons. Negative controls without primary antibodies were used. Internal positive controls consisted of known expression sites of the target molecules. External positive controls were employed when necessary. The antibodies, incubation protocols, and antigen retrieval methods are detailed in Table S2, with concise descriptions of each antibody's relevance to the peripheral nervous system and sensory corpuscles provided alongside. The full step-by-step single- and double-staining immunohistochemical protocols are provided in Table S3. For comprehensive backgrounds on the normal and pathological tissue antigens targeted by these antibodies, refer to Chetty et al.,[79] Dako's antibody manual,[99] and Gratzl and Langley.[100]

2.6 | Double immunofluorescence

Double immunofluorescence was performed on selected slides to evaluate the potential colocalization of CD10 with CD34 in the intermediate layer of Pacinian corpuscles. Antibodies and antigen retrieval methods are detailed in Table S2. The protocol utilized heat treatments between staining steps, enabling the use of primary antibodies from the same species for multiple immunofluorescence rounds.[101, 102] This approach involves heat inactivation of the primary antibodies from the initial staining cycle without affecting the fluorescent dyes or diminishing fluorescence intensity. Our laboratory has experience with these methods, routinely employing microwave-assisted heat inactivation between manual staining cycles. This technique was used in the present study. Briefly, CD10 mouse monoclonal antibody (Dako-Agilent, ready-to-use) was incubated for 24 h at 4°C, followed by sheep anti-mouse IgG Fab'2 fragment conjugated with Cy3 (Sigma-Aldrich) at a 1:200 dilution for 1 h at room temperature (RT). Next, a heat treatment was performed in a microwave at 750 W in citrate buffer for 20 min, followed by incubation with CD34 mouse monoclonal antibodies (Dako-Agilent, ready-to-use) for 24 h at 4°C. Alexa 488-labeled donkey anti-rabbit IgG (Invitrogen, Life Technologies Corp) was then applied at a 1:200 dilution for 1 h at RT. Subsequently, the slides were incubated with DAPI nuclear counterstain (Thermo Fisher Scientific, Cat. No. 62248) at a 1:1000 dilution for 10 min at RT. The complete step-by-step immunofluorescence protocol is provided in Table S4.

2.7 | Whole slide imaging and microphotographs

Selected slides were fully digitalized with a PathScan Combi digital pathology scanner (Excilone) in brightfield mode at ×20 magnification. Representative microphotographs were acquired with the PathScan software version 3.0.10. Slides were also examined and photographed using an Olympus BX51 microscope coupled to a digital camera (Olympus DP70).

3 | RESULTS

Findings from fetal specimens are presented according to fetal age, illustrating the progressive stages of penile neurodevelopment and associated morphological processes over time. In contrast, results from adult specimens are presented in a synchronic manner as a snapshot or distillate of the normal adult penile anatomy and histology, divided into specific subcategories of findings. Relevant age-related histological changes were also noted in the adult specimens. A consistent pattern of heightened ventral neural density was identified across both fetal and adult penile specimens.

3.1 | Fetal specimens

Penile innervation patterns in fetal specimens could be broadly divided into two general sequential phases of neurodevelopment, each characterized by consistent age-specific histological and neurohistological patterns:

1. **Pre-corpuscular and hyperinnervation stage (8–16 weeks of fetal age)**: Characterized by an almost complete absence of immature sensory corpuscles, heightened neural densities within mesenchymal and stromal extracorporeal compartments, and exuberant ventral intraepithelial nerve fibers within disproportionately thickened ventral preputial epithelial sheets (Figures 2–4).
2. **Corpuscular and neural pruning stage (17–24 weeks of fetal age)**: Marked by the widespread emergence of developing Pacinian corpuscles across all penile regions, persistent heightened ventral stromal neural densities, evidence of neural pruning, particularly affecting the previously dense ventral intraepithelial nerve fibers, and the thinning of the previously thickened ventral preputial epithelium (Figure 5 and Figures S1–S3).

Penile hypercellularity and the nerve diameter-to-body ratio decreased as development progressed, with younger specimens showing a higher proportion of cells and nerve tissue relative to penile volume compared to older specimens. Reticulin fibers (type III collagen), indicative of tissue immaturity, were consistently arranged in a dense mesh-like network throughout the penile connective tissues across all fetal ages (not shown). Heightened neural densities were observed across the ventral surfaces of the developing penis during both neurodevelopmental phases. The following subsections provide a detailed examination of each stage.

3.2 | Pre-corpuscular and hyperinnervation stage (8–16 weeks)

No developing penile sensory corpuscles were observed in fetal specimens aged 8–16 weeks. However, by the end of this stage, scarce developing Pacinian corpuscles began to appear in select sections of a minority of specimens (inset in Figure 4E). During this stage, the developing corporeal bodies and glans exhibited pronounced hypercellularity, with minimal or absent intracorporeal innervation, smooth muscle content, and vascular spaces (Figures 2A–C,F, 3A,C,E, and 4A,E). In contrast, at 8 weeks, the fetal phallus displayed a highly developed dorsal nerve with prominent fasciculation that fully invaded the glans mesenchyme and branched extensively to reach all basal epithelial targets (Figure 2A). The difference in innervation between the hyperinnervated extracorporeal mesenchymal and stromal tissues and the hypoinnervated developing corpora cavernosa was thus a distinctive characteristic of this stage. Notably, this thick primary branch of the dorsal nerve within the glans mesenchyme was observed in sagittal sections to supply the prospective frenular region ventrally (Figure 2A).

This ventral termination of the dorsal nerve within the glans was consistently observed across specimens of all ages but was more readily identifiable in younger specimens (up to 14 weeks) when analyzed in single sections because of the high nerve diameter-to-body ratio (Figures 2F and 3A,C,E). Simultaneously, at 8 weeks, a distinct and dense contingent of very thin nerve fibers innervated the ventral mesenchyme surrounding the developing urethra (Figure 2A). This ventral nerve supply contrasted with the dorsal innervation in its minimal to absent axonal fasciculation, highlighting a clear difference in neural architecture between these regions.

Intraepithelial VIM^+ spindle- or dendritic-shaped cells, originating from the underlying mesenchyme, were frequently observed at the onset of this stage but became increasingly rare as development advanced (inset in Figure 2A). The early dorsal prepuce began forming at 9–10 weeks through epithelial and mesenchymal remodeling, accompanied by increased subepithelial nerve fiber densities (Figure 2B–D). Sparse intraepithelial nerve fibers were observed during this period (arrow in Figure 2D). From this age onward, varying densities of intraepithelial nerve fibers ($PGP9.5^+$, $NGFR^+$, pan-TRK^+, $CD56^+$, $GAP\text{-}43^+$, and NSE^+) were present across all penile epithelia, often forming interanastomosing networks. These epithelia included the preputial and distal glans epithelia, the glandopreputial common epithelium (located between the glans and prepuce), the urethral epithelium, the epithelium of the developing urethral glands, and the scrotal epithelium. Significantly lower levels of intraepithelial nerve fibers were observed with SYN, NF, and S100.

By 10 weeks, intraepithelial nerve fibers were prominent in the distal glans, and subepithelial neural concentrations persisted at the developing glans-shaft boundary (Figure 2C,H). Additionally, a profusion of thick lateral $S100^+$ dorsal nerve branches, extending toward the prepuce, glans, and ventral aspects, was readily identified lateral to the midline (Figure 2E). These branches represent the future ventral extensions of the dorsal nerve in the adult. By 12 weeks, the ventral preputial epithelium acquired a thickness of up to 30 cell layers and was consistently associated with dense subepithelial stromal neural densities (Figure 2F). A proliferation of intraepithelial nerve fibers began to populate the thickening ventral preputial epithelium (Figure 2G,I,J).

By 12–14 weeks, a large number of perineal nerves were observed within the scrotum (Figure 3A), along with numerous dorsal nerve branches innervating the dorsal prepuce (Figure 3A,C,E). High neural densities persisted in the ventral prepuce and proximal ventral stroma, located beneath the disproportionately thickened ventral stratified squamous epithelium (Figure 3E). The typical ventral neural densities commonly appeared partly out of the plane of section (Figure 3A,C,E), and thus, care was necessary in the interpretation of sagittal histological profiles. This limitation was partially circumvented through serial and adjacent section analyses and by the use of transverse sections.

At 13–14 weeks, the cavernosal tunica albuginea was not yet fully distinct, although tunical perforating nerve fibers were present (Figure 3B and arrowheads in D). Significant interindividual variation was observed among fetal specimens in all aspects of tissue morphology. Despite this variability, intraepithelial nerve fibers in the distal glans (Figure 3F–H) and ventral prepuce (Figure 3I,J)

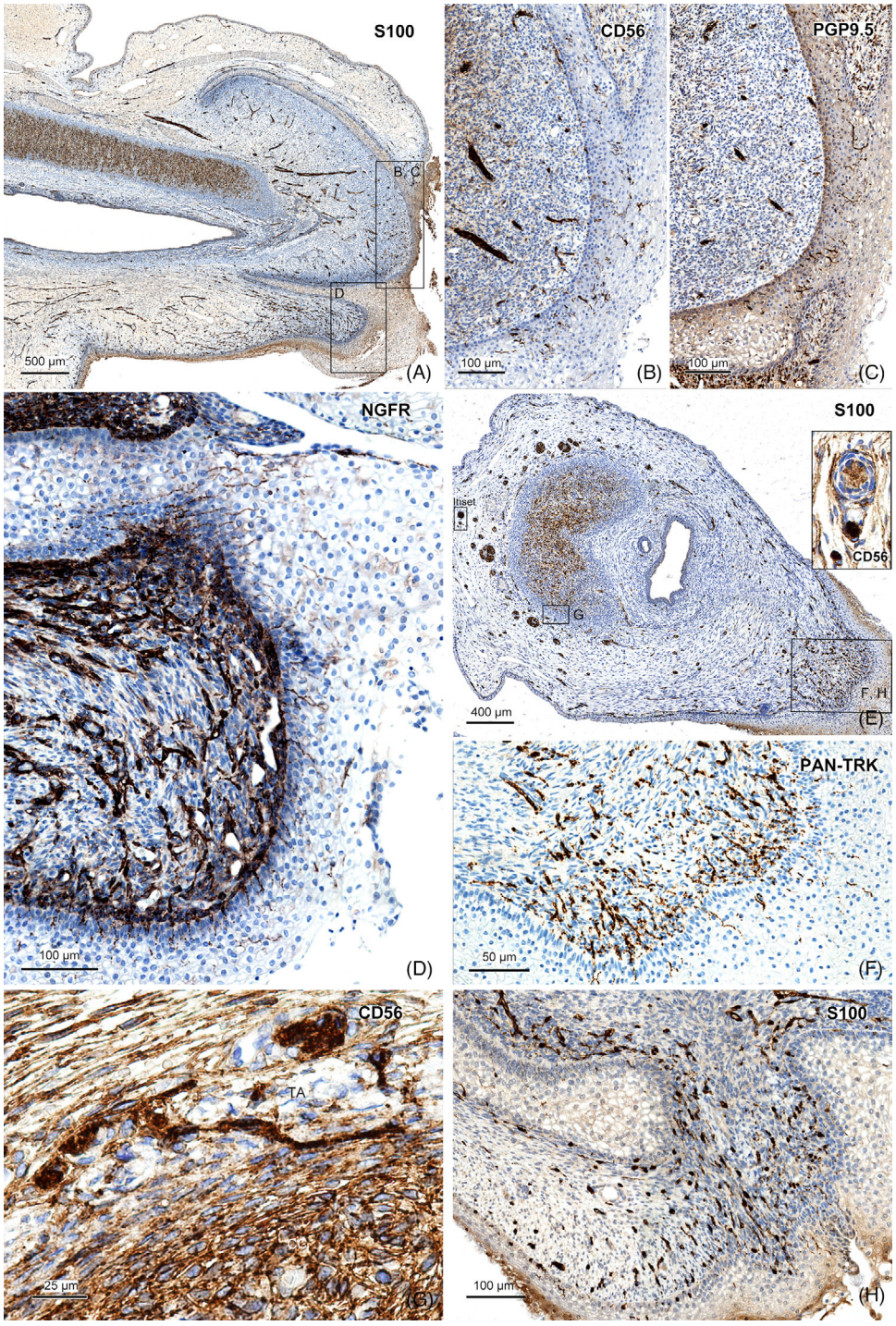

FIGURE 4 Preputial and distal glans innervation patterns in sagittally and transversely sectioned human fetal penile specimens. Pre-corpuscular stage of penile neurodevelopment. Approximate fetal ages: 14 (A–D) and 16 (E–H) weeks. (A) Sagittally sectioned 14-week specimen with typical ventral S100^{+} preputial stromal neural density associated to an overlying thickened distal ventral epithelium. These fibers reach their highest densities in the ventral prepuce within disproportionately thickened epithelial sheets, typically associated with a high ventral stromal neural density. (B) Approximately 46 µm lateral to A, showing dense CD56^{+} intraepithelial nerve fibers within the distal glans epithelium. (C) Approximately 58 µm lateral to A, providing a similar view as B, with continued observation of dense intraepithelial nerve fibers (protein gene product 9.5 [PGP9.5^{+}]) within the distal glans epithelium. (D) Approximately 50 µm medial to A, fetal penile intraepithelial nerve fibers (NGFR^{+} in this microphotograph) reach their highest densities in the ventral prepuce within disproportionately thickened epithelial sheets, invariably associated with a high ventral underlying stromal neural density and increased densities of blood vessels. (E) 16-week specimen sectioned transversely at the shaft level, proximal to the glans and prepuce, showing typical ventral epithelial thickening accompanied by dense stromal S100^{+} neural densities. The inset, located approximately 10 µm distal to the corresponding small rectangle, presents a higher magnification image suggesting a dorsal developing Pacinian corpuscle with a CD56^{+} inner core. (F) Approximately 26 µm proximal to E, illustrating ventral pan-TRK^{+} intraepithelial nerve fibers and corresponding underlying dense stromal neural density. The pattern of increased ventral neural density continues

remained consistently detectable. In the glans, intraepithelial fibers often appeared oriented parallel to the surface, likely because of the overlying periderm layer, which limits their longitudinal extension (Figure 3F,G).

By 14 weeks, intraepithelial nerve fibers were observed distally in the glans (Figure 4A–C) and reached their highest density levels within the thickened ventral preputial epithelium (Figure 4D). Transverse sections at 16 weeks revealed striking cutaneous and subcutaneous innervation biases toward the ventral aspect proximal to the prepuce (Figure 4E) and more distally in the ventral preputial and frenular regions (Figure 4F,H), correlating well with our observations in sagittal sections. Cavernosal tunical perforating nerve fibers were also readily visible in transverse sections, piercing a distinct cavernosal tunica albuginea (Figure 4G). Tunical perforating nerves were particularly numerous and thick in the proximal corpora cavernosa near the bulbar level but appeared thinner along the longitudinal penile axis. No evidence of a tunica albuginea or distinct lamina propria was identified superficially in the fetal glans during the pre-corpuscular stage.

3.3 | Corpuscular and neural pruning stage (17–24 weeks)

Developing Pacinian corpuscles were the only type of immature sensory corpuscle identified in fetal specimens during the corpuscular stage, suggesting that other sensory corpuscle types emerge at later developmental stages. Developing Pacinians could be identified virtually anywhere in the fetal penis, including the prepuce, glans, scrotum, bulb, the plane between the corpora cavernosa and corpus spongiosum, and adjacent to the tunica albuginea of both the cavernosal and spongiosal tissues. At 17 weeks, coronal (frontal) sections (Figure S1A) at the bulbar level revealed persistent intraepithelial nerve fibers in the ventral prepuce, yet they were less numerous and markedly thinner compared to earlier stages (arrows in Figure S1B–D). Simultaneously, the ventral preputial epithelium began to thin, contrasting with the thicker epithelia characteristic of the pre-corpuscular stage.

The corporeal bodies now displayed vascular spaces, innervation, and smooth muscle. The proximal corpora cavernosa exhibited numerous tunical perforating nerve fibers along the medial corporeal aspect (Figure S1E,F). Tunical perforating nerves at the proximal (crural) cavernosal level were also frequently observed dorsally and, less commonly, laterally. By 18 weeks, coronal sections at the urethral level (Figure S1G) demonstrated increased stromal neural densities near the ventral glans epithelium (Figure S1H,I), clusters of urethral intraepithelial nerve fiber networks (Figure S1J), lateral tunical perforating nerve fibers (Figure S1K), and frequent neural anastomoses between dorsal nerve fascicles (Figure S1L).

At 20 weeks, sagittal sections (Figure 5A) revealed developing Pacinian corpuscles within the glans (Figure 5B), in the plane between the corporeal bodies (Figure 5C), within the prepuce (Figure 5D), and in the penile bulb (Figure 5E). The prospective frenulum (Figure 5F,H) and ventral prepuce (Figure 5G,I) continued to display dense innervation. By this stage, the penile surface epithelia were uniformly thinner compared to the corpuscular stage, and ventral preputial intraepithelial nerve fiber densities were greatly diminished or absent. Immature Pacinian corpuscles were also identified in the frenular region (Figure S2A,B), associated with high nerve fiber densities (Figure S2C); in the scrotum (Figure S2D,E); in the perineal skin (Figure S2F); exceedingly rarely within the corpora cavernosa (Figure S2G,H); adjacent to the tunica albuginea of both cavernosal and spongiosal tissues (Figure S2I); occasionally in an intra-albugineal position (Figure S2J,K); and infrequently within the bulbospongiosus muscle (Figure S2L). By 20–24 weeks, fetal Pacinian corpuscles generally exhibited the characteristic immunohistochemical profile of mature Pacinian corpuscles.

Throughout this stage, transverse sections demonstrated persistent, striking innervation biases toward the ventral prepuce and frenular region (Figure S3A–G), aligning closely with observations from sagittal and coronal sections. A noteworthy phenomenon we documented in the developing frenular stroma was the presence of numerous Glut-1$^+$ red blood cells that appeared extravasated and were not associated with the adjacent CD31$^+$ blood vessels (Figure S3E). This phenomenon was also observed during the pre-corpuscular stage (not shown). Table 1 summarizes the main neurological and morphological processes associated with the pre-corpuscular and corpuscular stages of fetal penile neurodevelopment. Figure 6 presents a schematic illustration of the pre-corpuscular/hyperinnervation and corpuscular/neural pruning stages of fetal penile neurodevelopment in sagittal view.

3.4 | Adult specimens

As noted earlier, these findings are organized into specific subcategories that correspond to the research themes discussed in Section 1. In the older adult specimens, apart from minimal to intense atherosclerosis of intracorporeal arteries and varying degrees of intracorporeal tissue fibrosis (not shown), no other significant histopathological changes were observed in this cadaveric series. Unlike fetal specimens, reticulin fibers were almost absent in the adult penile connective tissues, instead being preferentially distributed around capillaries, peripheral nerve fibers, and adipocytes in the penile suspensory apparatus, as well as intra- and extracorporeal smooth muscle cells, and the skeletal muscle cells of the bulbospongiosus muscle (not shown).

in this specimen. (G) Approximately 94 μm proximal to the corresponding rectangle in E, depicting a CD56$^+$ tunical perforating nerve fiber with an oblique course identified in the lateral aspect of the shaft tunica albuginea. (H) Approximately 242 μm distal to E, showing the persistence of the heightened ventral S100$^+$ neural density at the frenular level. Thus, similar neurodevelopmental patterns of increased ventral neural densities are observed across specimens sectioned in different spatial planes (sagittal and transverse). CC, corpora cavernosa; TA, tunica albuginea.

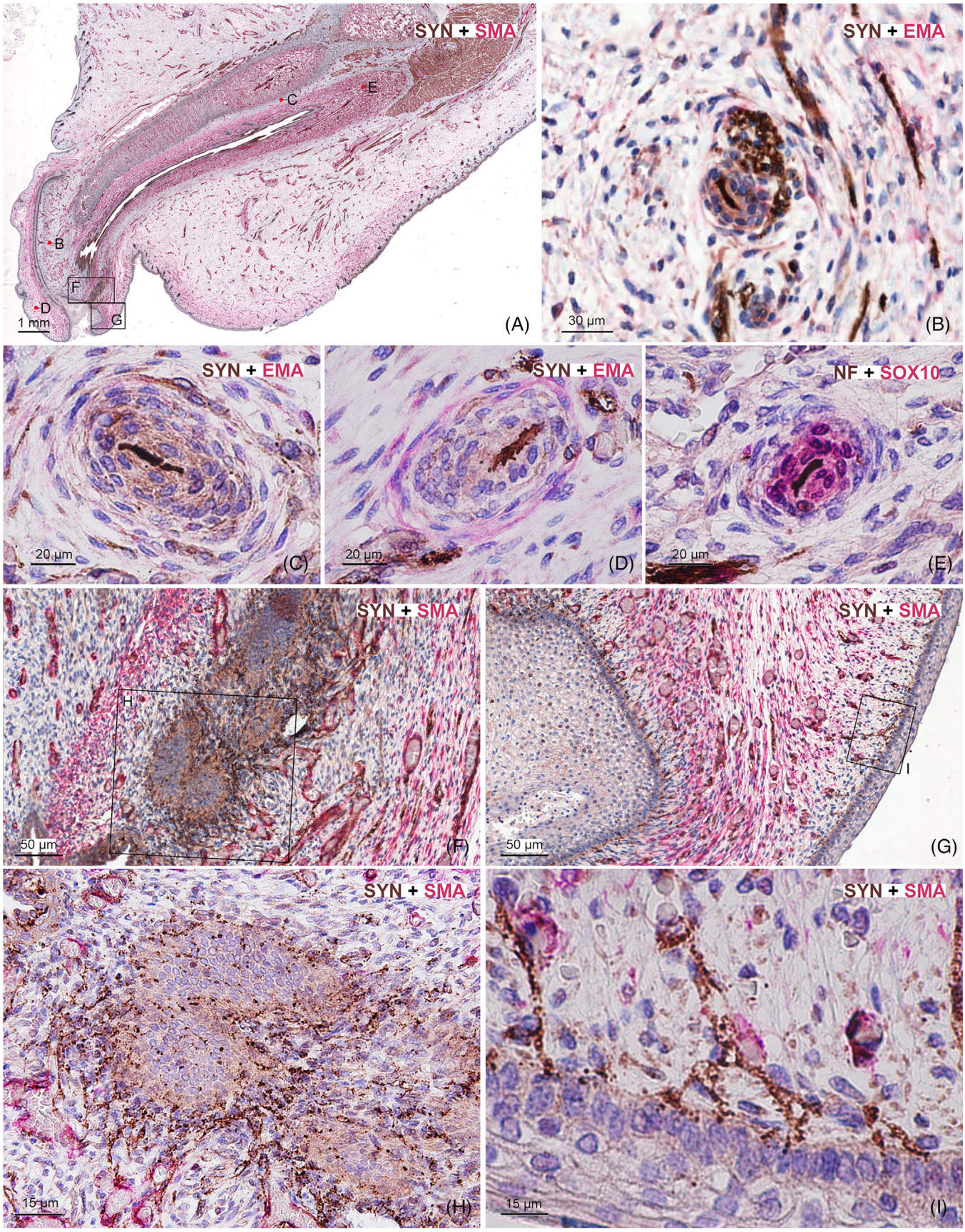

FIGURE 5 Neurological phenomena in a sagittally sectioned human fetal penile specimen of approximately 20 weeks of fetal age. Corpuscular stage of fetal penile neurodevelopment. (A) Low-magnification overview of a specimen immunostained for SYN (brown) and smooth muscle actin

3.5 | Immunohistochemical profiles of penile sensory corpuscles

The axonal immunoreactivity patterns of all sensory corpuscle types across all penile regions examined in this study were NF$^+$, SYN$^+$, NSE$^+$, PGP9.5$^+$, GAP-43$^+$, and pan-TRK$^+$. Intracorpuscular modified Schwann cells, regardless of sensory corpuscle type or penile region, were S100$^+$, SOX10$^+$, nestin$^+$, vimentin$^+$, CD56$^+$, Bcl2$^+$, Gap-43$^+$, and NGFR$^+$. Additionally, COL-IV specifically stained the basal laminae of these Schwann cells, highlighting their specialized extracellular matrix (ECM). For Pacinian and Golgi-Mazzoni corpuscles, regardless of their anatomical position, the outer core was Glut-1$^+$, EMA$^+$, VIM$^+$, COL-IV$^+$, NGFR$^+$, and CD10$^+$, whereas the irregular intermediate layer was CD34$^+$. Occasionally, a distinct α-SMA$^+$ capsular layer surrounding the Pacinian outer core was identified, observed in approximately 1 out of every 10 Pacinian corpuscles. The capsules of deep-dermal genital corpuscles were CD34$^+$, α-SMA$^+$, Glut-1$^+$, EMA$^+$, and CD10$^+$. A summary of this information is provided in Table 2.

3.6 | Glans, frenular, and ventral preputial nerve bundle innervation: lamina propria

Transverse sections of the glans and frenular region revealed a strikingly higher density of nerve bundles ventrally in the frenular area and ventrolateral glans (Figure 7). In the frenular region, nerve bundles formed an interconnected network that extended throughout the glans lamina propria (Figure 7A,B,D–F). The axons within these bundles ascended toward the dermis and lamina propria, giving rise to a variety of sensory corpuscles (Figures 7C,F, 8, and Figure S4). The dense frenular nerve bundles were located adjacent to equally dense dartoic smooth muscle bundles and richly innervated blood vessels with prominent autonomic innervation (Figure 7E,G). In contrast, the glans lamina propria lacked smooth muscle bundles and dense aggregations of nerve bundles. Along with nerve bundles and richly innervated vasculature and smooth musculature, the frenular region also contained an extensive network of lymphatic vessels that communicated with those in the glans lamina propria (Figure 7H). Thus, together, the frenular region and glans lamina propria formed an interconnected network of nerve bundles, blood vessels, and lymphatic vessels, whereas smooth muscle bundles were absent in the glans lamina propria. Using the classical anatomical position with the penis erect and the prepuce retracted as a reference, the nerve bundles in the frenular region (projections of the perineal and dorsal nerves) extended proximally throughout the ventral prepuce in a retrograde manner (Figure 7I).

3.7 | Sensory corpuscles in the glans and frenular region

A wide variety of sensory corpuscles in the glans and frenular region were spatially segregated in a highly organized manner (Figures 8–10 and Figure S4). These included genital, Krause, Pacinian, Paciniform, Golgi-Mazzoni, Ruffini-like, Meissner, and numerous other corpuscles that were difficult to classify. We present these data from the superficial to the deep histological strata.

3.7.1 | Lamina propria

The lamina propria of the glans was continuous with that of the frenular and ventral inner preputial regions. It was bounded superficially by the epithelium and underneath by a distinct layer composed of dense elastic fibers and coarse collagen oriented parallel to the surface. This specialized layer corresponds to the glans tunica albuginea, which will be described in detail in Section 3.16.

(SMA) (magenta), indicating the anatomical positions of the structures shown in the other images. The preputial and scrotal dartos, along with the intracorporeal smooth muscle, are labeled with SMA (magenta). Parts (B–D) are from a section approximately 162 µm lateral to A, whereas E is from a section approximately 122 µm lateral to A. (B–E) Typical developing and immature Pacinian corpuscles are shown in various anatomical regions: glans (B), between the corpus spongiosum and corpora cavernosa (C) (for an adult Pacinian in this position, see Figure 11N), prepuce (D), and within the penile bulb (E) (for adult bulbar Pacinians, see Figure 11). In B–E, the SYN$^+$ axons within the Pacinian inner cores are longitudinally sectioned (brown), with SYN$^+$ spine-like axonal processes extending from the sensory axon in D. The nascent outer core lacks epithelial membrane antigen (EMA) expression in B and C but is EMA$^+$ (magenta) in D, indicating developmental intraspecimen variability in expression of this marker. The intracorporeal bulbar Pacinian in E contains inner core SOX10$^+$ Schwann cell nuclei (magenta). (F) Higher magnification of the corresponding rectangle in A, showing a ventrally situated epithelial structure identified as the future frenulum associated with numerous SYN$^+$ nerve fiber profiles (brown) and blood vessels. (G) An intermediate magnification of the corresponding rectangle in A, showing the terminal SYN$^+$ axonal branching pattern in the ventral prepuce (brown). The outer ventral preputial epithelium has thinned to only four or five cells thick, a marked reduction in thickness compared to the pre-corpuscular stage. This thinning is accompanied by a significant decrease in preputial intraepithelial nerve fiber density, suggesting axon pruning and/or retraction of nerve fibers from their previous intraepithelial positions at an earlier developmental stage. The ventral preputial stroma is filled with developing SMA$^+$ dartos smooth muscle (magenta), along with SYN$^+$ nerve fibers (brown) reaching all basal epithelial surfaces, though many deep stromal nerve fibers are out of the plane of section. (H) Higher magnification of the epithelial frenular structure in F, highlighting the dense network of SYN$^+$ nerve fibers (brown) associated with the future frenulum. (I) High magnification view of the ventral preputial region indicated in G, where SYN$^+$ (brown) intensely stains the distinct peripheral axon branching pattern of nerve fibers that cover contiguous but apparently non-overlapping or partially overlapping epidermal territories. This pattern suggests axon self-avoidance through repulsive interactions between isoneuronal branches and/or competition for limited neurotrophic factors.

TABLE 1 Summary of main morphological and neurological processes across the fetal pre-corpuscular/hyperinnervation and corpuscular/neural pruning stages of penile neurodevelopment.

Feature	Pre-corpuscular/Hyperinnervation stage (8–16 weeks)	Corpuscular/Neural pruning stage (17–24 weeks)
Sensory corpuscles	Absent for most of this stage (Figures 2–4). Sparse developing Pacinian corpuscles were observed by the end of stage (inset in Figure 4E)	Developing sensory corpuscles, exclusively Pacinians, appear consistently from ~19 weeks (Figure 5 and Figure S2). Extracorporeal Pacinians observed in prepuce, glans, scrotum, surrounding the tunica albuginea, and perineal skin. Intracorporeal Pacinians in bulb (Figure 5A,E) and rarely in the corpora cavernosa (Figure S2D,G,H)
Nerve-to-body ratio	High nerve diameter-to-body ratio makes neural patterns easily identifiable in single sections without serial section analyses	A progressive decrease in the nerve diameter-to-body ratio necessitates extensive serial and semi-serial section analyses to delineate neural patterns
Intraepithelial fibroblasts	VIM^+ intraepithelial penile spindle- or dendritic-shaped cells are commonly noted between 8 and 10 weeks (inset in Figure 2A)	VIM^+ intraepithelial penile spindle- or dendritic-shaped cells continue to be observed
Extracorporeal innervation	By 8 weeks, dorsal nerve fibers reach the distal glans tip and early prepuce by 10 weeks (Figure 2A), with minimal intraepithelial fibers (arrow in Figure 2D). The main dorsal nerve trunk and its ventrolateral branches terminate near the future frenulum by the end of the indifferent stage, marking the earliest phase of penile morphogenesis (Figure 2A). Thinner very dense stromal nerves are evident ventrally. Neural anastomoses are frequent, with ventral convergence of extracorporeal branches toward the future frenular area	High stromal neural densities persist in the frenular area (Figure 5F–I, Figures S2C and S3), with autonomic innervation of perivascular and dartos smooth muscle evident by >24 weeks
Intraepithelial nerve fibers	A hallmark of this stage throughout all penile epithelia. Marked increases between 11 and 13 weeks (Figures 2G–J and 3E–J), peaking in the ventral prepuce and future frenular area within thick epithelial sheets (Figure 4D) (14–16 weeks)	Densities decrease across all penile epithelia (Figure S1B–D,I), with the ventral preputial epithelium thinning notably (Figure 5A,G,I, Figures S2A,D and S3F) as exuberant intraepithelial fibers undergo pruning (a hallmark of this stage) (Figure 5G,I). However, high stromal neural densities in the future frenular area persist (Figure 5F–I, Figures S2C and S3)
Epithelial features	Ventral preputial epithelium disproportionately thicker than dorsal (Figures 2F,G,I,J, 3A,E,I,J, and 4A,D–F). Dorsal epithelial remodeling at 10 weeks signals early development of prepuce, coronal sulcus, and glans-shaft junction (Figure 2B–D)	Epithelia thin to homogenous thin layers across all penile surfaces (Figure 5A,G,I and Figures S2A,D and S3F)
Corporeal bodies, urethra, and intracorporeal innervation	Corpora cavernosa, developing corpus spongiosum, and glans appear as hypercellular mesenchymal condensations with absent to sparse vasculature and innervation (Figure 2A–C,F). Urethral development begins with dense ventral axonal supply	Intracorporeal vascular spaces, innervation, and smooth muscle are present (18 weeks) (Figures 5A and Figures S1E–G, S2D, and S7F,G). Urethral development is complete after 20 weeks
Tissue structure	High levels of reticulin fibers indicate connective tissue immaturity. Hypercellularity and dense tissular texture are common throughout this stage	High levels of reticulin fibers indicate connective tissue immaturity. Hypercellularity and dense tissular texture diminish by 18 weeks, transitioning to a looser texture
Glans features	No distinct lamina propria or tunica albuginea. The dorsal nerve invades and ramifies throughout the glans, with thick branches innervating the ventral glans near the future frenulum (8–9 weeks) (Figures 2A and 3E)	Lamina propria appears by 19 weeks, but the tunica albuginea remains absent at 24 weeks
Preputial dartos	Dartos smooth muscle layer begins developing at 12 weeks, visible in sagittal, transverse, and coronal sections (Figure S7)	Development continues, with dartoic and vascular autonomic noradrenergic innervation evident by >24 weeks

Note: Processes that develop after the corpuscular stage include the bundling of preputial and glans axons within $Glut\text{-}1^+$ and EMA^+ compact perineurium, the establishment of autonomic vascular and dartoic preputial innervation, the reduction of reticulin fibers across penile connective tissues, the emergence of non-Pacinian sensory corpuscles, and the initiation of elastogenesis of the glans tunica albuginea.

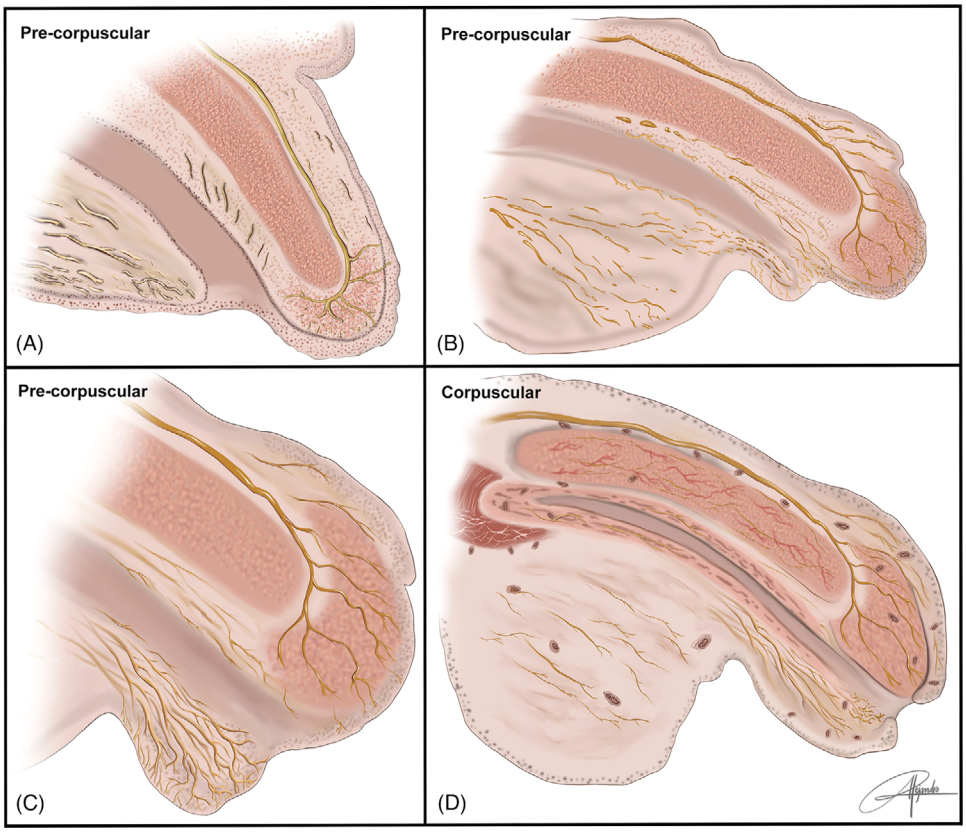

FIGURE 6 Schematic illustrations depicting the pre-corpuscular (hyperinnervation) and corpuscular (neural pruning) stages of human fetal penile neurodevelopment in sagittal view. (A–C) Pre-corpuscular stage. (D) Corpuscular stage. (A) 8 weeks. Preputial development has not yet begun. The prominent dorsal nerve has penetrated the glans, branching extensively and terminating ventrally in the prospective frenular region. Nerve fibers are present at the distal tip of the glans, with high mesenchymal neural density in the developing ventral periurethral region (urethral folds). Intraepithelial nerve fibers, however, remain sparse to absent. The penile surface epithelium begins to thicken, whereas corporeal vascular spaces and innervation are still absent. (B) 12 weeks. Early prepuce emerges with nerve fibers in its distal tips. Ventral preputial intraepithelial nerve fibers begin to peak in density within a disproportionately thickened epithelium. (C) 16 weeks. Preputial development progresses, with intraepithelial nerve fibers reaching their peak density within the thickened ventral preputial epithelium, which simultaneously attains its maximum thickness. Developing sensory corpuscles are not yet detectable. (D) 24 weeks. The prepuce fully covers the glans, extending beyond its distal tip. Immature Pacinian corpuscles are distributed across all penile regions, including the prepuce, glans, frenular region, scrotum, areas adjacent to the tunica albuginea, the plane between the corpora cavernosa and corpus spongiosum, the penile bulb, the perineal skin beneath the bulbospongiosus muscle, and rarely within the corpora cavernosa. Neural pruning of intraepithelial nerve fibers, a defining feature of this stage, occurs concurrently with the thinning of the ventral preputial epithelium. However, stromal neural densities beneath the epithelium remain high, particularly in the prospective frenular region. The corporeal bodies exhibit vascular spaces and innervation.

This tissue compartment contained numerous highly axonally branched sensory corpuscles, both papillary and non-papillary, distributed across the glans surface. However, these corpuscles were spaced out (Figure 8A) and did not form dense clusters, as commonly seen in the prepuce and frenulum (Figure 8B,C). Large segments of the glans lamina propria across numerous serial and adjacent sections were entirely devoid of corpuscular receptors. Nevertheless, a tendency for corpuscular and FNE aggregation was observed in the ventrolateral glans regions flanking the frenular area contralaterally (Figures 7E,F and 8D). Serial section analyses of multiple transverse sections of the glans across paraffin blocks revealed that nerve bundles and sensory corpuscles were most concentrated in the frenular region of the ventral prepuce, rather than in the glans lamina propria (Figures 7 and 8A–C). Clusters of up to 17 densely arborized corpuscular receptors were found concentrated within a few adjacent dermal papillae in the frenular region (Figure 8B). These dense clusters of nerve bundles and sensory corpuscles were consistently absent in the dorsolateral glans lamina propria. Figure 8D–M and Figure S4 illustrate the diversity of sensory corpuscles identified within the glans lamina propria.

The axonal components of sensory corpuscles in the glans lamina propria were visualized in our microphotographs using NF staining (Figure 8A,C,E–I,M and Figure S4A,J,M,O) and synaptophysin (Figure 8B,D,J–L and Figure S4I,K,N). Axons were also immunopositive for NSE (Figure S4G), PGP9.5 (not shown), GAP-43 (not shown), and pan-TRK (not shown). Notably, the glans lamina propria contained a low-density subpopulation of Golgi-Mazzoni (Figure S4A–I), Paciniform (Figure S4J–N), and small Pacinian corpuscles (Figure S4O). Unlike typical Pacinian corpuscles, Golgi-Mazzoni corpuscles exhibited larger inner cores with abundant axonal profiles (Figure S4G,I)

TABLE 2 Immunohistochemical profiles of adult penile sensory corpuscles identified in this study.

Marker	Pacinian corpuscles	Golgi-Mazzoni corpuscles	Meissner corpuscles	Ruffini-like corpuscles	Genital and Krause corpuscles
α-SMA	Capsule −/+	−	−	−	Capsule (deep-dermal type) −/+
Bcl-2	Inner core Schwann cells +	Inner core Schwann cells +	Schwann cells +	Schwann cells +	Schwann cells +
CD10	Outer core +	Outer core/capsule ±	−	−	Capsule (deep-dermal type) ±
CD31	N/A	N/A	N/A	N/A	N/A
CD34	Intermediate layer +	Inner core −/+ Intermediate layer + Outer core/capsule −/+	Capsule ±	Capsule ±	Capsule (deep-dermal type) +
CD56	Axons −/+ Inner core Schwann cells +	Inner core Schwann cells +	Schwann cells +	Schwann cells +	Schwann cells +
COL-IV	Outer core + Inner core ±	Inner core ± Outer core/capsule +	Basal lamina of Schwann cells +	Basal lamina of Schwann cells +	Basal lamina of Schwann cells +
D2-40	N/A	N/A	N/A	N/A	N/A
EMA	Outer core +	Outer core/capsule +	−	N/A	Capsule (deep-dermal type) ±
Gap-43	Axons ± Inner core Schwann cells ± Outer core −/+	Axons ± Inner core Schwann cells ± Outer core/capsule −/+	Axons ± Schwann cells ±	N/A	Axons ± Schwann cells ±
Glut-1	Outer core +	Outer core/capsule +	−	N/A	Capsule (deep-dermal type) ±
Nestin	Inner core Schwann cells +	Inner core Schwann cells +	Schwann cells +	Schwann cells +	Schwann cells +
NF	Axons +	Axons +	Axons +	Axons +	Axons +
NGFR	Axons ± Inner core Schwann cells + Outer core + Capsule +	Axons ± Inner core Schwann cells + Outer core/capsule +	Schwann cells +	Schwann cells +	Schwann cells +
nNOS	N/A	N/A	N/A	N/A	N/A
NPY	N/A	N/A	N/A	N/A	N/A
NSE	Axons +	Axons +	Axons +	Axons +	Axons +
Pan-TRK	Axons +	Axons +	Axons +	Axons +	Axons +
PGP9.5	Axons + Outer core +	Axons + Outer core/capsule +	Axons +	Axons +	Axons +
S100	Inner core Schwann cells +	Inner core Schwann cells +	Schwann cells +	Schwann cells +	Schwann cells +
SOX10	Inner core Schwann cells +	Inner core Schwann cells +	Schwann cells +	Schwann cells +	Schwann cells +
Synaptophys	Axons +	Axons +	Axons +	Axons +	Axons +
TH	N/A	N/A	N/A	N/A	N/A
Vimentin	Inner core Schwann cells + Outer core + Capsule +	Inner core Schwann cells + Outer core/capsule +	Schwann cells +	Schwann cells +	Schwann cells +
VIP	N/A	N/A	N/A	N/A	N/A

Note: Regardless of their anatomical location, the immunohistochemical properties of penile sensory corpuscles were consistent. The table details the specific corpuscular components that exhibit immunoreactivity, along with approximate percentages of corpuscles displaying these immunoreactivities. +, Marker positive in most corpuscles (>90%). ±, Marker positive in a moderate subpopulation of corpuscles (~40%–60%). −/+, Marker positive in a small subpopulation of corpuscles (~10%–20%). −, Marker not detected in all corpuscles. N/A, antibody not applied to sensory corpuscle.

Abbreviations: COL-IV, collagen type IV; EMA, epithelial membrane antigen; Glut-1, glucose transporter 1; NF, neurofilament; nNOS, neuronal nitric oxide synthase; NPY, neuropeptide Y; PGP9.5, protein gene product 9.5; SMA, smooth muscle actin; TH, tyrosine hydroxylase; VIP, vasoactive intestinal peptide.

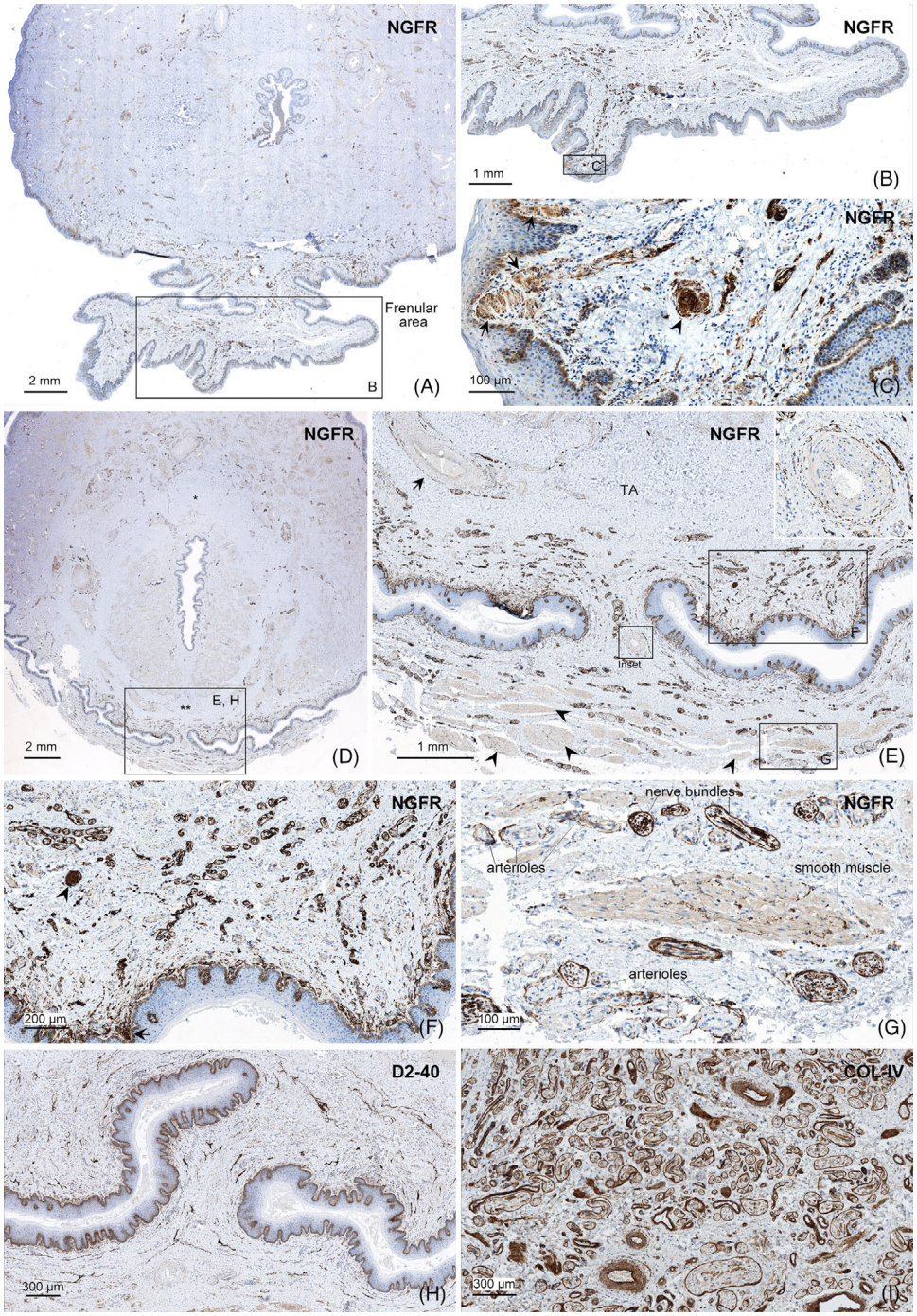

FIGURE 7 Frenular innervation patterns in three human adult penile specimens. (A) Transverse section through the glans and frenular region from a 63-year-old individual, immunostained for NGFR. Moderate to low levels of nerve bundles are observed in the dorsolateral glans lamina propria, contrasting with the increasing nerve bundle densities ventrolaterally and ventrally in the frenular area proper. A continuous network of nerve bundles and vasculature extends through the lamina propria of the glans, frenular region, and ventral prepuce, seamlessly connecting these anatomical regions. (B) Higher magnification of the corresponding rectangle in A (frenular region), showing an increase in $NGFR^+$ nerve bundle density toward the frenular area proper. (C) Higher magnification of the rectangle in B, highlighting superficial $NGFR^+$ nerve fibers that give rise to $NGFR^+$ corpuscular receptors, including Meissner corpuscles in the dermal papillae (arrows) and a deeper Krause corpuscle (arrowhead). NGFR immunostains the modified Schwann cells within these corpuscles, although axonal immunopositivity cannot be excluded. (D) Transverse section immunostained for NGFR from a 65-year-old individual, again showing heightened ventral $NGFR^+$ nerve bundle density as part of the continuous network of nerve bundles and vasculature that extends through the lamina propria of the glans, frenular region, and ventral prepuce. The dorsolateral glans lamina propria contains moderate to low levels of nerve bundles, in contrast to the elevated neural densities ventrolaterally and ventrally. The distal ligament (*) is observed dorsally, and the lower midline septum (**) is present ventrally. These fibrous collagenous structures are connected by fibrous extensions or a "urethral ring" surrounding the glanular urethra, which is also readily observed in the image. (E) Higher magnification of the rectangle in D (frenular region), showing a dense network of $NGFR^+$ nerve bundles that communicate through the continuous tissue plane formed by the ventral glans and ventral preputial lamina propria. Numerous unstained dartos smooth muscle bundles are observed on

and smaller outer cores or capsules. Golgi-Mazzoni corpuscles were also commonly found in the prepuce in low to moderate numbers (not shown), varying by specimen. Their immunohistological profile was identical to that of Pacinian corpuscles, as reported in the literature, with the exception that the CD34$^+$ intermediate layer of cells between the inner and outer cores frequently appeared irregular and extended cytoplasmic processes into the inner core, which itself also contained CD34$^+$ cells (Figure S4A). However, we also identified a population of Golgi-Mazzoni corpuscles with a well-defined CD34$^+$ intermediate layer, similar to that of Pacinians (not shown).

SYN, NSE, and PGP9.5 immunostained numerous intracorpuscular small-diameter accessory axons that were not highlighted by NF staining in serial sections. This contrast was particularly evident in the aforementioned corpuscles and genital corpuscles of the ventral preputial region near the frenulum (Figure S6). For comparison, examine the axonal profiles in Figure S4A against those in Figure S4G,I, and in Figure S4J,M compared to those in Figure S4K,N, respectively.

3.8 | Corpus spongiosum

The deep glans corpus spongiosum, a region typically rich in elastic fibers, contained moderate to low numbers of small Pacinian corpuscles and smaller Paciniform corpuscles (Figure 9). Elastic fibers were not observed within the Pacinian corpuscles themselves; however, they were abundantly interwoven with coarse collagen fibers surrounding the glans Pacinians (Figure 9J–N).

3.9 | Glans urethral lamina propria

The lamina propria of the glanular urethra exhibited sparse, low-to-moderate densities of small sensory corpuscles, which were absent in the lamina propria of the shaft and bulbar regions of the anterior urethra (Figure 10A–I).

3.10 | Bulbar sensory corpuscles

Adult intracorporeal sensory corpuscles were primarily sparse, isolated, and variably sized and shaped typical Pacinian corpuscles located in the bulbar region of the corpus spongiosum, supplemented occasionally by Paciniform corpuscles (Figure 11). Bulbar Pacinians were predominantly intratrabecular in position (Figure 11B–M) but were also found directly adjacent to the inner aspect of the bulbar tunica albuginea (not shown). Sensory corpuscles were absent from the lamina propria of the bulbar and shaft urethra. Additionally, Pacinian corpuscles were identified in the plane between the corpora cavernosa and corpus spongiosum near the external aspect of the bulbar tunica albuginea (Figure 11N). For comparison, see Figure 5A,C for a fetal Pacinian corpuscle in a similar anatomical location.

Sensory corpuscles were specifically searched for in the fibromuscular trabeculae of the corpora cavernosa and the shaft corpus spongiosum but were not observed in adult specimens. Thus, the adult corpora cavernosa was devoid of sensory corpuscles in this study, whereas the corpus spongiosum contained low-to-moderate density subpopulations of Pacinian corpuscles limited to the bulb and glans regions, suggesting a bimodal distribution. However, exceedingly rare fetal intracavernosal developing Pacinians were identified in fetal specimens (Figure S2G,H).

Collectively, the immunohistochemical profiles of bulbar and glans Pacinians were identical and matched those of preputial Pacinians identified in the same specimens, which served as internal controls whose immunohistology has been previously documented in the literature (Table 2). No elastic or reticular fiber contents were observed within Pacinian corpuscles, although dense elastic fibers were located near Pacinians in the spongiosal bulbar and glans trabeculae.

3.11 | Penile suspensory apparatus

The adipose tissue of the penile suspensory system contained numerous nerve bundles (Figure 11O) and typical Pacinian corpuscles (Figure 11P). The nerve bundles exhibited an exceptionally high density of nerve fibers, consisting of a mix of unmyelinated and myelinated fibers in varying proportions. Figure 11O highlights the reticulin fiber network surrounding the nerve fibers within the penile suspensory apparatus.

the preputial side (arrowheads), as detailed further in G. The inset (upper right corner) shows the thick-walled frenular artery with rich NGFR$^+$ autonomic adventitial innervation by nonmyelinated nerve fibers. In the upper left corner, an artery (arrow) with NGFR$^+$ autonomic innervation is visible within the layers of the ventral spongiosal tunica albuginea (TA). (F) Higher magnification of the rectangle in E, displaying NGFR$^+$ nerve bundles, a deep Krause corpuscle in the lamina propria (arrowhead), a papillary NGFR$^+$ corpuscle (arrow), and innervated arterioles in the frenular region. (G) Higher magnification of the rectangle in E, demonstrating dartos smooth muscle bundles with rich NGFR$^+$ autonomic innervation (see also Figure S8F), NGFR$^+$ nerve bundles, and frenular arterioles with dense NGFR$^+$ autonomic innervation. NGFR intensely stains both myelinated and unmyelinated axons within nerve bundles and the unmyelinated autonomic axons that supply the dartoic smooth muscle and preputial blood vessels, thus serving as a pan-axonal marker. Additionally, NGFR stains the nerve bundle perineurium. (H) A section located approximately 82 μm proximal to the frenular region in D, showing a network of D2-40$^+$ lymphatic vessels within the frenulum, freely communicating through the continuous tissue plane formed by the ventral glans and ventral preputial lamina propria. (I) Ventral prepuce from a 45-year-old individual, immunostained for collagen type IV (COL-IV), revealing numerous nerve bundles with intensely stained COL-IV$^+$ perineurium. As a rule, such nerve bundle aggregations were not found in the glans lamina propria. Endoneurial periaxonal collagen, blood vessels, and smooth muscle bundles also stain positive. TA, tunica albuginea.

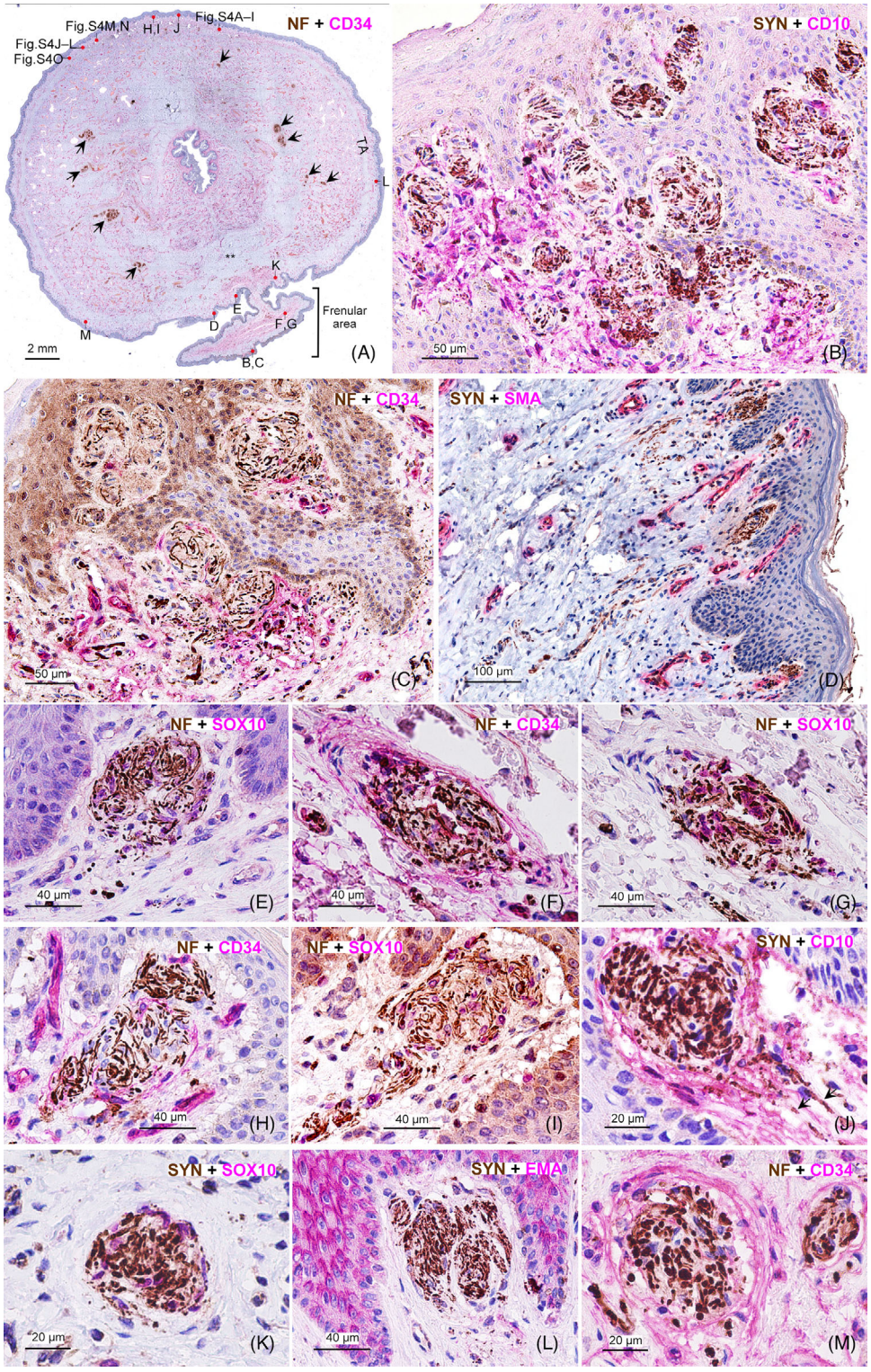

FIGURE 8 Glans and frenular corpuscular neuroreceptors. The figure is a composite, with E and M derived from different specimens (51 and 66 years old, respectively). The rest of the images were obtained from the specimen shown in A. (A) Transversely sectioned glans specimen from a 45-year-old individual immunostained for neurofilament (NF) (brown) and CD34 (magenta), showing the anatomical positions of the other images, including those in Figure S4. The strand of ventral frenular tissue is part of the ventral inner prepuce. Transverse sections of the glans from specimens fixed with the prepuce retracted typically exhibit this or similar histological profiles. Note the anatomical continuity between the frenular lamina propria and the glans lamina propria. Also note the unstained glans tunica albuginea (TA), situated between the $CD34^+$ (magenta) glans lamina propria and underlying corpus spongiosum. The NF^+ dorsal nerves (arrows) appear in cross-section, showing bilateral asymmetry, with larger and more numerous nerves on the right hemiglans (left part of the image) compared to the contralateral side. The distal ligament (*) and the lower midline septum (**) are located dorsal and ventral to the urethra, respectively. (B) Higher magnification of a section approximately 22 µm

3.12 | CD10 expression in the outer core of Pacinian and Golgi-Mazzoni corpuscles

CD10 was consistently expressed in the outer core of adult Pacinian corpuscles, specifically in the region closest to the inner core (Figure S5A–G,L). This pattern was observed in the majority of Pacinian corpuscles analyzed in this study. Double immunofluorescence staining for CD10 and CD34 excluded colocalization of these markers in the intermediate layer (Figure S5H–K,M–O). No differences were detected in the staining patterns or intensities of Pacinian corpuscles between the two CD10 antibody clones used in this study (Table S2). Additionally, CD10 was identified within Golgi-Mazzoni corpuscles, where it exhibited faint immunopositivity (Figure S4G).

3.13 | Preputial genital corpuscles

The prepuce contained a subpopulation of deep-dermal encapsulated typical genital corpuscles characterized by capsular expression of CD34, Glut-1, EMA, vimentin, α-SMA, and CD10 (Figure S6A–N). Additionally, the internal septa of some of these corpuscles were exclusively $CD34^+$, whereas the axons consistently expressed NF, NSE, PGP9.5, and NGFR. Similar to Golgi-Mazzoni corpuscles, SYN, NSE, and PGP9.5 immunostained numerous intracorpuscular small-diameter accessory axons that were not detected by NF staining in serial sections. For comparison, contrast the axons depicted in Figure S6C with those in Figure S6D,E, as well as those in Figure S6H with those in Figure S6I,J. These comparisons suggest that the small-diameter accessory axons represent a distinct subset of intracorpuscular neural components, as indicated by their specific immunoreactivities.

3.14 | Ontogeny of the preputial dartos

The adult preputial α-SMA^+ dartos smooth muscle layer was observed in transverse sections of the glans and prepuce (Figure S7H,I). This α-SMA^+ anatomical layer was also identified in fetal specimens through sagittal, transverse, and coronal sections, first appearing at 12 weeks of fetal age and persisting across specimens aged 14–24 weeks (Figure S7A–G). The orientation of the preputial smooth muscle bundles was notably multiaxial. This richly developed preputial smooth muscle layer occupied the central axis of the prepuce, positioned between the lamina propria of the inner prepuce and the dermis of the outer prepuce.

3.15 | Innervation of the preputial dartos smooth muscle

The preputial dartos smooth muscle exhibited dense innervation by unmyelinated nerve fibers, forming a fine network of dense NSE^+, $CD56^+$, $PGP9.5^+$, $NGFR^+$, SYN^+, and TH^+ fibers (Figure S8A–I). This robust innervation was supplemented by a markedly sparser network of $nNOS^+$, NPY^+, and VIP^+ fibers, which were detectable in specific regions within a limited number of sections from most specimens (Figure S8J–O).

proximal to the frenular region indicated in A. Concentration of frenular sensory corpuscles with dense SYN^+ axons (brown) within a $CD10^+$ dermal stroma (magenta). The image highlights the dense clustering of approximately 17 sensory corpuscles in the frenular area, contrasting with the isolated situation of sensory corpuscles in the glans proper. (C) Semi-serial section approximately 6 μm proximal to B, showing corpuscles from the same cluster with NF^+ axons (brown) amid a $CD34^+$ dermal stroma (magenta), contrasting with the more extensively stained $CD10^+$ stroma in B. Background staining is observed in the epithelium. (D) Higher magnification of a section from a different paraffin block from approximately the ventral glans region indicated in A. Three or four corpuscular receptors within adjacent frenular corial papillae, showing SYN^+ axons (brown) near smooth muscle actin $(SMA)^+$ capillaries (magenta). Parent fibers supplying the corpuscles can be observed in the lamina propria beneath the corpuscles. (E) Section from a different specimen (51 years old) from approximately the ventral glans region indicated in A. Frenular genital corpuscle with dense NF^+ axons (brown) and $SOX10^+$ Schwann cell nuclei (magenta). (F and G) Serial sections from a different paraffin block from approximately the region indicated in A. Serially sectioned deep-dermal fusiform Ruffini-like corpuscle, displaying NF^+ axonal arborizations (brown in F and G), $CD34^+$ fibroblast-like cells or possible telocytes (magenta in F), and $SOX10^+$ Schwann cell nuclei (magenta in G). The surrounding collagen appears artifactually broken because of common HIER effects on stromal collagen. (H and I) Serial sections from a different paraffin block from approximately the dorsal region indicated in A. Serially sectioned genital corpuscle located within a dorsal glans corial papilla, exhibiting loose NF^+ axonal proliferations (brown in H and I), $CD34^+$ corpuscular fibroblast-like cells or possible telocytes (magenta in H), and $SOX10^+$ Schwann cell nuclei (magenta in I). (J) Section from a different paraffin block from approximately the dorsal region indicated in A. Papillary corpuscle in the dorsal glans, with a dense SYN^+ axonal component (brown) surrounded by a $CD10^+$ dermal stroma (magenta). It is unclear whether $CD10^+$ cells are part of the corpuscle or external to it. Two parent fibers (arrows) approximate the corpuscle, suggesting polyinnervation. (K) Section from a different paraffin block from approximately the ventral glans region indicated in A. Small frenular Krause corpuscle in the deep lamina propria, with densely packed SYN^+ axons (brown) and $SOX10^+$ Schwann cell nuclei (magenta). Serial sections (not shown) confirmed the presence of loose $CD34^+$ fibroblast-like capsular cells. (L) Section from a different paraffin block from approximately the lateral glans region indicated in A. Lateral papillary glans genital corpuscle with a typical SYN^+ dense axonal mass (brown) and immunonegative epithelial membrane antigen (EMA) capsular component. The adjacent epithelium shows EMA immunopositivity (magenta) with an apicolateral membranous staining pattern. (M) Section from a different specimen (66 years old) from approximately the ventrolateral glans region indicated in A. Encapsulated Krause corpuscle in the ventrolateral glans deep lamina propria, with an NF^+ axonal component (brown) and a $CD34^+$ capsule (magenta), escorted by an adjacent NF^+ and $CD34^+$ smaller corpuscle. TA, tunica albuginea.

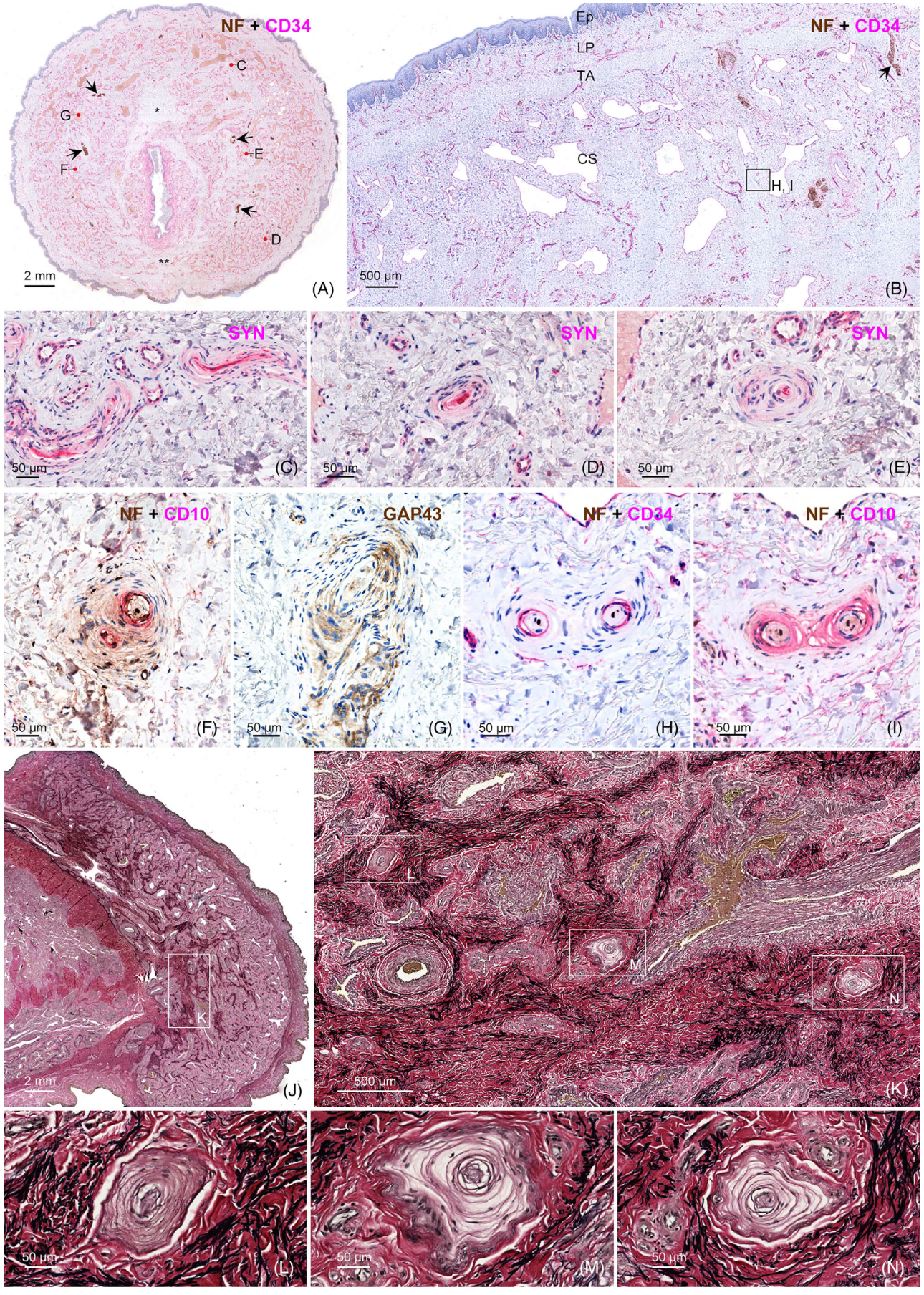

3.16 | Tunica albuginea of the glans

In contrast to all fetal specimens, a distinct glans tunica albuginea, composed of densely packed elastic and thick collagen fibers oriented parallel to the glans epithelium, was easily identified as an anatomical layer between the lamina propria and the corpus spongiosum (Figures 8A, 9B, 10A, and 12). The fibroelastic composition of this layer exhibited a multiaxial arrangement, with fibers oriented in transverse (Figure 12A–F,J) and sagittal (Figure 12G–I) planes. Coarse collagen fibers were clearly visible using H&E staining (Figure 12J) and MT staining (not shown). Multiple measurements of tunical thickness, performed on random regions from representative slides of three specimens, determined an average thickness of approximately 0.5 mm. This layer was frequently perforated by numerous neurovascular elements (arrows in Figure 12B,H).

The visibility of the glans tunica albuginea varied between specimens. It was more readily observed at low and high magnifications in younger specimens aged 45–66 years but was more difficult to demonstrate in older specimens. These differences may be age-related, although technical factors such as specimen handling and preparation likely contributed. Furthermore, even in specimens where this layer was clearly demonstrated, localized areas exhibited disorganization, irregularity, and reduced prominence of elastic fibers. A sharply defined transition was commonly observed between the deepest layers of the glans tunica albuginea and the underlying corpus spongiosum (Figure 12I,J). However, detailed analysis revealed continuity between the elastic and collagen fibers of the glans trabeculae and the tunica albuginea (arrows in Figure 12C–F,J). The transition between the tunica albuginea's most superficial layers and the lamina propria was less distinct, particularly in H&E and MT stains. This occasionally led to the misconception that the tunica albuginea was merely a deeper region of the lamina propria with an increased concentration of elastic fibers. Closer examination using carefully oriented transverse and sagittal sections at multiple magnifications, combined with high-quality automated histochemical staining, confirmed that the tunica albuginea is distinct from the lamina propria. This distinction is based on the pronounced parallel orientation of elastic and coarse collagen bundles relative to the glans epithelium. The glans tunica albuginea constitutes the outermost component of the intricate glans fibroelastic skeleton, encasing the corpus spongiosum of the glans. Refer to Figure 1C (arrowheads indicating the EF glans layer) to compare our histological demonstration of the glans tunica albuginea with Krstić's classical illustration.

Low-power immunohistochemical analysis of sections stained for CD34 (Figures 8A, 9B, and 10A) and vimentin (not shown) further identified the glans tunica albuginea as a distinct, unstained, hypocellular fibrous tissue layer, connected to the underlying fibroelastic skeleton of the glans corpus spongiosum. Elastic fibers within the glans lamina propria extended superficially, forming intricate networks and meshes of varying sizes in the papillary layer, closely contacting the basal epithelial surface (not shown). Figure 8 and Figure S4 show the diverse sensory corpuscles located within the glans lamina propria, positioned between the tunica albuginea and the epithelium.

4 | DISCUSSION

In this study, we have provided detailed light-microscopic immunohistological analyses of human penile tissues from the earliest fetal stages of penile development to adulthood, presenting a wealth of novel findings across diverse areas of contemporary penile research. These areas include the ontogeny of penile innervation; the innervation of the glans, frenular delta, prepuce, and corporeal bodies; an emphasis on the immunohistology of sensory corpuscles across these regions;

FIGURE 9 Human adult Pacinian corpuscles deep in the glans corpus spongiosum (CS) in three specimens: (A, C–G) 51-year-old individual, (B, H, I) 54-year-old individual, and (J–N) 48-year-old individual. The human adult penile glans contains a distinct but relatively low-density subpopulation of small Pacinian corpuscles located deep in the glans CS. (A) Transverse section through the distal glans, immunostained for neurofilament (NF) (brown) and CD34 (magenta), showing the anatomical positions of the other images. Small dorsal nerve fascicles are visible in cross-section (arrows). The urethral lamina propria (LP) contains a dense population of $CD34^+$ cells. The distal ligament (*) and the lower midline septum (**) are present dorsal and ventral to the urethra, respectively, connected by a fibrous "urethral ring." (B) Transverse section through the dorsal glans, immunostained for NF (brown) and CD34 (magenta), showing the anatomical positions of H and I. The four histological layers of the glans are shown: epithelium (Ep), LP, tunica albuginea (TA), and CS. A tunical perforating nerve bundle is visible in the upper right corner (arrow). (C–E) Small Pacinian corpuscles with SYN^+ inner core axons found in a section approximately 10 μm proximal to A. The two Pacinians in C are longitudinally sectioned, whereas those in D and E are transversely sectioned. (F) Section from a different paraffin block from approximately the anatomical region indicated in A, showing a Pacinian corpuscle with a single NF^+ axonal punctate profile (brown) and a $CD10^+$ circular layer (magenta) surrounding the inner core. Background staining is present in the outer core. (G) Section from a different paraffin block from approximately the anatomical region indicated in A, showing a larger Pacinian corpuscle with $GAP43^+$ outer core immunoreactivity. (H and I) Serially sectioned Paciniform corpuscle with double inner cores, showing NF^+ (brown in H and I) single axonal profiles within each inner core. (H) shows $CD34^+$ intermediate layers (magenta) and $CD34^+$ endothelium (magenta) lining a venous space in the superior part of the image. Part (I) displays a distinct $CD10^+$ circular layer (magenta) surrounding the inner core and occupying the first layers of the outer core. (J) Sagittal section through a distal glans specimen stained for elastic fibers, showing the anatomical positions of K–N. Note the paucity of elastic material within the corporeal tunica albuginea and the higher density of elastic fibers in the glans CS. (K) Higher magnification of the rectangle in J, displaying three small Pacinian corpuscles. Note the high density of elastic material (black) in the glans fibroelastic skeleton. (L–N) Higher magnifications of the corresponding rectangles in K, showing three small Pacinians near each other in a region close to the distal ligament of the glans. Note the high density of thick elastic material (black) interwoven with dense collagenous tissue surrounding each Pacinian, and the absence of elastic material within the corpuscles.

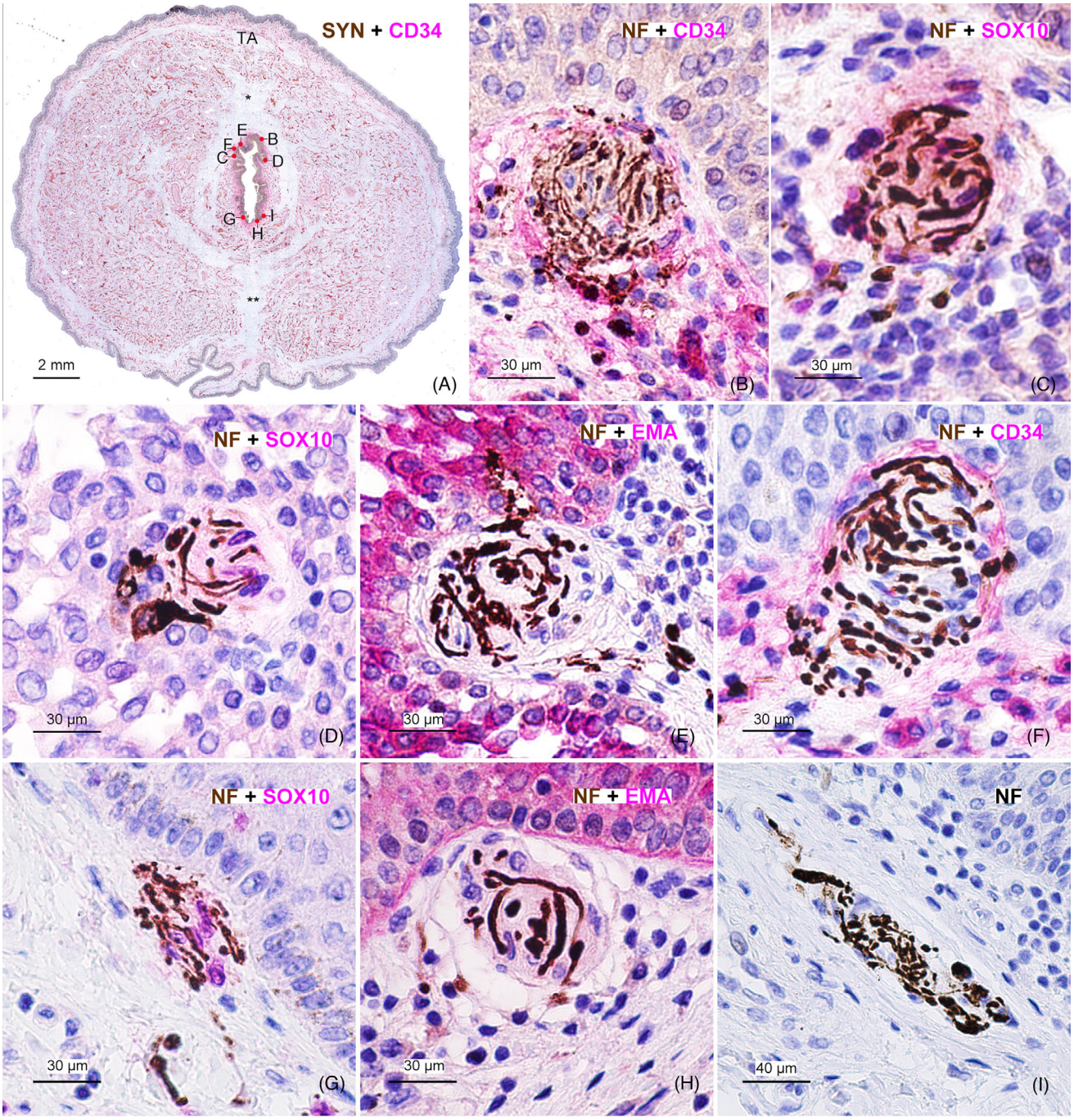

FIGURE 10 Human adult penile distal urethral sensory corpuscles. (A–I) 51-year-old specimen. The glans portion of the anterior urethra contains low to moderate densities of small non-Pacinian corpuscular receptors in the lamina propria, typically located near the epithelium. (A) Low-power view of a transversely sectioned glans specimen at the fossa navicularis, showing the anatomical locations of the corpuscles in the other images. The glans tunica albuginea (TA) appears as an unstained band parallel and adjacent to the epithelium, contrasting with $CD34^+$ tissue elements (magenta) in the lamina propria and corpus spongiosum. Note the midline distal ligament (*) dorsal to the urethra, the lower midline septum (**) ventrally, and the fibrous "urethral ring" that connects these ligamentous structures. Fibrous tissues surround the urethra, connecting the distal ligament to the lower median septum and the glans tunica albuginea, forming the glans fibrous skeleton. (B) Rounded subepithelial urethral corpuscle with dense NF^+ axons (brown), surrounded by $CD34^+$ cells (magenta) in the lamina propria. (C) Corpuscle with NF^+ axons (brown) and $SOX10^+$ Schwann cell nuclei (magenta). (D) Corpuscle with NF^+ axons (brown) and $SOX10^+$ Schwann cell nuclei (magenta) in an apparent intraepithelial location. This corpuscle may have been artifactually displaced during specimen preparation. (E) Urethral corpuscle with NF^+ axons (brown), lacking an epithelial membrane antigen (EMA^+) capsule. The EMA^+ urethral epithelium (magenta) is visible. (F) Sensory corpuscle with NF^+ axons (brown), surrounded superolaterally by $CD34^+$ cells (magenta). No clear capsule is observed in the basal part of the corpuscle. (G) Small sensory corpuscle with NF^+ axons (brown) and $SOX10^+$ Schwann cell nuclei (magenta). (H) Urethral corpuscle with NF^+ axons (brown), lacking an EMA^+ capsule. Note the EMA^+ urethral epithelium (magenta). (I) Fusiform Ruffini-like corpuscle parallel to the basal epithelial surface, with intensely stained NF^+ axons. TA, tunica albuginea.

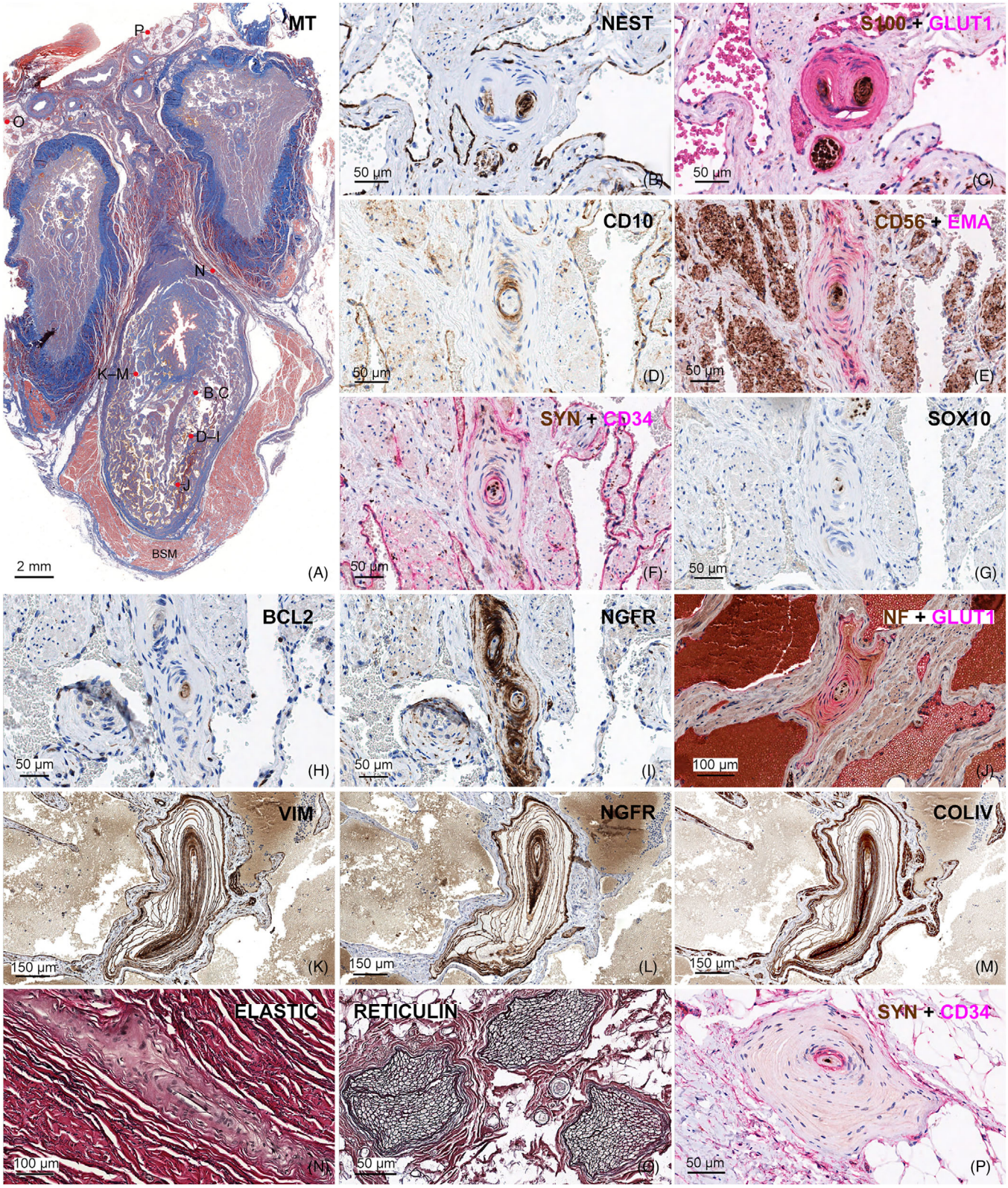

FIGURE 11 Human adult penile bulbar Pacinian corpuscles. The figure is a composite, with images J–M derived from an embalmed specimen, whereas the rest were obtained from the FFPE specimen shown in A (66-year-old). See Figure 5A,E for a fetal bulbar Pacinian. (A) Low-magnification image of a transversely sectioned specimen at the penile root stained for Masson's trichrome (MT), showing the penile bulb ventrally and separate cavernous bodies dorsally. The bulbospongiosus muscle (BSM, red) embraces the bulb, and parts of the penile suspensory apparatus are visible dorsal to the cavernous bodies. The anatomical positions of the other images are indicated. (B and C) Serial sections showing a small Paciniform corpuscle within a bulbar spongiosal trabecula near the bulbar septum, located approximately 66 μm distal to the region indicated in A. The corpuscle has double inner core that expresses nestin (B) and S100 (brown in C), whereas the outer core intensely expresses

the development and innervation of the preputial dartos; and the presence and structure of the tunica albuginea encasing the glans corpus spongiosum. We employed a diverse array of immunohistochemical markers with high specificity and sensitivity, targeting neural, smooth muscle, and vascular tissue components, alongside high-quality special stains to highlight connective tissue elements. Rather than artificially unifying a series of disparate topics, this study frames the penis as an integrated organ,[103] with each component contributing to its overall functions, including its proximal role in the provision of sexual pleasure and its evolutionary role in reproduction.

Although our emphasis has primarily focused on neurosensory structures, particularly through revealing the ontogenetic innervation pattern of the frenular delta, we have also explored the ontogeny and autonomic innervation of the preputial dartos, a dense smooth muscle layer embedded within the prepuce. Additionally, our findings regarding the glans tunica albuginea suggest a distinctive connective tissue configuration with implications for the organization and distribution of glans innervation, among other aspects. This study provides the most detailed primary data on glans sensory innervation since Halata and Munger's 1986 study,[13] integrating multi-scale microphotographs to illustrate neural distribution and tissue architecture. It is also the first to clearly visualize, through immunohistochemistry, the cavernosal tunical perforating nerve branches and the neural anastomoses between penile nerves. The cavernosal tunical perforating nerves likely originate from branches of the cavernous and pudendal nerves, suggesting pro-erectile and sensory functions, whereas the functional significance of the neural anastomoses remains to be elucidated.

Notably, these findings extend far beyond minor aspects of penile morphology, instead shedding light on major anatomical and histological landmarks of the fetal and adult penis that had previously remained obscure. This discussion partially mirrors the structure of Section 1, synthesizing our findings to highlight their implications for understanding penile neurodevelopment, morphology, sensory function, and potential clinical and ethical implications, while situating them within the broader scientific literature through detailed analyses. Section 4 concludes by addressing penile neurotomy (PN) and circumcision, highlighting the relevance of our findings to these controversial practices.

4.1 | Ontogeny of human penile innervation and its role in sexual sensation: toward a neurodevelopmental biology of the human penis

For the first time in the scientific literature, we have mapped the neurological ontogeny of the human penis, providing immunohistochemical evidence that informs over a century of discussion on penile sexual sensation and its neuroanatomical basis (Table S1). Striking neurodevelopmental phenomena of axonal pathfinding, pruning, and refinement appear to occur in the ventral penis during fetal development, specifically in the prospective frenular and ventral preputial regions, potentially holding the key to understanding penile sexual sensation. Dysregulation of these processes may contribute to the development of hypospadias, a hypothesis previously explored by Aksel et al.,[22] although their approach emphasized the role of neurovascular crosstalk.

Crucially, we have precisely documented the fetal ages (17–24 weeks) during which sensory corpuscles become histologically detectable in the human penis, defining distinct pre-corpuscular and corpuscular stages of penile sensory development. The initial pre-corpuscular stage is characterized by axonal hyperinnervation and exuberant ventral intraepithelial nerve fibers that establish a dense neural foundation. This phase is dominated by axon progressive processes, such as neural growth and proliferation, with such vigorous neurite extension that the intraepithelial nerve fibers appear almost as if they are striving to extend beyond the confines of the fetal penis.

glucose transporter 1 (Glut-1) (magenta in C). Note the nestin$^+$ (B) endothelial cells lining the vascular sinusoids filled with Glut-1$^+$ red blood cells (magenta in C). A small, rounded nerve bundle with Glut-1$^+$ perineurium (magenta in C) lies beneath the Paciniform. (D–I) Semi-serial sections showing a small bulbar intratrabecular Pacinian corpuscle, obtained from a different paraffin block several mm proximal to A from approximately the bulbar region indicated in A. The outer core is CD10$^+$ (D), epithelial membrane antigen (EMA$^+$) (magenta in E) and NGFR$^+$ (I), whereas the inner core lamellar cells are CD56$^+$ (brown in E), SOX10$^+$ (G), and BCL2$^+$ (H). The intermediate layer is CD34$^+$ (magenta in F), with six SYN$^+$ punctate axonal profiles (brown in F) visible within the inner core. Spurious staining is present in the trabecular smooth muscle in E, likely because of signal amplification for CD56. The vascular sinusoids are lined by CD34$^+$ endothelium (magenta in F). Contrast the single inner core in D–F with the triple inner core in I, highlighting the complexity of Pacinian structure depending on the plane of sectioning. (J) Small intrabulbar Pacinian with multiple neurofilament (NF$^+$) inner core axonal profiles (brown) and Glut-1$^+$ outer core (magenta) obtained from a different specimen from approximately the bulbar anatomical region indicated in A. Background staining is observed in the outer core interlamellar spaces. Although Glut-1 typically marks red blood cells, the magenta staining within the vascular sinusoids surrounding the Pacinian is background, likely because of the embalming mixture used in this specimen. (K–M) Serial sections of a large intratrabecular Pacinian corpuscle with highly complex interconnections between the outer core lamellar cells, expressing VIM (K), NGFR (L), and collagen type IV (COL-IV) (M) in the inner and outer cores and capsule. This Pacinian is from a different specimen from approximately the bulbar region indicated in A. (N) Flattened Pacinian corpuscle located in the plane between a cavernosal body and bulb, obtained from a paraffin block several mm proximal to A. Note the numerous elastic fibers (black) interwoven with collagen fibers surrounding the Pacinian and the absence of elastic fibers within the Pacinian itself. Most elastic fibers appear as short, rectangular profiles, reflecting their oblique orientation relative to the plane of section. For a fetal Pacinian in this anatomical position, see Figure 5A,C. (O) Large nerve bundles within the adipose tissue of the penile suspensory apparatus stained for reticulin (COL-III), which is richly distributed around peripheral nerve fibers. The nerve bundles are several mm proximal to the region indicated in A. These nerve bundles are heavily loaded with both unmyelinated and myelinated axons (not shown). (P) Typical Pacinian corpuscle with a single SYN$^+$ axonal profile (brown) surrounded by a CD34$^+$ intermediate layer (magenta), located within the penile suspensory system several mm distal to the region shown in A.

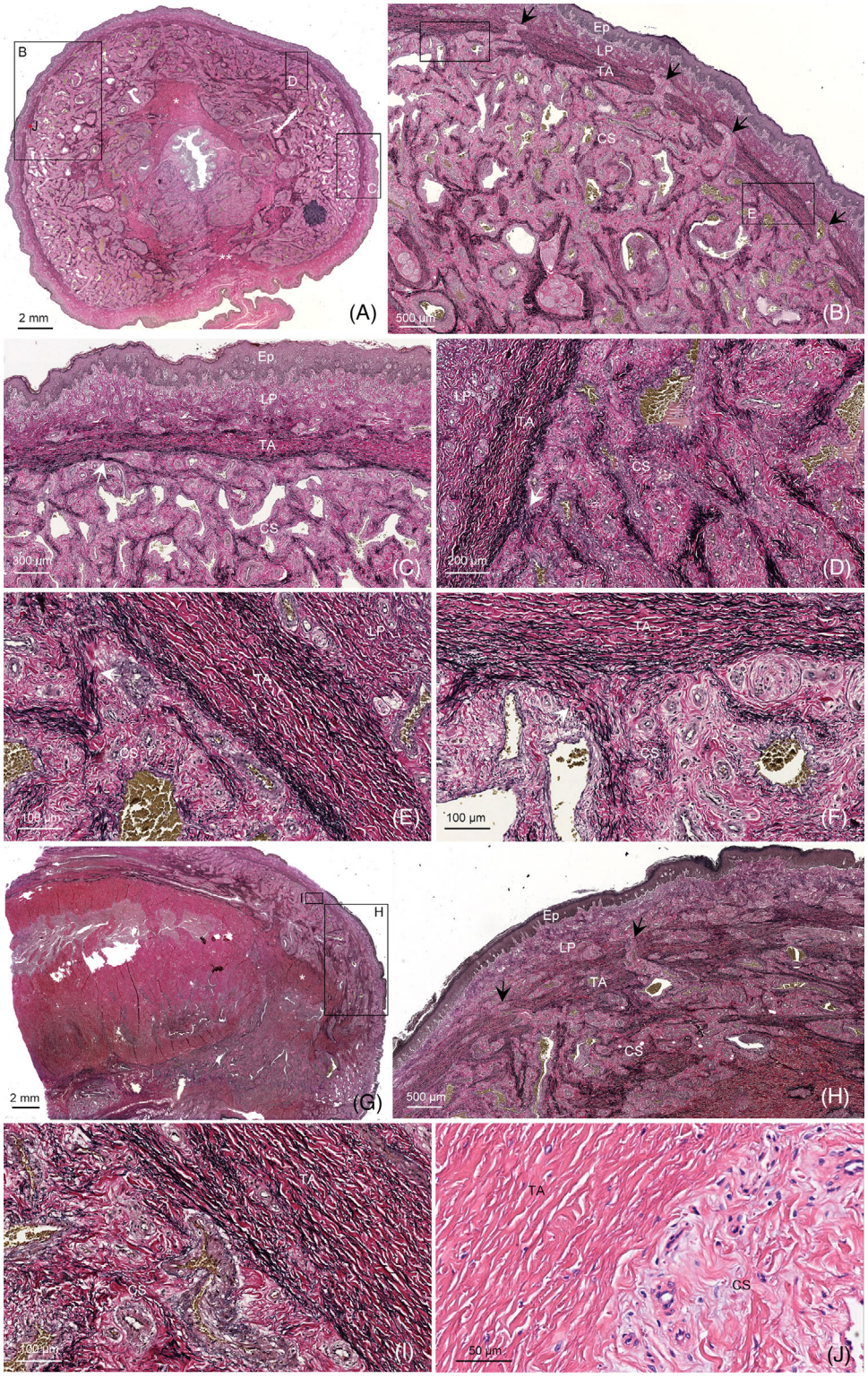

FIGURE 12 Tunica albuginea of the human adult penile glans in two specimens, one sectioned transversely and the other sagittally, stained for elastic fibers and HE. The glans contains a distinct histological layer between the lamina propria (LP) and the underlying glans corpus spongiosum (CS), composed of coarse collagen fibers and interwoven dense elastic fibers arranged in a thick multiaxial band parallel to the epithelium (Ep). Refer to Figure 1C for a detailed illustration of this histological layer by Krstić, which closely aligns with our current histological findings. (A) Transversely sectioned specimen from a 45-year-old individual, showing the anatomical positions of the other images. The distal or corporoglans ligament (*) and the lower midline septum (**), both structures with a low content of elastic fibers, are located dorsal and ventral to the urethra, respectively. The dark spot ventrolaterally is an artifact. The strand of tissue ventrally is part of the frenular region and ventral prepuce. (B) Higher magnification of the corresponding rectangle in A, showing the four histological layers of the glans: Ep, LP, tunica albuginea (TA), and CS. The glans tunica albuginea exhibits numerous perforating neurovascular elements (arrows). (C) Higher magnification of the corresponding rectangle in A,

This is followed by the corpuscular stage, where evidence of targeted ventral axonal pruning coincides with the emergence and organization of sensory corpuscles (fundamentally Pacinians), progressively refining the neural architecture toward its mature postnatal form. Thus, the corpuscular phase involves axon regressive events to refine the neural pattern to a more organized and mature circuitry. Across both developmental stages, however, heightened neural densities are observed in the ventral mesenchyme and stroma, and these densities persist postnatally in the frenular region and ventral glans.

Overall, our fetal results establish a basis for a detailed understanding of the neurodevelopmental biology of the human penis, inviting further exploration of axonal guidance strategies,[104] navigation through intermediate and final targets, molecular gradients of guidance cues, and axonal progressive and regressive events.[59] Table 1 details the main characteristics of fetal penile neurodevelopment during the pre-corpuscular and corpuscular stages. Preliminary, unpublished data from our laboratory suggest that a similar neurodevelopmental framework may also govern the fetal innervation of the vulva and clitoris. The following descriptions expand on the concepts introduced in Section 1.1.

4.2 | Pre-corpuscular and hyperinnervation stage (8–16 weeks)

Following the indifferent stage of sexual development, the penis begins to form at approximately 8–9 weeks of fetal age. As documented in our previous report,[56] in Aksel et al.,[22] and in the current study, dorsal nerve fibers are present at the distal tips of the fetal glans at these stages of development. These early fibers express NF, NSE, S100, CD56, PGP9.5, pan-TRK, and NGFR and continue to express these molecules into adulthood. Aksel et al.[22] reported an absence of nerve fibers at the distal tips of the fetal phallus at the indifferent stage, suggesting that navigating axons have reached an intermediate target but have not yet extended to their final distal destination. By 10 weeks of fetal age, nerve fibers are also observed at the distal preputial tip where the earliest signs of the developing prepuce begin to emerge. This indicates that navigating axons have crossed multiple intermediate targets to reach their final destinations at the distal penis by 8–10 weeks of fetal age. Notably, the developing corpora cavernosa, appearing at this stage as a hypercellular mesenchymal condensation lacking innervation, likely serves as a crucial intermediate target that exerts a strong chemoattractive influence on the pudendal nerve. This effect appears to contribute to the fasciculation of axons into the dorsal nerves, aligning them closely along the dorsal tunical surface.

The observation that the corpora cavernosa lack innervation at 8–10 weeks indicates an obvious sequence of innervation in the human penis, with extracavernosal sensory innervation established first, followed by the subsequent development of intracavernosal autonomic innervation. This suggests a developmental division of labor that contributes to the dual sensory-autonomic functionality of the penis. A series of experimental studies in rats, summarized by Georgiadis and Kringelbach,[3] highlight the critical role of genital sensory input during early sexual experiences in shaping sexual behavior patterns and motivations. Our findings on the early onset of sensory innervation relative to intracavernosal autonomic innervation in fetal penile development align with this body of work, suggesting that prenatal penile sensory input may contribute to the development of sexual sensation pathways. Prenatal penile afferent input, even if rudimentary and limited, might stimulate synaptic growth and differentiation, facilitating the organization and wiring of sensory pathways essential for functional postnatal sensory and sexual responses. This early sensory input could also hypothetically promote the development of intracavernosal autonomic innervation, potentially further stimulated by the emergence of developing Pacinians during the corpuscular phase. In any case, the specialized sensory function of the human penis may depend on a very early establishment of its sensory innervation pattern during fetal development.

It remains unknown whether the distal tips of the genital tubercle exert long-range axonal chemoattraction at the indifferent stage. However, we postulate that once axons reach their final targets at the distal tips of the developing glans and prepuce by 8–10 weeks, short-range

showing elastic fibers within the glans tunica albuginea arranged parallel to the epithelial surface, with zones of delamination (arrow) where they connect with the underlying glans fibroelastic skeleton. The four histological layers of the glans are visible again. (D) Higher magnification of the corresponding rectangle in A, further demonstrating the fibroelastic structure of the glans tunica albuginea between the LP and the underlying glans CS, with zones of delamination (arrow) connecting with the underlying glans fibroelastic skeleton. (E) Higher magnification of the corresponding rectangle in B, highlighting zones where elastic fibers of the tunica albuginea delaminate (arrow) to integrate with the fibroelastic skeleton of the CS beneath. (F) Additional magnification of the transverse section (corresponding rectangle in B), showing detailed views of elastic and collagen fiber arrangement in the tunica albuginea and their connection to the underlying glans fibroelastic skeleton (arrow). (G) Sagittally sectioned specimen from a 73-year-old individual, showing the anatomical positions of H and I. The corporeal tunica albuginea, poor in elastic fibers, extends distally to form the distal or corporoglans ligament (*). This ligament gradually increases in elastic fiber content, emitting fibroelastic extensions in all directions that ultimately communicate with the glans tunica albuginea. (H) Higher magnification of the corresponding rectangle in G, showing the glans tunica albuginea with a more irregular appearance and neurovascular perforators (arrows) connecting the LP and CS. (I) Higher magnification of the corresponding rectangle in G, providing detailed views of the elastic and collagen fiber arrangement within the tunica albuginea, along with the sharp transition between this layer and the CS. (J) High magnification view of a section from a different paraffin block from the same specimen and approximately the same lateral region indicated in A. HE-stained section showing a sharp transition between the glans tunica albuginea and the underlying CS. However, upon closer inspection of this microphotograph, collagen fibers in the glans tunica albuginea and CS are continuous, a feature observed throughout the whole penile circumference. In contrast, elastic fibers in the glans tunica albuginea, arranged parallel to the epithelial surface, delaminate in specific zones toward the underlying CS (arrows in C–F). TA, tunica albuginea.

axonal chemoattraction becomes a continuous process, contributing to the synchronized development of nerve fibers alongside their epithelial targets. By 8–10 weeks, Aksel et al.,[22] along with our current study, demonstrated that the thick dorsal nerve of the penis terminates in the ventral aspect of the glans near the prospective frenulum. Adult electrophysiological and anatomical dissection studies[86] have documented these ventral branches of the dorsal nerve within the glans corpus spongiosum, and they are illustrated in the adult penis in Figure 1A. Thus, the specialized sexual sensations and dense neural structures of the adult frenular area may depend on this early fetal innervation, as it establishes the sensory neural architecture within a fetal tissue environment where molecular cues guide axons to form stable, specialized connections and enable later exuberant branching, features that might not be replicated in later developmental stages.

By these fetal stages, the urethral groove remains open, whereas the urethral folds exhibit a dense supply of axons. Throughout urethral formation, the rapidly proliferating ventral epithelium remains notably thicker than the dorsolateral penile epithelia, as demonstrated in our previous[6] and in the current study. This thickened ventral epithelium may originate from the perineal thick epithelium initially observed in the sexually indifferent perineal region, as described by Hülsman et al.[105] van der Putte[90] also described this thickened stratified squamous ventral epithelium in the urethral folds, and sagittal penile microphotographs in other publications[42] display this feature, though its significance is rarely explicitly discussed. Hülsman et al.[105] noted that, although the function of thick skin in human embryos remains unknown, non-cornified thick skin in fetal rodents generally appears more permeable to chemicals than thinner, cornified skin epithelia. By this reasoning, one hypothesis is that the thickened ventral penile epithelium may be more permeable to endocrine and environmental factors, potentially linking this feature to both normal and abnormal urethral development. This increased permeability could expose the developing urethral region to hormonal imbalances or environmental disruptors, which may interfere with urethral closure and contribute to hypospadias formation.

The formation of the thickened ventral epithelium might depend on molecular signals from the underlying stroma. An alternative hypothesis, therefore, is that if stromal signaling is disrupted, the ventral epithelium may not thicken adequately, potentially leading to a lack of exposure to the hormonal or molecular cues essential for proper urethral closure. In this scenario, a factor contributing to the cascade of events leading to hypospadias may arise not from excess permeability but from the absence of the necessary epithelial thickening to receive essential developmental signals. This hypothesis aligns with van der Putte's work,[90, 106] which postulates that hypospadias results from underdevelopment of the stromal tissue beneath (or "dorsal to," in the embryological terminology he employs) the developing urethral orifice.

The thickened ventral penile epithelium may have additional functions critical to penile neurodevelopment. At approximately 12–16 weeks of fetal age, the developing ventral preputial epithelium reaches its maximum thickness and contains a dense and prominent network of pan-TRK$^+$, NGFR$^+$, CD56$^+$, PGP9.5$^+$, and NSE$^+$ intraepithelial nerve fibers. These fibers are also NF$^+$, S100$^+$, and SYN$^+$, though at extremely lower densities. The immunopositivity for pan-TRK and NGFR suggests that these fibers are equipped with the receptors needed to respond to neurotrophins (NTs). By this stage, intraepithelial fibers are found not only in the ventral prepuce but throughout all penile epithelia, with their notable density and exuberance primarily confined to the ventral prepuce and future frenular region. These microphotographs of exuberant ventral intraepithelial nerve fibers, static captures of dynamic in vivo axonal development, evoke foundational neuroscience concepts of nerve competition for neurotrophic sources,[107, 108] neurotropic influence of epithelial structures,[109] and the chemoattraction of axons over short and long distances by diffusible neurotropic substances.[107, 108]

As outlined in Section 1, we propose that this thickened ventral epithelium serves as a source of diffusible axonal guidance molecules with chemoattractant effects on penile sensory nerves, potentially forming a gradient of guidance cues that direct the precise innervation patterns observed in later stages of development. Concentrations of guidance cues and neuronal growth-promoting molecules would be highest in the developing ventral penile surface, gradually decreasing toward the dorsolateral and proximal penile regions. This gradient could direct the perineal nerve and the ventral branches of the dorsal nerve toward target areas of the developing ventral penis, including the future frenular region, where key sensory structures ultimately concentrate, supporting region-specific innervation essential for future sensory function. The gradient might contribute to the formation of the uniquely dense intraepithelial nerve fibers observed specifically in the ventral prepuce. In this way, this gradient may also help explain the adult macroscopic pattern of penile innervation, particularly the horsetail-shaped distribution of the ventral branches of the dorsal nerve observed in anatomical dissection studies.[110] This hypothesis leaves open the possibility of countergradients of axonal guidance cues in other penile regions, which could complement or modulate the proposed ventral gradient, ensuring balanced and region-specific sensory innervation across the entire penile surface.

The absence of developing sensory corpuscles throughout all of these progressive axonal processes defines this phase as the pre-corpuscular stage of penile sensory development. Although the specific molecules governing penile axonal progression and exuberant terminal branching remain unknown, as noted in Section 1, they may include NTs such as NGF, BDNF, NT-3, and GDNF, along with morphogens like BMP and Shh.[61, 62] Additionally, canonical axonal guidance molecules, including netrins, semaphorins, ephrins, and Slit-Robo ligands, and the corresponding axonal receptors, could play crucial roles in directing penile axonal growth and targeting.[59] Substrate-derived attractants, such as fibronectin and the basement membrane component laminin, along with cell adhesion molecules, are also anticipated to play roles in penile axon pathfinding. These molecules function as adhesive cues along permissive tissue substrata, facilitating axonal extension, guidance, and selective fasciculation.[59] The reader is referred to the works of Gordon-Weeks[111] (tables 3.1–3.4), Mencio et al.[112] (table 1), and Kolodkin and Pasterkamp[113] for detailed listings of molecules implicated in axonal pathfinding.

4.3 | Corpuscular and neural pruning stage (17–24 weeks)

As fetal penile development progresses, the thickened ventral preputial epithelium becomes markedly thinner, and the intraepithelial nerve fibers drastically decrease in density or disappear, suggesting the possibility of axonal pruning. Although the mechanisms behind this epithelial thinning remain unknown, it is possible that large preputial epithelial chunks shed or fragment into the amniotic fluid during penile development, suggesting that ventral preputial epithelial thinning and neural pruning may, at least in part, involve epithelial shedding. Additionally, the fetal glandopreputial common epithelium gradually disintegrates or luminizes to form the postnatal preputial sac (a virtual space), suggesting that the intraepithelial fibers it once contained are no longer present.

To our knowledge, Seto[32] was the first to propose a hypothesis of axonal regression in this specific context, suggesting that fetal penile intraepithelial nerve fibers degenerate and that their parent fibers ultimately form the genital corpuscles typically observed postnatally in these regions. Seto[32] stated (p. 289): "The intraepithelial fibres in the common epithelium accordingly attain the highest development in the 7th month, decrease abruptly in the 10th month and completely disappear with the final separation of the glans and prepuce epithelia. The genital nerve bodies not yet formed in the fetal stage are probably formed later by the thick stem fibres of these degenerated intraepithelial fibres." Seto thus proposed an ontogenetic relationship between fetal penile intraepithelial fibers and the densely arborized genital corpuscles observed postnatally, suggesting that the pruning of intraepithelial fibers represents a regressive event necessary for the subsequent maturation and reorganization of their parent fibers into specialized corpuscular sensory structures. In light of this scenario, it is necessary to consider potential mechanisms of axonal pruning and reorganization, which Seto[32] vaguely describes as "degeneration" followed by restructuring of parent or stem fibers to form mature genital corpuscles.

Classical models of axon pruning encompass two categories: small-scale and large-scale pruning.[60] Small-scale pruning is a stochastic and localized process of axonal elimination that refines neural networks by selectively eliminating exuberant or misguided axonal branches, rather than entire neurons (cell death) or large segments of axons. Terminal arbors can be eliminated by competition for neurotrophic factors and axosome shedding, and the pruning may also be regulated by neural activity. The intrinsic and extrinsic molecular factors mediating this type of pruning remain largely unknown. In contrast, large-scale pruning involves the elimination of entire axons, long axonal segments, or even entire neural populations to shape the structure and function of neural circuits.

In the fetal ventral prepuce, developmental axonal pruning appears to be a localized, small-scale process, potentially involving mechanisms that are unique or previously undescribed. The disproportionately thick ventral preputial epithelium thins, possibly as its epithelial cells are shed into the amniotic fluid, and the exuberant nerve fibers contained within this epithelium may undergo pruning during this process. This pruning process appears distinct from the large-scale elimination of entire neurons or substantial portions of axons, focusing instead on fine-tuning of existing neural pathways. As the thick ventral epithelium is shed, intraepithelial fibers remain within the glandopreputial common epithelium, albeit at reduced densities. These fibers are further pruned as development advances and the preputial sac takes shape.

At the same time, heightened stromal neural densities persist ventrally in the future frenular region, where we observed very high levels of SYN^+ axons. The typical $S100^+$ frenular neural densities observed in our transverse sections closely resemble, and are further supported by, a microphotograph presented by Cunha et al.[23] (see their Fig. 17F). Thus, the initial phenomenon of axonal pruning (a regressive event in neural development) in the fetal penis appears to be predominantly restricted to the exuberant intraepithelial fibers of the ventral prepuce, whereas the pruning of nerve fibers in the glandopreputial common epithelium occurs at later fetal stages and/or postnatally. Late-stage neural pruning in the stroma during the corpuscular stage cannot be excluded. However, if it occurs, it is more challenging to document compared to the pruning of the ventral exuberant fibers of the pre-corpuscular stage.

It is important to note that, although the corpuscular phase involves axonal regression, these events appear to be targeted and region-specific, predominantly affecting the ventral prepuce and glandopreputial common epithelium. Notably, these localized pruning processes occur within a broader context of ongoing axonal growth and proliferation, reflecting a dynamic balance between progressive and regressive neural events during the corpuscular phase of fetal penile neurodevelopment. Regardless of the underlying mechanisms driving axonal regression and pruning, our study found that this process coincided with the emergence of the first developing Pacinian corpuscles, which remained the only identifiable corpuscle morphotype until 24 weeks of fetal age. This suggests that other types of sensory corpuscles in the human penis develop at later fetal stages or postnatally. Winkelmann's[65, 66, 114] observations on the neonatal and adult prepuce (based on histological analysis of thousands of sections[66]) further support this notion, indicating that all other types of sensory corpuscles, at least within the prepuce, develop at later fetal stages and attain their characteristic postnatal morphologies only after the neonatal period. A major atlas[115] of human prenatal histology also supports this concept, indicating that Pacinian corpuscles are the earliest to emerge during human fetal development, with other corpuscle types appearing later.

As expected, the anatomical positions of immature fetal Pacinian corpuscles in the penis mirror their future adult locations. We identified developing Pacinian corpuscles in the glans, prepuce, frenular region, scrotum, penile bulb, and the tissue plane between the corpora cavernosa and corpus spongiosum. Additional locations included extracavernosal sites near the tunica albuginea along both longitudinal and transverse penile axes, within the tunica albuginea itself, intracavernosally (in one instance), within the bulbospongiosus muscle, and in the perineal skin region. Of these locations, the only ones not reproduced in adult tissues were the intra-albugineal, intracavernosal, and bulbospongiosus muscle positions, likely because of an insufficient number of sections analyzed. The oldest fetus analyzed, approximately

24 weeks of fetal age, exhibited Pacinian corpuscles that still lacked the typical adult morphology, although their molecular profiles closely matched the adult patterns.

The early and exclusive emergence of Pacinian corpuscles during this stage underscores their unique mechanosensory role and foundational importance in the maturation of the penile nervous system. These early Pacinians establish a baseline mechanosensory framework in the penis, potentially critical for various developmental processes and providing a specialized sensory modality fully functional at birth. Immature Pacinians and developing nerve fibers might respond to mechanical stimuli in utero, delivering mechanosensory input that refines neural pathways linking the peripheral and central nervous systems, thereby influencing the maturation of the somatosensory cortex and related brain regions. Such feedback could also hypothetically stimulate the subsequent development of fetal intracorporeal innervation and autonomic reflex pathways essential for postnatal erectile and ejaculatory functions. This early differentiation thus positions Pacinians as pivotal drivers of the human penile nervous system. The recent finding[116] that Piezo2-dependent mechanosensory activity shapes the development of touch receptors further supports the notion that fetal Pacinians and nerve fibers may actively refine peripheral and central neuroarchitecture, representing an in utero regulatory mechanism for the emergence of functional penile innervation.

During the corpuscular stage, we also documented the peripheral axonal branching pattern of nerve fibers in the distal preputial epithelial tips. Instead of penetrating the epithelium, these fibers branched two or three times from their parent fibers before contacting the basal surface of the epithelium, suggesting a developmental strategy for maximizing sensory coverage and signal integration. This distinct branching pattern likely represents another developmental phase different from the pre-corpuscular stage, governed by a unique tissue environment and a distinct or partially overlapping set of molecular cues. The noteworthy presence of red blood cells (Glut-1$^+$) in the developing frenular region has also been observed by Cunha et al.[23] (see their Figure 7), who suggested that it may indicate ongoing morphogenetic activity in the formation of the urethral meatus. However, they did not report that many of these cells appear extravasated and unassociated with CD31$^+$ blood vessels. The potential connection between red blood cells and axonal guidance in this context, if any, warrants further investigation.

In summary, fetal penile innervation appears to progress from an initial phase of axonal hyperinnervation, characterized by exuberant ventral intraepithelial fibers within disproportionately thickened epithelia and an absence of developing sensory corpuscles (pre-corpuscular stage), to a pruned pattern with thinner ventral epithelia and the emergence of developing Pacinian corpuscles (corpuscular stage). This process culminates in the refined postnatal and adult pattern, marked by a diversity of corpuscular receptors and nerve bundles encased in perineurium, with higher neural densities concentrated in the distal ventral aspect (frenular delta and region). Postnatal neural pruning phenomena in the human penis cannot be excluded and require thorough analysis. Figure 6 depicts a schematic overview of the pre-corpuscular/hyperinnervation and corpuscular/neural pruning stages of fetal penile neurodevelopment, illustrated in sagittal section.

Moving forward, it will be essential to develop a more mechanistic understanding of the neuroembryological processes described here, which offer a framework for exploring the molecular interactions that underlie them. As discussed, the intrinsic and extrinsic molecular cues involved (including axonal guidance molecules, NTs, morphogens, and their respective receptors) may not only shape postnatal penile innervation patterns critical for sexual sensation and function, but their dysregulation may also contribute to the development of congenital penile anomalies such as hypospadias.[22]

4.4 | Adult specimens

Our study utilized a unique combination of low-, medium-, and high-power microphotographs to situate sensory corpuscles and nerve bundles within broader anatomical regions, providing panoramic views of the innervation patterns. The ventral innervation bias observed in fetal tissues appears to persist into adulthood, with higher concentrations of nerve bundles and distinctive clusters of sensory corpuscles in the adult frenular region. In this area, clusters of up to 17 sensory corpuscles, densely packed together, are a unique feature. These corpuscular receptors and nerve bundles arise from direct projections of the perineal nerve and ventral projections of the dorsal nerve (Figure 1A). In contrast, although the glans has high densities of sensory corpuscles, these corpuscles consistently appear in isolation rather than forming clusters, as observed in the prepuce and frenular region. Glans sensory corpuscles are distributed across three tissue compartments: (i) those in the lamina propria, which include a variety of types such as genital corpuscles, Krause corpuscles, Golgi-Mazzoni corpuscles, small Pacinian and Paciniform corpuscles, as well as others that are challenging to classify; (ii) those located deeper within the glans corpus spongiosum, typically limited to small Pacinian, smaller Paciniform, and Golgi-Mazzoni corpuscles; and (iii) those found in the lamina propria of the glanular urethra, which are usually small but can exhibit densely arborizing axons. These corpuscles are generally non-Pacinian and are positioned near the urethral epithelium.

We postulate that the high-density sensorineural terminal architecture of the human penis, concentrated in the frenular region, the remainder of the prepuce (including the coronal sulcus), and the glans, progressively diminishes toward the proximal penile regions. Together, this arrangement, along with an opposing proximodistal density gradient of nitrergic autonomic fibers in the intracavernosal compartment (with higher densities proximally that gradually decrease distally), constitutes what we refer to as the gradient hypothesis, an organizational model that integrates sensory and autonomic distribution patterns across penile tissues.[6] A detailed immunohistochemical study by Jang et al.[28] complements our findings by providing elegant visual documentation of the dense S100$^+$ sensorineural anatomy in the frenular region (see their figures 2C and 3D, with 4C and 5C as respective higher magnification views) and suggests that deep ventral incisions

could compromise this innervation and result in sensory damage. Further research is needed to clarify whether the specific deep ventral nerve structures that Kinsey[17] suggested underlie penile erogenous sensation play a role (Table S1).

4.5 | Penile sensory corpuscles and their molecular profiles: novel identification of CD10 in Pacinian corpuscles and perineurial markers in genital corpuscle capsules

Our findings on the immunohistochemical profiles of penile sensory corpuscles build upon our previous works, which analyzed the protein compositions of penile sensory corpuscles.[6,46] In this study, we presented data on the immunohistochemical properties of adult sensory corpuscles from the prepuce, glans, urethra, and intracorporeal regions. The molecular profiles of the specific types of sensory corpuscles were consistent across all these regions. Table 2 summarizes these data. Although most of the immunoreactivities identified in this study have been previously reported in sensory corpuscles from extra-genital regions,[117] our work is the first to demonstrate these molecular profiles in specific regions of the human fetal and adult penis. Regardless of the functional significance of these molecules in sensory corpuscles, our data demonstrate that they serve as reliable markers for identifying specific components of sensory corpuscles in the penis. To the best of our knowledge, this study is also the first to report the presence of CD10 in Pacinian corpuscles and the localization of perineurial markers (Glut-1, EMA, CD10, α-SMA, and VIM) in the capsules of deep-dermal genital corpuscles.

4.6 | CD10: a regulator of Pacinian morphology?

The distinct gradient of CD10 immunostaining in the Pacinian outer core, concentrated near the inner core, suggests a role in spatially regulated ECM remodeling via localized enzymatic degradation of bioactive peptides. CD10, a membrane-bound endopeptidase, might modulate the availability of signaling peptides that govern ECM synthesis and degradation, thereby influencing Pacinian interlamellar architecture. Its enrichment in outer core regions with narrower interlamellar spaces supports a model in which high CD10 activity limits ECM accumulation through enhanced peptide turnover, maintaining tight lamellar packing, whereas reduced or absent outer core peripheral CD10 expression permits ECM buildup and interlamellar loosening. As shown by double immunofluorescence, the CD10 immunolocalization is distinct from that of CD34 in the intermediate layer; however, their spatial proximity suggests that CD10-mediated peptide regulation may also influence the activity of $CD34^+$ cells. This finding points to CD10 as a potential modulator of Pacinian corpuscle morphology (and possibly morphogenesis) through targeted enzymatic control of ECM dynamics. We did not investigate CD10 expression in fetal Pacinians during the corpuscular phase of penile sensory development, leaving room for further studies to explore this aspect. Further elaboration on this hypothesis is provided in the relevant section of the Supporting Information section.

4.7 | Preputial genital corpuscles show molecular continuity with nerve sheaths and features for fine-tuning erogenous sensation

In this study, we identified a distinct subpopulation of ventral preputial genital corpuscles whose capsules express both endoneurial (CD34) and perineurial (Glut-1, EMA, α-SMA, CD10, VIM) markers, suggesting structural and molecular continuity with peripheral nerve sheaths, similar to what has been described for Pacinian corpuscles.[117] This population of corpuscles was preliminarily documented in our earlier study on WT1 expression in sensory corpuscles.[46] These corpuscles were identical to the deep-dermal encapsulated genital corpuscles previously identified by Halata and Munger[13] in the glans (refer to their Figure 10) and showed direct continuity between the perineurium of the supplying nerve bundle and the corpuscular capsule. Serial sectioning revealed heterogeneous axonal populations within these corpuscles: Larger NF^+ axons likely associated with fast conduction, and smaller, densely packed SYN^+ and NSE^+ axons lacking detectable NF expression, suggesting potential neurosecretory or modulatory sensory roles. This molecular heterogeneity implies a refined capacity for sensory signal modulation, possibly related to the encoding of affective, pleasant touch. These findings highlight a previously unrecognized population of genital corpuscles with specialized structural and functional features, potentially involved in fine-tuning erogenous sensation and contributing to the nuanced sensory dynamics of genital tissues. A more detailed analysis is available in the corresponding section of the Supporting Information Section.

4.8 | Novel identification of Pacinian corpuscles within the penile bulb suggests a bimodal distribution of intracorporeal sensory corpuscles spanning the bulb and glans

Excluding the glans corpus spongiosum, this study (together with our recent work[46]; see figure 3 therein) provides the first unambiguous histological identification of mechanosensory end organs located deep within the human penile erectile tissues. Specifically, we identified sparse, isolated Pacinian corpuscles along with their immunohistochemical profiles within the fetal and adult penile bulb. These corpuscles shared the same molecular profile as those in the glans and prepuce. Together with glans Pacinians, they form a bimodal distribution of intracorporeal sensory corpuscles, present proximally in the bulb and distally in the glans, but absent or extremely rare in the shaft corpus spongiosum and corpora cavernosa. This distribution suggests a specialized role in detecting mechanical changes related to vascular engorgement in these regions and reflexive processes such as ejaculation. We found only one intracavernosal fetal Pacinian despite exhaustive sampling, supporting the rarity of such end organs within

the corpora cavernosa. Although intracorporeal corpuscular receptors in the human penis have been sporadically mentioned in the literature, such reports are typically anecdotal and lack clear histological documentation.[31, 118] Our findings support the idea that penile intracorporeal mechanosensory input is predominantly mediated by FNEs, whereas Pacinians may contribute to reflex modulation and erogenous sensation in the bulb and glans. For an expanded analysis and full contextual discussion of these findings within the literature, refer to the Supporting Information section under the same title.

4.9 | The preputial dartos: its ontogeny and functional innervation revealed

Our focus now shifts to the preputial dartos, which at first glance is unrelated to penile sensory mechanisms. This study provides the first near-complete ontogenetic mapping of the human preputial dartos, revealing it as the earliest developing penile smooth muscle layer, with a dense, multi-directional arrangement of α-SMA$^+$ muscle bundles and extensive adult noradrenergic innervation. Using multiple sectioning planes and immunohistochemical markers, we documented its autonomic innervation by TH$^+$, CD56$^+$, NSE$^+$, SYN$^+$, and NGFR$^+$ fibers forming diffuse plexuses, with much lower densities of VIP$^+$, NPY$^+$, and nNOS$^+$ fibers, suggesting a global en passant pattern of autonomic control. These data indicate a primarily sympathetic regulation of dartoic tone and contractibility, potentially modulating preputial tension, thermoregulation, and sexual function. We propose that involuntary dartos contractions may dynamically influence the spatial positioning and sensitivity of nearby sensory corpuscles, enhancing tactile and erogenous sensation during movement, erection, and orgasm. We also showed that the frenular region contains richly innervated smooth muscle bundles, possibly contributing to orgasmic contraction reflexes. Variability in dartos preservation following circumcision (depending on surgical incision depth and extense of resection) may influence penile structure and sensitivity by altering this muscle layer and its integrated innervation. For a more detailed discussion of these findings and the supporting literature, refer to the corresponding section in the Supporting Information Section.

4.10 | Tunica albuginea of the glans: resolving an anatomical question and elucidating its functional significance

Our histological analysis revealed a distinct fibroelastic layer approximately 0.5 mm thick between the glans lamina propria and the underlying corpus spongiosum, corresponding to a superficial tunica albuginea of the glans. Special elastic stains demonstrated this layer's complex three-dimensional network of elastic fibers, oriented longitudinally, transversely, and obliquely. These fibers connected radially with the trabeculae of the glans corpus spongiosum and with distal extensions of the tunica albuginea of the corporeal bodies, forming an integrated fibroelastic scaffold. Numerous perforating nerve bundles and blood vessels traversed this layer, suggesting a role in neurovascular distribution.

These findings support classical anatomical descriptions by Krstić,[40] Szymonowicz and Krause,[41] and align with recent data by Lee et al.[39] They challenge prevailing three-layer glans models[13, 42, 43] and substantiate a four-layer structure: epithelium, lamina propria, tunica albuginea, and corpus spongiosum. This refined model has implications for anatomical teaching and penile cancer staging and may explain characteristic patterns of carcinoma spread in the glans, including horizontal dissemination to the inner prepuce and vertical progression only in aggressive tumors that destruct the tunica albuginea or breach tunical discontinuities.[42, 119] The presence of this histological layer in the clitoral glans or its possible sexual dimorphism remains unexplored and warrants further study.

Functionally, the glans tunica albuginea appears adapted to support glans firmness during erection through its high elastic fiber content, distinguishing it from the more collagenous, thick, and rigid tunicae of the corporeal bodies. It likely facilitates controlled glans expansion, distributes intraspongiosal pressure in the glans, and protects against mechanical trauma during penetration. Moreover, by embedding dorsal nerve branches and organizing their distribution, it contributes to the spatial architecture of glans innervation in the lamina propria. Compression of sensory structures (corpuscles and FNEs in the lamina propria), situated between the epithelium and tunica albuginea, by engorged glans sinusoids may enhance tactile feedback through interoceptive stimuli. Our fetal data suggest that elastogenesis of the glans tunica albuginea begins after 24 weeks of fetal age, once nerves have already navigated and reached their final targets in the fetal distal glans (pre-corpuscular stage), indicating a role in maintaining rather than providing axonal guidance during fetal neurodevelopment.

Last, the glans tunica albuginea may help explain the mechanism of action and persistence of hyaluronic acid gel injections used for glans augmentation and the treatment of premature ejaculation.[120, 121] It defines the superficial tissue compartment composed of the lamina propria and the immediately subjacent tunica albuginea, where the injected hyaluronic acid primarily diffuses. However, these injections pose a risk of damaging the tunica albuginea, potentially compromising its structural integrity and affecting glans erection. Our identification of the glans tunica albuginea highlights the need for a more rigorous evaluation of the safety profile of glans-injected bulking agents to mitigate potential risks to glans architecture and function. The corresponding section of the Supporting Information Section offers a more detailed examination of our crucial finding regarding the glans tunica albuginea.

4.11 | Penile neurotomy

PN, an experimental and not recommended[122–126] intervention for lifelong premature ejaculation, involves severing or cauterizing the penile perineal nerves and/or the ventral branches of the dorsal nerve that supply the frenular delta (Figure 1A),[127–130] an anatomical epicenter of specialized sexual sensation (Figure 1B). PN originated in Brazil

in the late 1980s,[131, 132] and quickly raised ethical alarm, leading to the 1997 resolution of the Brazilian Federal Council of Medicine (Conselho Federal de Medicina),[133] which deemed the procedure experimental and restricted its use to approved research settings. In intact patients, PN is usually performed during circumcision together with a complete frenulectomy.[127] A variety of surgical loupes and magnification devices are typically used to locate and sever the targeted nerves. The implications of such aggressive nerve-ablative disruption extend beyond the intended prolongation in ejaculatory latency time, with documented cases of permanent erogenous sensation loss, erectile dysfunction,[134] and profound psychological sequelae.[135] Psychotic episodes have been reported,[135, 136] likely stemming from the deep neural and hedonic impact of compromising frenular delta innervation, a structure uniquely adapted for transmitting pleasurable sensations tied to sexual reward and satisfaction.[4, 10]

Despite an alarming lack of robust scientific evidence, ethical regulations,[133] and the absence of recommendation in urological guidelines,[122–126] PN has proliferated internationally within urology since the 1990s, often executed under dubious circumstances,[133, 137–139] including cases where young adults presumptively underwent the procedure without informed consent during circumcision.[137] Between the more than 4000 PN cases reported in a multicentric trial by Dias Bautista et al.[129] in 2001 and the 44,000 cases documented in South Korea[136] alone by 2013, the historical tipping point appears to have occurred in the adoption of this practice—despite limited scientific evidence and the absence of ethical or regulatory oversight that should have prevented the uncontrolled dissemination of this experimental procedure. The historical trajectory of PN serves as a clear example of how surgical practices should not be disseminated and integrated into the standard surgical armamentarium for treating specific conditions. There is an urgent need for robust regulatory oversight to mitigate the harm associated with this historically and ethically fraught practice.

4.12 | Penile circumcision

Our results reinforce the relevance of Cold and Taylor's[11] 1999 conclusions (p. 42), which now seem more pertinent than ever: "The prepuce is a specialized, specific erogenous tissue in both males and females. Therefore, surgical excision should be restricted to lesions that are unresponsive to medical therapy…Preputial plasty should be considered in place of circumcision whenever possible, so as to preserve the corpuscular sensory receptors, dartos muscle, penile mucosa and complete function of the penis…Although a Fourcroy grade 1 female circumcision would excise less tissue than in a male, this comparison cannot be used to justify female circumcision. Excision of normal, erogenous genital tissue from healthy male or female children cannot be condoned, as the histology confirms that the external genitalia are specialized sensory tissues… Removal of normal genital anatomy in children and infants should be deferred until the individual can make an informed decision. If external genital tissue must be excised to combat a disease process that threatens the child's health, and is unresponsive to medical therapy, then the amount of tissue should be limited so as to preserve the anatomy and function of the external genitalia."

Regarding adult circumcision, the current knowledge of preputial and penile neuroanatomy and structure underscores the importance of meticulous patient selection for this procedure. Specifically, when adult circumcision is to be performed, factors such as the position of the circumcision scar line, the amount of inner prepuce retained, the tightness of the remaining penile skin, and whether a frenulectomy is performed should be carefully discussed and agreed upon by both the patient and the surgeon, with all decisions clearly documented in the informed consent. Recent survey findings underscore this need for dialogue: Callegari et al.[140] showed that preferences regarding the amount of inner preputial remnant retained after circumcision vary considerably among individuals, reinforcing the importance of engaging patients in personalized discussions to align surgical decisions with their expectations.

The findings of this study, which highlight the complexity and richness of preputial and penile innervation, musculature, and vasculature, should be integrated into informed consent discussions and documents to ensure comprehensive counseling for parents contemplating the procedure for their children and for individuals considering adult circumcision. Although penile sensory loss can be clinically assessed using tools such as Semmes-Weinstein monofilaments, biothesiometry, and somatosensory evoked potentials (SSEPs), it has been argued that objective evaluations do not always align with a patient's sensory experience in an erotic context.[4] For example, SSEPs may be normal even in patients with significant sensory deficits because of the complexity and redundancy of sensory pathways.[141, 142] Validated patient-reported outcome measures, such as the Self-Assessment of Genital Anatomy and Sexual Function in Male questionnaire, provide site-specific assessments of genital sensation and sexual function that could enrich patient counseling and enhance procedural outcome evaluations both before and after penile surgery.[4] Circumcision incisions should always be performed as superficially as is possible. Given that the frenular delta region is widely regarded as a primary contributor to penile sexual sensation,[4, 5, 8, 9, 24] special care must be taken with ventral incisions to avoid damaging the dense and complex neuroanatomy in this area.[6, 8, 28] Our work offers valuable insights for penile surgeons, providing a rich perspective on the exquisitely innervated and structurally complex tissues they routinely resect, cauterize, and mobilize, tissues whose neural composition may often be underestimated or overlooked.

4.13 | Limitations

The limitations of this study include the absence of postnatal tissue analysis spanning the neonatal period to early adulthood, the use of an alcohol-based fixative in the arterial perfusion method for some adult specimens, the lack of quantitative data for neural density analyses, possible imprecisions in fetal age determination, and the inability to directly observe neural pruning phenomena during fetal penile development. Regarding the first limitation, the absence of tissues from this

age range excludes the analysis of critical developmental stages during which penile neurodevelopment continues, including the emergence of non-Pacinian sensory corpuscles. We acknowledge this gap and are actively working to address it. For the second limitation, as described in Section 2, we conducted preliminary analyses to ensure the preservation of critical tissue antigens and optimized immunohistochemistry conditions for the alcohol-based fixative. These analyses yielded good results, as demonstrated by the quality of the microphotographs presented in this study. For the third limitation, although the inclusion of numerical data through stereological or image analysis techniques is valuable, it is not always essential for studies evaluating neural densities. When a sufficiently large and representative number of sections per paraffin block is analyzed, semiquantitative assessments can provide reliable and accurate insights into the patterns of neural density distribution in a tissue. Concerning the fourth limitation, as noted by Himelreich Perić et al.[143] and Li et al.,[144] fetal ages reported in peer-reviewed studies are best approximations and are subject to interindividual variability in developmental pace. Nonetheless, we are confident that the sequence of neurodevelopmental processes documented in this study (from a pre-corpuscular phase of axonal hyperinnervation to the emergence of sensory corpuscles and neural pruning) reflects the chronological trajectory of penile innervation, irrespective of fetal staging imprecisions. Finally, the lack of direct observation of neural pruning limits our ability to precisely characterize the mechanisms driving axonal remodeling in the prospective frenular region and ventral prepuce during penile morphogenesis.

4.14 | Concluding remarks

> "The most important source of sensory nerve signals for initiating the male sexual act is the *glans penis*. The glans contains an especially sensitive sensory end-organ system that transmits into the central nervous system that special modality of sensation called *sexual sensation*. The slippery massaging action of intercourse on the glans stimulates the sensory end organs, and the sexual signals in turn pass through the pudendal nerve, then through the sacral plexus into the sacral portion of the spinal cord, and finally up the cord to undefined areas of the brain." **Guyton and Hall Textbook of Medical Physiology,[145] p. 1026**

Sexual science aims to bridge the gap between rigorous scientific inquiry and the complexities of human sexual anatomy, function, and experience. Our current immunohistological and morphological investigation of the human fetal and adult penis contributes to this field by advancing our understanding of its peripheral sensory structures, their development, and their role in sexual physiology. Over 70 years ago, Kinsey[17] urged anatomists to identify the precise nerves responsible for penile sexual sensation (Table S1); our study represents a step toward fulfilling that call with modern immunohistological tools. Although this may seem self-evident to anyone attuned to the sensations of their penis during sexual activity, our work scientifically validates the existence of a ventral penile anatomical region that serves as a center of sexual sensation, commonly referred to as the frenular delta.[10] In essence, the presence of a sensory center in the penis, akin to a "G-spot," emerges as a neuroanatomical reality, rooted in its embryological origins and underscoring its vital role in sexual sensation, function, and experience.

Although the classical description in Guyton and Hall[145] positions the glans as the primary source of penile sexual afferent signals, our study—alongside existing literature and the experiential knowledge of most sexually functional individuals[4, 5, 8, 9, 24]—supports a revised paradigm in which the distal ventral penile surface, particularly the frenular delta and surrounding region, constitutes the principal neurological locus of penile sexual sensation. That the "female G-spot" has inspired decades of controversy whereas the penile erotogenic center—so evident in structure and sensation—has remained underexamined in the scientific literature underscores persistent blind spots in sexual medicine and urology. However, we hope to have provided not only a scientific contribution that offers new perspectives into penile neurodevelopment and morphology but also a divertimento, an enjoyable exploration for the neurohistology aficionado who, paraphrasing del Río Hortega,[146] is captivated by the pictorial beauty and artistic emotion revealed through the polychromatic lens of histology.

A specter haunts the field of sexual science: the specter of a neuroscience of the human genitalia solidly grounded in basic morphological sciences. Some argue that the neuroscience of the human penis remains underdeveloped, particularly regarding its sensory function.[147] Others may consider penile morphology a static field with little left to discover, yet the complexity of the structures we have observed and the embryological mysteries they present suggest otherwise. In some cases, as with the glans tunica albuginea, anatomical information has been forgotten and must be redescribed. Although significant progress has been made in elucidating penile neuroanatomy, vulvar neuroanatomy and morphology remain grossly underexplored, leaving substantial gaps in our understanding of their role in sexual function and experience. In this work, we have attempted to lay the groundwork for a neurodevelopmental understanding of the peripheral mechanosensory components of the human penis. Studies of vulvar and clitoral sexual neuroanatomy are underway in our laboratory, aiming to address the long-standing imbalance in research. We seek to give voice to the specter, hoping to shed light on what has been overlooked, misunderstood, or willfully ignored.

AUTHOR CONTRIBUTIONS

Alfonso Cepeda-Emiliani conceptualized the study and drafted the manuscript. Alfonso Cepeda-Emiliani, Tomás García-Caballero, Rosalía Gallego, and Lucía García-Caballero collaborated on subsequent drafts and the final version. Alfonso Cepeda-Emiliani, Marina Gándara-Cortés, María Otero-Alén, Juan Suárez-Quintanilla, Tomás García-Caballero, Rosalía Gallego, and Lucía García-Caballero performed histological and immunohistological analyses. Alfonso Cepeda-Emiliani, Marina Gándara-Cortés, María Otero-Alén, Juan Suárez-Quintanilla, Tomás García-Caballero, Rosalía Gallego, and Lucía García-Caballero

interpreted the results. All authors revised and approved the final manuscript.

ACKNOWLEDGMENTS

We express our deepest gratitude to those who donated their bodies to science, and to their families, for enabling anatomical research that advances scientific knowledge and improves patient care. We are grateful to Professor María Teresa Vázquez Osorio for providing access to specimens from the Body Donation and Dissecting Room Center of the Complutense University of Madrid. We also thank Alejandro García-Pérez for contributing the artwork in Figures 1A,B and 6A–D, as well as the anonymous reviewers for their valuable feedback.

CONFLICT OF INTEREST STATEMENT

The authors declare no conflicts of interest.

DATA AVAILABILITY STATEMENT

Data supporting results of this study are available from the corresponding author upon reasonable request.

ORCID

Alfonso Cepeda-Emiliani https://orcid.org/0000-0003-2170-2733
María Otero-Alén https://orcid.org/0000-0002-0640-5776
Juan Suárez-Quintanilla https://orcid.org/0000-0001-8114-6834
Marina Gándara-Cortés https://orcid.org/0000-0001-5129-0712
Tomás García-Caballero https://orcid.org/0000-0002-7938-1437
Rosalía Gallego https://orcid.org/0000-0002-6015-4680
Lucía García-Caballero https://orcid.org/0000-0003-0116-1263

REFERENCES

1. McKenna KE. What is the trigger for sexual climax?. *Arch Sex Behav*. 2022;51(1):383-390. doi:10.1007/s10508-021-02164-9
2. Tajkarimi K, Burnett AL. The role of genital nerve afferents in the physiology of the sexual response and pelvic floor function. *J Sex Med*. 2011;8(5):1299-1312. doi:10.1111/j.1743-6109.2011.02211.x
3. Georgiadis JR, Kringelbach ML. Intimacy and the brain: lessons from genital and sexual touch. In: Olausson H, Wessberg J, Morrison I, McGlone F, eds. *Affective Touch and the Neurophysiology of CT Afferents*. Springer; 2016:301-321.
4. Claeys W, Bronselaer G, Lumen N, Hoebeke P, Spinoit AF. The self-assessment of genital anatomy, sexual function, and genital sensation (SAGASF-M) questionnaire in a Belgian Dutch-speaking male population: a validating study. *Andrology*. 2023;11(3):489-500. doi:10.1111/andr.13348
5. Ruesink GB, McGlone FP, Olausson H, et al. A psychophysical and neuroimaging analysis of genital hedonic sensation in men. *Sci Rep*. 2022;12(1):10181. doi:10.1038/s41598-022-14020-4
6. Cepeda-Emiliani A, Gándara-Cortés M, Otero-Alén M, et al. Immunohistological study of the density and distribution of human penile neural tissue: gradient hypothesis. *Int J Impot Res*. 2023;35(3):286-305. doi:10.1038/s41443-022-00561-9
7. Colonnello E, Limoncin E, Ciocca G, et al. The lost penis syndrome: a new clinical entity in sexual medicine. *Sex Med Rev*. 2022;10(1):113-129. doi:10.1016/j.sxmr.2021.08.001
8. Schober JM, Meyer-Bahlburg HF, Dolezal C. Self-ratings of genital anatomy, sexual sensitivity and function in men using the "self-assessment of genital anatomy and sexual function, male" questionnaire. *BJU Int*. 2009;103(8):1096-1103. doi:10.1111/j.1464-410X.2008.08166.x
9. Sorrells ML, Snyder JL, Reiss MD, et al. Fine-touch pressure thresholds in the adult penis. *BJU Int*. 2007;99(4):864-869. doi:10.1111/j.1464-410X.2006.06685.x
10. McGrath K. The frenular delta: a new preputial structure. In: Denniston G, Hodges F, Milos M, eds. *Understanding Circumcision: A Multi-Disciplinary Approach to a Multi-Dimensional Problem*. Kluwer Academic/Plenum; 2001:199-206.
11. Cold CJ, Taylor JR. The prepuce. *BJU Int*. 1999;83:34-44. doi:10.1046/j.1464-410x.1999.0830s1034.x
12. Taylor J, Lockwood A, Taylor A. The prepuce: specialized mucosa of the penis and its loss to circumcision. *Br J Urol*. 1996;77(2):291-295. doi:10.1046/j.1464-410x.1996.85023.x
13. Halata Z, Munger BL. The neuroanatomical basis for the protopathic sensibility of the human glans penis. *Brain Res*. 1986;371(2):205-230. doi:10.1016/0006-8993(86)90357-4
14. Hyrtl J. Practical remarks on the surgical anatomy of the penis. *Med Surg Rep*. 1875;32:327-330. https://ia800400.us.archive.org/22/items/medicalsurgicalr1875phil/medicalsurgicalr1875phil.pdf
15. Van de Velde TH. *Ideal Marriage: Its Physiology and Technique*. William Heinemann Medical Books; 1940:119.
16. Willy A, Vander L, Fisher O. *The Illustrated Encyclopedia of Sex*. Cadillac Publishing; 1950:48.
17. Kinsey AC, Pomeroy WB, Martin CE, Gebhard PH. *Sexual Behavior in the Human Female*. W.B. Saunders Company; 1953:573.
18. Zwang G. *La Fonction Érotique*. Éditions Robert Laffont; 1972.
19. Young JZ. *An Introduction to the Study of Man*. Oxford University Press; 1974:187.
20. Masters WH, Johnson VE. *Homosexuality in Perspective*. Little, Brown and Company; 1979:73.
21. Love B. *The Encyclopedia of Unusual Sex Practices*. Barricade Books Inc; 1992:104.
22. Aksel S, Derpinghaus A, Cao M, Li Y, Cunha G, Baskin L. Neurovascular anatomy of the developing human fetal penis and clitoris. *J Anat*. 2024;245(1):35-49. doi:10.1111/joa.14029
23. Cunha GR, Sinclair A, Cao M, Baskin LS. Development of the human prepuce and its innervation. *Differentiation*. 2020;111:22-40. doi:10.1016/j.diff.2019.10.002
24. Bronselaer GA, Schober JM, Meyer-Bahlburg HFL, T'Sjoen G, Vlietinck R, Hoebeke PB. Male circumcision decreases penile sensitivity as measured in a large cohort. *BJU Int*. 2013;111(5):820-827. doi:10.1111/j.1464-410X.2012.11761.x
25. Moldwin R, Valderrama E. Nerve distribution patterns within prepucial tissue: clinical applications in penile nerve blocks. *Anesth Analg*. 1990;70(2):S270-S270.
26. Kaneko S, Bradley WE. Penile electrodiagnosis: penile peripheral innervation. *Urology*. 1987;30(3):210-212. doi:10.1016/0090-4295(87)90235-4
27. Yang CC, Bradley WE. Innervation of the human glans penis. *J Urol*. 1999;161(1):97-102.
28. Jang HS, Hinata N, Cho KH, Bando Y, Murakami G, Abe SI. Nerves in the cavernous tissue of the glans penis: an immunohistochemical study using elderly donated cadavers. *J Anat Soc India*. 2017;66(2):91-96. doi:10.1016/j.jasi.2017.11.001
29. Dogiel AS. Die nervenendigunngen in der schleimhaut der aussen genitalorgane des menschen [The nerve endings in the mucosa of the external genital organs of humans]. *Arch F Mikr Anat*. 1893;41:585-612.
30. Ramón y Cajal S. *Texture of the Nervous System of Man and the Vertebrates*. Springer Vienna; 1999:422. doi:10.1007/978-3-7091-6435-8
31. Ohmori D. Über die Entwicklung der Innervation der Genitalapparate als peripheren Aufnahmeapparat der genitalen Reflexe [On the development of the innervation of the genital apparatus as a peripheral receptor apparatus of genital reflexes]. *Z Anat Entwickl Gesch*. 1924;70:347-410.

32. Seto H. *Studies on the Sensory Innervation (Human Sensibility)*. 2nd ed. Charles C Thomas Publisher; 1963.
33. Bischoff A. Skin receptors of the human prepuce. In: Rohen JW, ed. *Functional Morphology of Receptor Cells*. Akademie der Wissenschaften und der Literatur. 1978:64-87.
34. Abraham A. *Iconography of Sensory Nerve Endings*. Akadémiai Kiadó; 1981.
35. Cold CJ, McGrath KA. Anatomy and histology of the penile and clitoral prepuce in primates: an evolutionary perspective of the specialised sensory tissue of the external genitalia. In: Denniston GC, Hodges FM, Milos MF, eds. *Male and Female Circumcision: Medical, Legal, and Ethical Considerations in Pediatric Practice*. Kluwer Academic/Plenum Publishers; 1999:19-29. doi:10.1007/978-0-585-39937-9_3
36. De Girolamo A, Cecio A. Contributo alla conoscenza dell'innervazione sensitiva del prepuzio nell'uomo [Contribution to the knowledge of sensory innervation of the prepuce in man]. *Boll Soc Ital Biol Sper*. 1968;44:1521-1522.
37. Zaliznyak M, Isaacson D, Duralde E, et al. Anatomic maps of erogenous sensation and pleasure in the penis: are there difference between circumcised and uncircumcised men?. *J Sex Med*. 2023;20(3):253-259. doi:10.1093/jsxmed/qdac032
38. Bryk F. *Circumcision in Man and Woman: Its History, Psychology and Ethnology*. American Ethnological Press; 1934.
39. Lee SH, Koh KS, Song WC. Macro/microscopic distribution of the dorsal nerve of penis in human glans penis. *J Anat*. 2020;237(5):849-853. doi:10.1111/joa.13263
40. Krstić R. *Human Microscopic Anatomy: An Atlas for Students of Medicine and Biology*. Springer; 1991:385.
41. Szymonowicz L, Krause R, *Lehrbuch Der Histologie Und Der Mikroskopischen Anatomie: Mit Besonderer Berücksichtigung Des Menschlichen Körpers, Einschliesslich Der Mikroskopischen Technik*. 2nd ed. Curt Kabitzsch (A. Stuber's Verlag); 1909.
42. Velazquez EF, Barreto JE, Cañete-Portillo S, Cubilla AL. Penis and distal urethra. In: Mills S, ed. *Histology for Pathologists*. 5th ed. Wolters Kluwer; 2019:1009-1028.
43. Ro JY, Grignon DJ, Ayala AG. *Atlas of Surgical Pathology of the Male Reproductive Tract*. Saunders; 1997.
44. Özbey H. Further misconceptions in glans penis anatomy and hypospadias surgery. *J Pediatr Urol*. 2023;19(4):391-393. doi:10.1016/j.jpurol.2023.04.035
45. Martín-Alguacil N, Cooper RS, Aardsma N, Mayoglou L, Pfaff D, Schober J. Terminal innervation of the male genitalia, cutaneous sensory receptors of the male foreskin. *Clin Anat*. 2015;28(3):385-391. doi:10.1002/ca.22501
46. Cepeda-Emiliani A, Otero-Alén M, García-Caballero T, Gallego R, García-Caballero L. The human mechanosensory corpuscles: a new Schwann cell localization of the Wilms' tumor protein WT1. *J Histochem Cytochem*. 2025;73(5–6):197-221. doi:10.1369/00221554251338066
47. Bourlond A, Winkelmann R. L'innervation du prépuce chez le nouveau-né [The innervation of the prepuce of the newborn infant]. *Arch Belges Dermatol Syphiligraphie*. 1965;21(12):139-153.
48. Pérez Casas A, Vega Álvarez J, López Muñiz A, Romo Hidalgo E, Suárez Garnacho S, Bengoechea Gonzáles E. Inervación microscópica del pene. I. Cubiertas del pene y glande [Microscopic innervation of the penis. I. Prepuce and glans penis]. *Arch Esp Urol*. 1988;41(1):1-7.
49. Yucel S, Baskin LS. Identification of communicating branches among the dorsal, perineal and cavernous nerves of the penis. *J Urol*. 2003;170(1):153-158. doi:10.1097/01.ju.0000072061.84121.7d
50. Baskin LS, Lee YT, Cunha GR. Neuroanatomical ontogeny of the human fetal penis. *Br J Urol*. 1997;79(4):628-640. doi:10.1046/j.1464-410x.1997.00119.x
51. Yucel S, Baskin LS. Neuroanatomy of the male urethra and perineum. *BJU Int*. 2003;92(6):624-630. doi:10.1046/j.1464-410X.2003.04435.x
52. Liu X, Liu G, Shen J, et al. Human glans and preputial development. *Differentiation*. 2018;103:86-99. doi:10.1016/j.diff.2018.08.002
53. Yucel S, Baskin L. The detailed topographical anatomy of the perineal nerves on the penis and perineum: surgical implications. *Eur Urol Suppl*. 2004;3(2):106-106.
54. Akman Y, Liu W, Li YWU, Baskin LS. Penile anatomy under the pubic arch: reconstructive implications. *J Urol*. 2001;166(1):225-230. doi:10.1016/S0022-5347(05)66131-9
55. Baskin LS, Erol A, Li YW, Liu WH. Anatomy of the neurovascular bundle: is safe mobilization possible?. *J Urol*. 2000;164(3 pt 2):977-980. doi:10.1097/00005392-200009020-00014
56. Cepeda-Emiliani A, García-Caballero L, Gándara-Cortés M, García-Caballero T, Gallego R. Immunohistological and neurodevelopmental study of the peripheral neural substrates of penile sexual sensation: implications for penile surgeries. In: *Abstracts of the 26th Congress of the World Association for Sexual Health*. World Association for Sexual Health; 2023:234.
57. Moore KL, Dalley AF, Agur AMR. *Clinically Oriented Anatomy*. 8th ed. Wolters Kluwer; 2018.
58. Rouvière H, Delmas A. *Anatomie Humaine - Descriptive, Topographique et Fonctionnelle (Tome 2, Tronc)*. 15th ed. Masson; 2002:614.
59. Tessier-Lavigne M, Kolodkin AL, eds. *Neuronal Guidance: The Biology of Brain Wiring*. Cold Spring Harbor Laboratory Press; 2011.
60. Vanderhaeghen P, Cheng HJ. Guidance molecules in axon pruning and cell death. In: Tessier-Lavigne M, Kolodkin AL, eds. *Neuronal Guidance: The Biology of Brain Wiring*. Cold Spring Harbor Laboratory Press; 2011:329-346.
61. Koutsioumpa C, Santiago C, Jacobs K, et al. Skin-type-dependent development of murine mechanosensory neurons. *Dev Cell*. 2023;58(20):2032-2047. doi:10.1016/j.devcel.2023.07.020
62. Hiltunen JO, Laurikainen A, Klinge E, Saarma M. Neurotrophin-3 is a target-derived neurotrophic factor for penile erection-inducing neurons. *Neuroscience*. 2005;133(1):51-58. doi:10.1016/j.neuroscience.2005.01.019
63. Montagna W, Kligman AM, Carlisle KS. *Atlas of Normal Human Skin*. Springer-Verlag; 1992.
64. Winkelmann R. *Nerve Endings in Normal and Pathologic Skin*. Charles C Thomas Publisher; 1960.
65. Winkelmann RK. The erogenous zones: their nerve supply and its significance. *Proc Staff Meet Mayo Clin*. 1959;34(2):39-47.
66. Winkelmann R. The mucocutaneous end-organ: the primary organized sensory ending in human skin. *AMA Arch Dermatol*. 1957;76(2):225-235. doi:10.1001/archderm.1957.01550200069015
67. Qi L, Iskols M, Greenberg RS, et al. Krause corpuscles are genital vibrotactile sensors for sexual behaviours. *Nature*. 2024;630(8018):926-934. doi:10.1038/s41586-024-07528-4
68. Csillag A. *Atlas of the Sensory Organs*. Humana Press; 2005.
69. Xin Z, Chung W, Choi Y, Seong D, Choi Y, Choi H. Penile sensitivity in patients with primary premature ejaculation. *J Urol*. 1996;156(3):979-981.
70. Bläuer M, Vaalasti A, Pauli SL, Ylikomi T, Joensuu T, Tuohimaa P. Location of androgen receptor in human skin. *J Invest Dermatol*. 1991;97(2):264-268. doi:10.1111/1523-1747.ep12480373
71. Handler A, Zhang Q, Pang S, et al. Three-dimensional reconstructions of mechanosensory end organs suggest a unifying mechanism underlying dynamic, light touch. *Neuron*. 2023;111(20):3211-3229.e9. doi:10.1016/j.neuron.2023.08.023
72. Nikolaev YA, Ziolkowski LH, Pang S, et al. 3D architecture and a bicellular mechanism of touch detection in mechanosensory corpuscle. *Sci Adv*. 2023;9(37):eadi4147. doi:10.1126/sciadv.adi4147

73. García-Mesa Y, García-Piqueras J, Cobo R, et al. Sensory innervation of the human male prepuce: Meissner's corpuscles predominate. *J Anat*. 2021;239(4):892-902. doi:10.1111/joa.13481
74. Tobeigei F, Zaki MSA, Shati AA, et al. Why human prepuce is a valuable resource in science? Histological, ultrastructural, immunohistochemical and statistical analysis. *Int J Morphol*. 2022;40(4):895-901.
75. Erdem E, Caliskan MK, Karagul MI, Akbay E, Coskun Yilmaz B, Aygun YC. Histological and morphological development of the prepuce from birth to prepubertal age. *Investig Clin Urol*. 2024;65(2):180-188. doi:10.4111/icu.20230034
76. Özdemir-Sancı T, Sancı A, Nakkaş H. Foreskin neurovascular structure: a histological analysis comparing 0–3 years and 6–11 years children. *J Pediatr Urol*. 2024;20(4):704.e1-704.e7. doi:10.1016/j.jpurol.2024.03.016
77. Shih C, Cold CJ, Yang CC. Cutaneous corpuscular receptors of the human glans clitoris: descriptive characteristics and comparison with the glans penis. *J Sex Med*. 2013;10(7):1783-1789. doi:10.1111/jsm.12191
78. Ortiz-Rey JA, Álvarez-Álvarez C, Antón-Badiola I, San Miguel-Fraile P, de la Fuente-Buceta A. Human Meissner corpuscles express Bcl-2 but not Bax protein. *Neurosci Lett*. 2002;329(2):240-242. doi:10.1016/S0304-3940(02)00613-4
79. Chetty R, Cooper K, Gown AM. *Leong's Manual of Diagnostic Antibodies for Immunohistology*. 3rd ed. Cambridge University Press; 2016.
80. Maguer-Satta V, Besançon R, Bachelard-Cascales E. Concise review: neutral endopeptidase (CD10): a multifaceted environment actor in stem cells, physiological mechanisms, and cancer. *Stem Cells*. 2011;29(3):389-396. doi:10.1002/stem.592
81. Wang S, Xiao Y, An X, Luo L, Gong K, Yu D. A comprehensive review of the literature on CD10: its function, clinical application, and prospects. *Front Pharmacol*. 2024;15:1336310. doi:10.3389/fphar.2024.1336310
82. Hejbøl EK, Hajjaj MA, Nielsen O, Schrøder HD. Marker expression of interstitial cells in human skeletal muscle: an immunohistochemical study. *J Histochem Cytochem*. 2019;67(11):825-844. doi:10.1369/0022155419871033
83. Schutz PW, Cheung S, Yi L, Rossi FMV. Cellular activation patterns of CD10+ fibro- adipogenic progenitors across acquired disease states in human skeletal muscle biopsies. *Free Neuropathol*. 2024;5:3. doi:10.17879/freeneuropathology-2024-5162
84. Cadoni A, Mancardi GL, Zaccheo D, et al. Expression of common acute lymphoblastic leukemia antigen (CD 10) by myelinated fibers of the peripheral nervous system. *J Neuroimmunol*. 1993;45(1–2):61-66. doi:10.1016/0165-5728(93)90164-T
85. Allen K, Wise N, Frangos E, Komisaruk B. Male urogenital system mapped onto the sensory cortex: functional magnetic resonance imaging evidence. *J Sex Med*. 2020;17(4):603-613. doi:10.1016/j.jsxm.2019.12.007
86. Yang CC, Bradley WE. Peripheral distribution of the human dorsal nerve of the penis. *J Urol*. 1998;159(6):1912-1916. doi:10.1016/S0022-5347(01)63194-X
87. Yang CC, Bradley WE. Innervation of the human anterior urethra by the dorsal nerve of the penis. *Muscle Nerve*. 1998;21(4):514-518. doi:10.1002/(sici)1097-4598(199804)21:4⟨514::aid-mus10⟩3.0.co;2-x
88. Yang CC, Bradley WE. Neuroanatomy of the penile portion of the human dorsal nerve of the penis. *Br J Urol*. 1998;82(1):109-113. doi:10.1046/j.1464-410x.1998.00669.x
89. Yang CC, Bradley WE. Reflex innervation of the bulbocavernosus muscle. *BJU Int*. 2000;85(7):857-863. doi:10.1046/j.1464-410x.2000.00560.x
90. van der Putte SCJ. *The Development of the Perineum in the Human: A Comprehensive Histological Study With a Special Reference to the Role of the Stromal Components*. Springer; 2005.
91. Lakshmanan S. Human prepuce: some aspects of structure and function. *Indian J Surg*. 1980; 44(1966):134-137.
92. Jefferson G. The peripenic muscle; some observations on the anatomy of phimosis. *Surg Gynecol Obstetr*. 1916; 23(2):177-181.
93. Burnstock G, Verkhratsky A. Peripheral nervous system. In: Burnstock G, Verkhratsky A, eds. *Purinergic Signalling and the Nervous System*. Springer Berlin Heidelberg; 2012:307-432. doi:10.1007/978-3-642-28863-0_7
94. Fahmy MAB, ed. *Complications in Male Circumcision*. Elsevier; 2019.
95. de Carvalho JPM, Costa WS, Sampaio FJB, Favorito LA. Anencephaly does not cause structural alterations in the fetal penis. *J Sex Med*. 2012;9(3):735-742. doi:10.1111/j.1743-6109.2011.02589.x
96. Pueschel SM, Orson JM, Boylan JM, Pezzullo JC. Adolescent development in males with down syndrome. *Am J Dis Child*. 1985;139(3):236-238. doi:10.1001/archpedi.1985.02140050030014
97. Drey EA, Kang MS, McFarland W, Darney PD. Improving the accuracy of fetal foot length to confirm gestational duration. *Obstet Gynecol*. 2005;105(4):773-778. doi:10.1097/01.AOG.0000154159.75022.11
98. Cizkova K, Flodrova P, Baranova R, Malohlava J, Lacey M, Tauber Z. Beneficial effect of heat-induced antigen retrieval in immunocytochemical detection of intracellular antigens in alcohol-fixed cell samples. *Appl Immunohistochem Mol Morphol*. 2020;28(2): 166-174. doi:10.1097/PAI.0000000000000689
99. Dako. *FLEX Ready-to-Use Atlas of Stains*. 4th ed. Dako; 2012.
100. Gratzl M, Langley K. *Markers for Neural and Endocrine Cells: Molecular and Cell Biology, Diagnostic Applications*. VCH Publishers; 1991.
101. Suzuki T, Take G, Ikeda K, Mitsuya T. A novel multicolor immunofluorescence method using heat treatment. *Acta Medica Okayama*. 2005;59(4):145-151. doi:10.18926/AMO/31955
102. Zhang W, Hubbard A, Jones T, et al. Fully automated 5-plex fluorescent immunohistochemistry with tyramide signal amplification and same species antibodies. *Lab Invest*. 2017;97(7): 873-885. doi:10.1038/labinvest.2017.37
103. Taylor J. The smart penis. In: Denniston GC, Hodges FM, Milos MF, eds. *Genital Cutting: Protecting Children From Medical, Cultural, and Religious Infringements*. Springer; 2013:55-58. doi:10.1007/978-94-007-6407-1_3
104. Pasterkamp RJ, Kolodkin AL. SnaphShot: axon guidance. *Cell*. 2013;153(2):494-494. doi:10.1016/j.cell.2013.03.031
105. Hülsman CJM, Gao H, Kruepunga N, et al. The development of the external genitals in female human embryos and foetuses. Part 1: perineal thick skin, clitoris and labia. *J Anat*. 2024;246(2):190-204. doi:10.1111/joa.14139
106. van der Putte SCJ. Hypospadias and associated penile anomalies: a histopathological study and a reconstruction of the pathogenesis. *J Plast Reconstr Aesthet Surg*. 2007;60(1):48-60. doi:10.1016/j.bjps.2006.05.020
107. Purves D, Lichtman JW. *Principles of Neural Development*. Sinauer Associates Inc.; 1985.
108. Patterson PH, Purves D, eds. *Readings in Developmental Neurobiology*. Cold Spring Harbor Laboratory; 1982.
109. Ramón y Cajal S. Acción neurotrópica de los epitelios. (Algunos detalles sobre el mecanismo genético de las ramificaciones nerviosas intraepiteliales, sensitivas y sensoriales) [Neurotropic action of epithelia: some details on the genetic mechanism of intraepithelial, sensory and sensorial nerve branching]. *Trab Lab Invest Biol*. 1919;17:181-228.
110. Osmonov D, Wilson SK, Heinze T, et al. Anatomic considerations of inflatable penile prosthetics: lessons gleaned from surgical body donor workshops. *Int J Impot Res*. 2023;35(7):672-678. doi:10.1038/s41443-023-00715-3
111. Gordon-Weeks PR. *Neuronal Growth Cones*. Cambridge University Press; 2000.

112. Mencio CP, Hussein RK, Yu P, Geller HM. The role of chondroitin sulfate proteoglycans in nervous system development. *J Histochem Cytochem*. 2021;69(1):61-80. doi:10.1369/0022155420959147
113. Kolodkin A, Pasterkamp R. SnapShot: Axon guidance II. *Cell*. 2013;153(3):722. e1. doi:10.1016/j.cell.2013.04.004
114. Winkelmann R. The cutaneous innervation of human newborn prepuce. *J Invest Dermatol*. 1956;26(1):53-67. doi:10.1038/jid.1956.5
115. Nishimura H, ed. *Atlas of Human Prenatal Histology*. Igaku-Shoin; 1983:6.
116. Santiago C, Siegrist J, Africawala N, et al. Activity-dependent development of the body's touch receptors. *Neuron*. 2025;113:1-16. doi:10.1016/j.neuron.2025.04.015
117. Cobo R, García-Piqueras J, Cobo J, Vega JA. The human cutaneous sensory corpuscles: an update. *J Clin Med*. 2021;10(2):227. doi:10.3390/jcm10020227
118. Bengoechea González ME, Vega Alvarez JA, López Muñiz A, Romo Hidalgo E, Suárez Garnacho S, Pérez Casas A. Estudios sobre la inervación microscópica del pene. II. Cuerpos cavernosos y vasos profundos [Microscopic innervation of the penis. II. Corpora cavernosa and deep vessels]. *Arch Esp Urol*. 1988;41(1):9-14.
119. Velazquez EF, Soskin A, Bock A, Codas R, Barreto JE, Cubilla AL. Positive resection margins in partial penectomies: sites of involvement and proposal of local routes of spread of penile squamous cell carcinoma. *Am J Surg Pathol*. 2004;28(3):384-389. doi:10.1097/00000478-200403000-00012
120. Kim JJ, Kwak TI, Jeon BG, Cheon J, Moon DG. Effects of glans penis augmentation using hyaluronic acid gel for premature ejaculation. *Int J Impot Res*. 2004;16(6):547-551. doi:10.1038/sj.ijir.3901226
121. Valenzuela R, *HA for premature ejaculation*. 2025. Accessed March 2, 2025. https://www.youtube.com/watch?v=KNVUtb4D-6M
122. Salonia A, Capogrosso P, Boeri L, et al. European Association of Urology Guidelines on Male Sexual and Reproductive Health: 2025 Update on Male Hypogonadism, Erectile Dysfunction, Premature Ejaculation, and Peyronie's Disease. *Eur Urol*. 2025;88(1):76-102. doi:10.1016/j.eururo.2025.04.010
123. Romano L, Arcaniolo D, Spirito L, et al. Comparison of current international guidelines on premature ejaculation: 2024 update. *Diagnostics (Basel)*. 2024;14(16):1819. doi:10.3390/diagnostics14161819
124. Shindel A, Althof SE, Carrier S, et al. Disorders of Ejaculation: an AUA/SMSNA Guideline. *J Urol*. 2022;207(3):504-512. doi:10.1097/JU.0000000000002392
125. Althof SE, McMahon CG, Waldinger MD, et al. An update of the International Society of Sexual Medicine's Guidelines for the Diagnosis and Treatment of Premature Ejaculation (PE). *Sex Med*. 2014;2(2):60-90. doi:10.1002/sm2.28
126. Montague D, Jarow J, Broderick G, et al. AUA guideline on the pharmacologic management of premature ejaculation. *J Urol*. 2004;172(1):290-294.
127. Tullii RE, Di Iorio JM, Vaccari R, Trefiletti S, Degni M. Neurectomy: new therapeutic technique for premature ejaculation. *Int J Impot Res*. 1992;4(suppl 2):205.
128. Ladines L, Santos B, Fischer R. M139–A comparison of two groups of patients using different indications of neurotomy. *Int J Impot Res*. 2001;13(suppl l1):S74. doi:10.1038/sj.ijir.3900665
129. Dias Bautista A, Donis Romero A, Fischer Santos B, et al. M140–A multicentric evaluation of more than 4,000 cases of neurotomy. *Int J Impot Res*. 2001;13(suppl l1):S74. doi:10.1038/sj.ijir.3900665
130. Santos BOF, Vieira ALD. Neurotripsy—an alternative in the treatment of premature ejaculation. *Int J Impot Res*. 1996;8:149.
131. Fischer Santos B. *Manual Do Prazer Do Homem*. Imprensa Livre Editora; 2003.
132. Romero AD. *Da Tragédia Ao Prazer Sexual—Histórias de Vida*. Scortecci Editora; 2003.
133. Conselho Federal de Medicina. *RESOLUÇÃO CFM No 1.478/1997*. Publicada No D.O.U. de 12 de Agosto de1997, Seção I. Conselho Federal de Medicina; 1997. https://sistemas.cfm.org.br/normas/arquivos/resolucoes/BR/1997/1478_1997.pdf
134. Akhvlediani N. MP76-16 reconstruction of the dorsal nerves branches after excessive penile neurotomy. *J Urol*. 2024;211(5S):e1248-e1249.
135. Anaissie J, Yafi FA, Hellstrom WJG. Surgery is not indicated for the treatment of premature ejaculation. *Transl Androl Urol*. 2016;5(4):607-612. doi:10.21037/tau.2016.03.10
136. Yang DY, Ko K, Lee WK, et al. Urologist's practice patterns including surgical treatment in the management of premature ejaculation: a Korean nationwide survey. *World J Mens Health*. 2013;31(3):226-231. doi:10.5534/wjmh.2013.31.3.226
137. McMorrow RW, *Inside the unregulated Chinese hospitals that make men impotent*. Vice Media; 2016. https://www.vice.com/en/article/chinas-21st-century-eunuchs-v23-n3/
138. Shin S, Jang SG, Min K, Lee W, Kim SY. The legal doctrine on the liability of physicians in medical malpractice lawsuits involving complex regional pain syndrome. *J Korean Med Sci*. 2018;33(9):e46. doi:10.3346/jkms.2018.33.e46
139. Shin SH, Kim SY, Jang SG, Lee W. Analysis of closed medical litigation in urology. *Investig Clin Urol*. 2017;58(5):317-323. doi:10.4111/icu.2017.58.5.317
140. Callegari M, Muncey W, Kim T, Rhodes S, Woo L, Hannick J. Where to draw the line? Understanding preferences in mucosal collar length after circumcision: a crowdsourced survey from the U.S. general population. *Can Urol Assoc J*. 2022;16(9):E473-E478. doi:10.5489/cuaj.7691
141. Chandanwale A, Ramteke A, Barhate S. Intra-operative somatosensory-evoked potential monitoring. *J Orthop Surg (Hong Kong)*. 2008;16(3):277-280. doi:10.1177/230949900801600301
142. Mulhall JP, Stahl PJ, Stember DS. Penile sensory loss. In: Mulhall JP, Stahl PJ, Stember DS, eds. *Clinical Care Pathways in Andrology*. Springer; 2014:135-140. doi:10.1007/978-1-4614-6693-2_19
143. Perić MH, Takahashi M, Ježek D, Cunha GR. Early development of the human embryonic testis. *Differentiation*. 2023;129:4-16. doi:10.1016/j.diff.2022.07.001
144. Li Y, Overland M, Derpinghaus A, et al. Development of the human fetal testis: morphology and expression of cellular differentiation markers. *Differentiation*. 2023;129:17-36. doi:10.1016/j.diff.2022.03.002
145. Hall J. *Guyton and Hall Textbook of Medical Physiology*. 13th ed. Elsevier; 2016.
146. del Río Hortega P.. Art and artifice in the science of histology. *Histopathology*. 1993;22(6):515-525. doi:10.1111/j.1365-2559.1993.tb00171.x
147. Tunçkol E, Purkart L, Eigen L, Vida I, Brecht M. Fiber counts and architecture of the human dorsal penile nerve. *Sci Rep*. 2023;13(1):8862. doi:10.1038/s41598-023-35030-w

SUPPORTING INFORMATION

Additional supporting information can be found online in the Supporting Information section at the end of this article.

How to cite this article: Cepeda-Emiliani A, Otero-Alén M, Suárez-Quintanilla J, et al. The sensory penis: A comprehensive immunohistological and ontogenetic exploration of human penile innervation. *Andrology*. 2025;1-41. https://doi.org/10.1111/andr.70118